Aus der Klinik für Augenheilkunde und Experimentelle Ophthalmologie
der Medizinischen Fakultät Charité – Universitätsmedizin Berlin

DISSERTATION

Effects of ascorbic acid on TRP channel-mediated Ca^{2+} homeostasis and cell viability in etoposide-resistant and -sensitive retinoblastoma cells

Auswirkungen von Ascorbinsäure auf die TRP-Kanal-vermittelte Ca^{2+}-Homöostase und Zelllebensfähigkeit in Etoposid-resistenten und -empfindlichen Retinoblastomzellen

zur Erlangung des akademischen Grades
Doctor medicinae (Dr. med.)

vorgelegt der Medizinischen Fakultät
Charité – Universitätsmedizin Berlin
von

Jakub Jan Oronowicz
aus Szczecin, Polen

Datum der Promotion: 26.06.2022

CONTENTS

This text serves as the extended version of the publication [1] and therefore provides a supplement for the content described there. Some paragraphs and figures were taken over directly in order to maintain a precise formulation.

Oronowicz J, Reinhard J, Reinach PS, Ludwiczak S, Luo H, Omar Ba Salem MH, Kraemer MM, Biebermann H, Kakkassery V, Mergler S: *Ascorbate-induced oxidative stress mediates TRP channel activation and cytotoxicity in human etoposide-sensitive and -resistant retinoblastoma cells*. *Lab Invest* 2020.

DOI: 10.1038/s41374-020-00485-2

ABBREVIATIONS

2-APB	2-aminoethyl diphenylborinate
Asc	Ascorbic acid
CPZ	Capsazepine
GABA	Gamma-aminobutyric acid
GPCR	G protein-coupled receptor
H_2O_2	Hydrogen peroxide
La^{3+}	Lanthanum-III-chloride
NAC	N-acetylcysteine
NOMPC	No mechanoreceptor potential C
PTX	Pertussis toxin
RB	Retinoblastoma
ROS	Reactive oxygen species
TRPs	Transient receptor potential channels
TRPA1	Transient receptor potential ankyrin 1
TRPC5	Transient receptor potential canonical 5
TRPM2	Transient receptor potential melastatin 2
TRPM7	Transient receptor potential melastatin 7
TRPM8	Transient receptor potential melastatin 8
TRPV1	Transient receptor potential vanilloid 1
TRPV4	Transient receptor potential vanilloid 4
WERI-Rb1	Wills Eye Research Institute-Retinoblastoma-1 (human retinoblastoma cell line)
$\%_{e\text{-}r/e\text{-}s}$	A percentage of control in the etoposide-resistant / etoposide-sensitive group of cells

ABSTRACT IN ENGLISH

Introduction: *Cell viability and survival are both dependent on cellular mechanisms maintaining Ca^{2+} homeostasis. Intracellular Ca^{2+} is substantially regulated by transient receptor potential channels (TRPs), which are overexpressed in various tumors. Ascorbic acid (Asc) administered in high doses (1 mM) is reported to reduce tumor cell survival, through promoting prooxidative responses. This study was undertaken to investigate whether high doses of Asc have cytotoxic effects through perturbing intracellular Ca^{2+} regulation by stimulating Ca^{2+} influx through augmenting TRPs activity in retinoblastoma (RB) cells.*

Methods: *An etoposide-resistant and etoposide-sensitive RB cell lines (WERI-Rb1) were used and cultivated in RPMI-1640 Medium. For measuring the intracellular Ca^{2+} concentration and whole-cell currents, fluorescence Ca^{2+} imaging and the planar patch-clamp technique were used. Unspecific and specific TRP channel blockers were used as tools for characterizing TRPs involved in Asc-mediated Ca^{2+} influx. In addition, Trypan Blue staining was performed to determine the ability of RB cells to survive exposure to Asc.*

Results: *Extracellular application of 1 mM Asc induced increases in the fluorescence ratio f_{340}/f_{380}, which is proportional to a rise in intracellular Ca^{2+} concentration ($[Ca^{2+}]_i$). Interestingly, this effect reached higher levels in the etoposide-resistant WERI-Rb1 cells compared to their etoposide-sensitive counterpart. The Asc-induced increases of f_{340}/f_{380} could be clearly suppressed in the presence of different TRP channel blockers such as La^{3+} (500 µM), 2-APB (100 µM), Capsazepine (CPZ) (100 µM) and the broad-spectrum blocker N-Acetylcysteine (NAC) (10 mM). These results are in line with the corresponding rises in the whole-cell currents. Preincubation of the RB*

cells with pertussis toxin (PTX) (50 ng/ml), an uncoupler of Gi/o binding proteins to their cognate GPCR coupled receptor, suppressed the Asc-induced Ca^{2+} influx. Microscopic analyses revealed that 1 mM Asc treatment reduced cell viability by almost 94 % in both WERI Rb1 cell lines.

Conclusions: *The effects of pharmacological doses of Asc on TRP channel-modulated Ca^{2+} homeostasis are described for the first time on RB cells. Therefore, it is assumed that 1 mM Asc acting as a prooxidant reduces etoposide-resistant and -sensitive WERI-Rb1 cell survival through altering intracellular Ca^{2+} regulation as a consequence of stimulation of a Gi/o-protein-mediated pathway linked to TRP channel activity. Based on the cytotoxic effects of Asc, on both etoposide-resistant and etoposide-sensitive RB cells, the development of TRP modulating drugs could be a possible approach to treat even cytostatic resistant tumor cells. Moreover, the results suggest that Asc should be evaluated as an adjuvant to improve therapeutic management of retinoblastoma cures.*

ABSTRACT IN GERMAN

Einleitung: *Das Überleben von Zellen hängt von Mechanismen zur Aufrechterhaltung der Calciumhomöostase ab. Intrazelluläres Ca^{2+} wird im Wesentlichen durch transient receptor potential channels (TRPs) reguliert, die in verschiedenen Tumoren überexprimiert sind. Es wird berichtet, dass in hohen Dosen (1 mM) verabreichte Ascorbinsäure (Asc) das Überleben von Tumorzellen durch Förderung prooxidativer Reaktionen verringert. Diese Studie untersucht, ob hohe Asc-Dosen zytotoxische Wirkungen haben, indem sie die intrazelluläre Ca^{2+}-Regulation durch Stimulierung des Ca^{2+}-Einstroms und Erhöhung der Aktivität des TRPs in Retinoblastomzellen (RB) beeinflussen.*

Methoden: *Eine Etoposid-resistente und Etoposid-sensitive WERI-Rb1-Zelllinie wurde verwendet und in RPMI-1640-Medium kultiviert. Zur Messung der intrazellulären Ca^{2+}-Konzentration und der Ganzzellströme wurden Fluoreszenz-Ca^{2+}-Imaging und die planare Patch-Clamp-Technik verwendet. Unspezifische und spezifische TRP-Blocker wurden zur Charakterisierung von TRPs verwendet, die am Asc-vermittelten Ca^{2+}-Einstrom beteiligt sind. Zusätzlich wurde eine Trypanblau-Färbung durchgeführt, um die Überlebensfähigkeit von RB-Zellen gegenüber Asc zu bestimmen.*

Ergebnisse: *Die extrazelluläre Zugabe von 1 mM Asc induzierte einen Anstieg des Fluoreszenzverhältnisses f_{340}/f_{380}, das proportional zu einem Anstieg der intrazellulären Ca^{2+}-Konzentration ist. Interessanterweise erreichte dieser Effekt in den Etoposid-resistenten WERI-Rb1-Zellen höhere Werte. Die Asc-induzierten Anstiege von f_{340}/f_{380} konnten in Gegenwart verschiedener TRP-Blocker wie z.B. La^{3+} (500 µM), 2-APB (100 µM), Capsazepine (CPZ) (100 µM) und N-Acetylcystein (NAC) (10 mM) deutlich unterdrückt werden. Diese Ergebnisse stimmen mit den entsprechenden Anstiegen der Ganzzellenströme überein. Die Vorinkubation der RB-Zellen mit dem GPCR-Blocker Pertussis-Toxin (PTX) (50 ng/ml) unterdrückte den Asc-induzierten Ca^{2+}-Einstrom.*

Mikroskopische Analysen zeigten, dass eine 1 mM Asc-Behandlung das Überleben der Zellen in beiden RB-Zelllinien um fast 94 % verringerte.

Schlussfolgerungen: *Die Auswirkungen pharmakologischer Dosen von Asc auf die TRP-modulierte Ca^{2+}-Homöostase wurden erstmals in RB-Zellen beschrieben. Daher wird angenommen, dass 1 mM Asc als Prooxidationsmittel das Überleben von Etoposid-resistenten und -sensitiven WERI-Rb1-Zellen durch Veränderung der*

intrazellulären Ca^{2+}-Regulierung verringert. Dies geschieht als Folge der Stimulation eines Gi/o-Protein-vermittelten Weges, der mit der TRP-Aktivität verbunden ist.

Basierend auf den zytotoxischen Effekten von Asc sowohl auf Etoposid-resistente als auch Etoposid-sensitive RB-Zellen, könnte die Entwicklung von TRP-modulierenden Medikamenten ein möglicher Ansatz sein, um auch Zytostatika-resistente Tumorzellen zu behandeln. Darüber hinaus könnte Asc als eine mögliche adjuvante Therapie evaluiert werden, um das Gesamtkonzept für die Behandlung von Retinoblastomen zu verbessern.

1 INTRODUCTION

More than two decades ago, ascorbic acid (Asc) was already identified as a cytotoxic agent which supports anti-tumor treatment [2-4]. Intravenously administrated pharmacological doses of Asc (i.e. 1-20 mM) are reported to have some therapeutic effects. It was demonstrated that Asc reduced tumor cell survival in more than 40 different cell lines, e.g. lung, ovarian, breast cancer as well as Y-79 RB cell line [5, 6]. Despite controversies, using ascorbate in therapies is becoming more popular due to its favorable effects in different groups of patients [7-11]. Knowing that the millimolar levels of extracellular ascorbate, administrated as an adjuvant, selectively kill tumor cells [12, 13], this clinical approach seems to be safe since reported pharmacological doses of Asc did not affect the viability of healthy cells [4, 14]. It minimizes the possibility of side effects in case of therapeutic failure.

1.1 Ascorbic acid at pharmacological doses

Asc is present in supplements, food, medicines and also in different body tissues such as the brain, eyes, adrenal glands and leukocytes [15]. Notably, Asc has antioxidative properties at physiological, micromolar concentration (similar to its reported value in plasma [15]). Nonetheless, Asc has prooxidative effects at millimolar, pharmacological doses. It is able to generate reactive oxygen species (ROS), hydrogen peroxide (H_2O_2) and hydroxyl radicals [5, 11, 16].

As already mentioned, Asc is reported to be present at high millimolar levels in the eye. It is hypothesized to have a protective function in reducing the damaging effects of short wavelength solar radiation [17]. Notably, several studies reported that Asc is present at high intracellular concentration in different cell types and fluids in the

humans eye: aqueous humour: 0.4 - 1.1 mM; retina > 1 mM; lens: 2.5 to 3.4 mM; corneal epithelium ~12.5 mM [1, 18, 19]. Using the Asc in form of intravenous administrated therapy, it may be able to reach much higher doses at the external retina side. This property is important since the previous report suggests that not the intra- but rather the extracellular concentration of Asc impacts the cell death [12].

Furthermore, Asc is also known for modulation of cellular redox systems [13, 18], GABA receptors [20] or even tumor growth [21].

In this study, the same concentration of Asc (1 mM) was used as tested by *Uetaki et al*. in their previous report [11].

1.2 Role of TRP channels and Ca^{2+} in maintaining cell viability

As pharmacological doses of Asc have prooxidative properties, their effects on modulating physiological responses through oxidation-sensitive TRPs warranted consideration [5, 22-28]. In mammals, TRPs constitute a heterogeneous superfamily of more than 28 genes. They encode seven subfamilies: TRPA (ankyrin), TRPC (canonical), TRPM (melastatin), TRPML (mycolipin), TRPN (NOMPC), TRPP (polycyclin) and TRPV (vanilloid), [29, 30]. Through being regulated by different extra- and intracellular stimuli, they function as transducers and biosensors. Specifically, they can be activated by variety of environmental factors, e.g. anisoosmolarity [31], different ligands (capsaicin [32]), pH decrease [33], temperature [34], UV-light [35] and others [1, 36]. Moreover, TRPs can be stimulated by the activation of other cell surface proteins - G protein-coupled receptors (GPCRs) [37]. They function as a unit, composing a signaling axis [38, 39].

Relationships among TRPs and tumors were already widely described at different levels: diagnostic, progression, therapy. Multiple studies suggest a correlation

between TRP channel expression/function and malignant transformation [40]. Specifically, e.g. TRPM8 is overexpressed in different tumors such as prostate, breast, lung or colon compared to health tissues [41, 42]; time dependent increases in expression of TRPM1 is a diagnostic indicator of melanoma [43]; TRPV2 can serve as therapeutic target in bladder cancer [44]. Taken together, these representative findings form the basis for defining the roles of TRP functional modulation in tumorigenesis [45-47].

As it is well known that cell viability is linked to the homeostatic regulation of intracellular Ca^{2+} levels, much interest has been dedicated to characterizing the role of TRPs in this process. Modulation of their activity may lead to an uncompromised imbalance in Ca^{2+} homeostasis. Intracellular Ca^{2+} levels above 100 nM were reported to suppress the tumorigenesis by increasing the apoptosis rates, decreasing the cell proliferation or stimulating the autophagy [48-51].

Demonstrating a contribution by TRPs in mediating pathological responses resulting from an accumulation of cytotoxic levels of Ca^{2+} may indicate a crucial focal point for possible drug targeting therapies in mediating selective increases in cytotoxic effects in tumor cells.

1.3 Retinoblastoma

The neoplastic properties of Retinoblastoma (RB) cells are dependent on the expression of cellular mechanisms that mediate control of Ca^{2+} influx. Changes in the expression levels of voltage-operated Ca^{2+} channels [52, 53] and TRPs [54, 55] in these cells are indicative of this relationship. RB is the most common primary eye neoplasm in childhood [56]. Mutations in both RB1 alleles cause the RB protein (pRB) to lose its tumor suppression functions, which induces increases in the

proliferation of these cancer cells [57, 58]. RB survivability varies among different social groups. The survival rate in lower-income countries is less than 50%, while in developed countries it has significantly improved to over 90% [59, 60]. There are several therapeutic methods that provide some temporary alleviation of the symptomology but none of them provide a cure since frequently a diagnosis is only made after incurable metastasis has already occurred. One therapy that has been applied is etoposide treatment, but in the worst cases the primary option is enucleation [58]. Unfortunately, due to some complex and not fully understood factors RB cells can develop a resistance to etoposide, which is an antineoplastic agent. Etoposide-resistant cells behave more aggressively than their etoposide-sensitive counterpart and present a greater risk for local relapse [61].

Overall, it is unclear whether some new or already existing approaches can be developed and improved to treat different forms of this tumor. Therefore, we probed for a relationship between Asc-induced toxicity and TRPs activation in both etoposide-resistant and -sensitive WERI-Rb1 cells.

1.4 Aim of study

This study was conducted to determine if presumed prooxidative effects of a pharmacological dose (1 mM) of Asc can explain why its administration has unique cytotoxic effects on both etoposide-resistant and etoposide-sensitive WERI-Rb1cell lines. This evaluation entailed comparing the genetic and functional expression of certain TRPs in Asc-dependent Ca^{2+} modulation since the control of intracellular Ca^{2+} levels is a critical determinant of cell viability.

2 MATERIALS AND METHODS

2.1 Materials

In this study, materials are specified as previously described [1]. In brief, patch-clamp solutions were purchased from Nanion Company (Munich, Germany). Capsazepine was provided by Cayman Chemical Company (Ann Arbor, Mi, USA), but all other reagents (including Ascorbic acid) were obtained from Sigma-Aldrich (Deisenhofen, Germany). Culture medium and its supplements were provided by Biochrom AG (Berlin, Germany) or GIBCO Invitrogen (Karlsruhe, Germany) and the fluorescence dye Fura2/AM was obtained from PromoCell (Heidelberg, Germany).

2.2 Cell culture and cultivation

Established etoposide-resistant and -sensitive WERI-Rb1 cells were used [61, 62]. The human RB cell lines were obtained from Dr. Stephan (University Children's Hospital in Essen, Germany) [63]. Cells were incubated in culture flasks in medium containing: RPMI-1640 [64], 100 IU/ml penicillin/streptomycin and 10% fetal bovine serum (FBS), at 37°C in 80% humidity and 5% CO_2, as previously described [54, 65, 66]. For the experiments, the 12-well culture plates with cell-seeded coverslips were prepared 48-72 hours before measurements (Fig. 1A). Poly-L-lysine was used to ensure the cell adherence on the coverslips since fixed cells are necessary specifically for the fluorescence-optic measurements. The cultivation of both tumor cell types proceeded in the same way, with regular medium exchange [1].

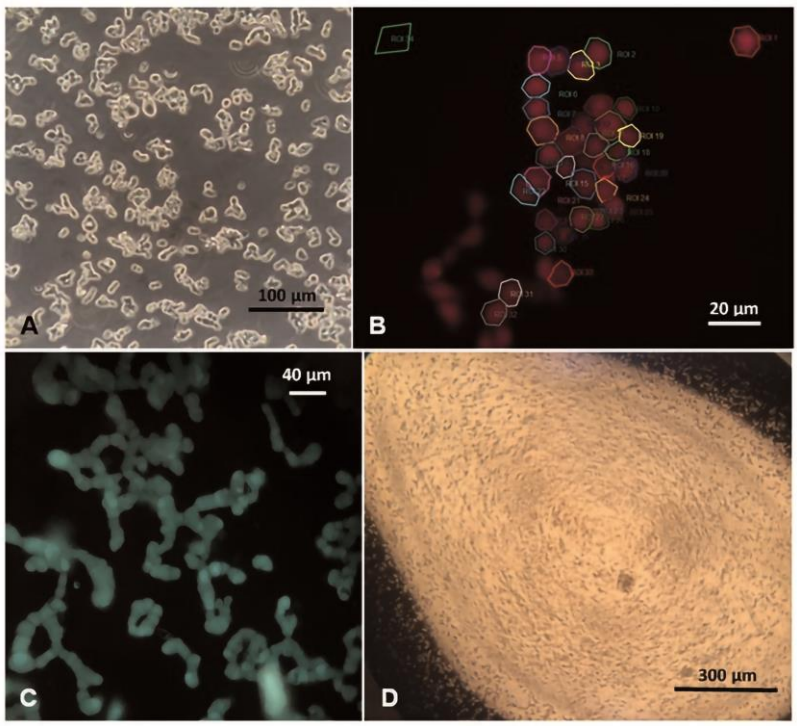

Fig. 1. Various microscopic images of etoposide-resistant WERI-Rb1 cells. a) Light microscopic view of freshly diluted cell culture. **b)** Calcium imaging; microscopic image at 510 nm emitted wavelength (colored by the software). Multiple circumscribed zones present the cells selected for the measurement - regions of interest (ROIs). **c)** Fluorescence microscopic image (510 nm) of chain-structured cell groups. **d)** Light microscopic image: single-cell suspension diluted for patch-clamp measurements.
Photos taken by J. Oronowicz. Figure by Oronowicz et al. [1].

2.3 Microscopic analyses of cell density and viability

In order to determine the effects of 1 mM Asc on WERI-Rb1 cell culture density, two sets of experiments were designed [1]:

1) 1 mM Asc was added to the freshly centrifuged cells on the first day and then the Asc concentration was diluted with RPMI-1640 medium four days later. The cell density was determined on the first, the fifth and also on the seventh day (two days after medium dilution).
2) Cell density was evaluated on the fifth day after culturing the RB cells in RPMI-1640 medium (without Asc). Thereafter, 1 mM Asc was added and WERI-Rb1 cultures were reassessed after another four days.

To investigate whether RB cell density corresponds with their viability, the 0,4% Trypan Blue dye exclusion experiments were conducted, using the fact that only

dead cells are stainable with this dye [67]. At first, Trypan Blue was added to the cell suspension (diluted 1:1). Afterwards, dead cells were counted using the Neubauer counting chamber (A. Hartenstein GmbH, Wuerzburg, Germany). Their quantity is presented as a percentage of all visible cells.

2.4 Fura-2/AM

Fura-2/AM is a Ca^{2+}-sensitive fluorescence dye that was used to measure the intracellular Ca^{2+} concentration ($[Ca^{2+}]_i$) [68]. Its fluorescence output at 510 nm resulting from alternate excitation at 340 and 380 nm changes depends on variations in intracellular free Ca^{2+} levels and provides a direct measure of its variability. The fluorescence intensity at the excitation wavelength of 340 nm is directly proportional with an increasing $[Ca^{2+}]_i$ whereas the 380 nm fluorescence signals are inversely proportional to $[Ca^{2+}]_i$ (Fig. 2) [68]. The isobestic point (at which fluorescence intensity is independent from Ca^{2+} concentration) is at about 360 nm excitation wavelength.

With the aforementioned two fluorescence signals, there is a direct relationship between increases in the fluorescent ratio f_{340}/f_{380} and rises in $[Ca^{2+}]_i$) [68].

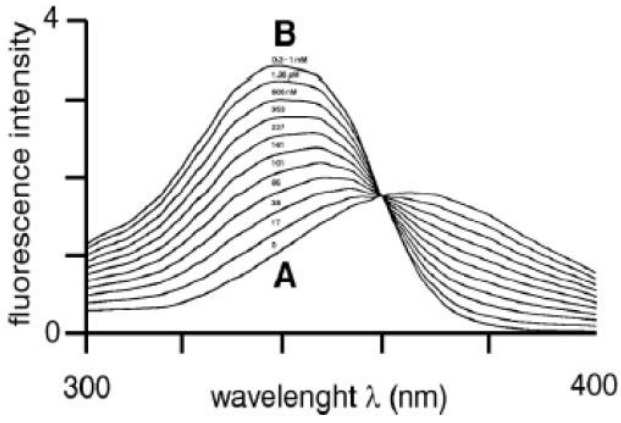

Fig. 2. Excitation spectral changes of Fura-2/AM fluorescence in solutions with a different free Ca^{2+} concentration covering a range from < 1 nM up to > 10 µM. The wavelengths between 300 nm and 400 nm excite the largest fluorescence intensity of the dye (at 510 nm - emission maximum).

Figure derived from Grynkiewicz et al. [68].

2.5 Fluorescence calcium imaging

To detect very small changes in cytosolic Ca^{2+}, this method, first used by Tsien et al, is one of the most sensitive procedures for this purpose [68]. For the experiments, the sterile cell-seeded coverslips were prepared and preincubated with 1 μM Fura-2/AM (diluted in culture medium) at 37°C and 5% CO_2. Additionally, to delineate the channel subtypes modulated by exposure to Asc, following TRP channel antagonists were used: 10 mM N-Acetylcysteine (NAC) as a broad spectrum blocker that suppresses TRPV1, TRPM2 and TRPA1 [69-72]; 500 μM Lanthanum-III-chloride (La^{3+}) as a nonselective TRP channel antagonist [73]; 100 μM 2-aminoethyl diphenylborinate (2-APB) as a blocker of TRPM2, TRPC5 and also store operated Ca^{2+} channels [74-76]; 100 μM capsazepine (CPZ) that suppresses TRPM8 and TRPV1 [73]. The cells were pretreated with NAC for up to 5 days (longest possible time without affecting the cell viability and measuring conditions [69]), whereas with other blockers the exposure time was only 20 - 30 min. They were also loaded with Gi/o inhibitor – pertussis toxin (PTX) (for 18 h) to determine if TRP activation by Asc is induced through the activation of a Gi/o GPCRs [1]. If the drugs were dissolved in dimethyl sulfoxide (DMSO), its concentration was kept below 0.1% which is reported to be non-cytotoxic [77]. Before each measurement, in order to stop Fura-2/AM uptake, RB cells were washed with a Ringer-like solution (containing in mM: 150 NaCl, 6 CsCl, 1 $MgCl_2$, 10 HEPES acid, 10 glucose and 1.5 $CaCl_2$ at pH ~ 7.35) and after that placed in a chamber of the inverted microscope containing the same solution. All experiments were performed at room temperature ~ 20 – 23°C. Adaptation of the cells lasted long enough to reach a certain stability level (data not shown). Drugs were applied by exchanging the bath contents by alternate additions with a pipette and removal with a suction pump. Fura-2/AM fluorescence was

measured in a setup composed of: a LED light source (LED-Hub by Omikron, Rodgau-Dudenhoven, Germany), an inverted microscope (Olympus BX50WJ) and a digital imaging system (Olympus Europa Holding GmbH, Hamburg, Germany) with a camera (Olympus XM-10). The imaging software (cellSens, Olympus Europa Holding GmbH, Hamburg, Germany) (Fig. 1B/C) was used to calculate the fluorescence ratio f_{340}/f_{380} (described in paragraph before) as a relative index of intracellular Ca^{2+} levels [68]. Results were normalized, control value was set to 0.1. Possible bleaching effects were compensated by drift correction using the TIDA-software (HEKA, Lampertheim, Germany) [1].

2.6 pH Measurements

All pH measurements in this study were performed with the pH-meter "Lab 850" (Si Analytics Gmbh, Mainz, Germany), with solutions, which had a room temperature ≈ 20 - 23°C or 37°C if needed. For certain experiments, the pH value of the Ringer-like solution was reduced using HCl instead of Asc.

2.7 Planar patch-clamp recordings

For the patch-clamp recordings, a setup of planar patch-clamp (Port-a-Patch®, Nanion, Munich, Germany) in combination with an EPC 10 amplifier (HEKA, Lamprecht, Germany) and PatchMaster v2x90.1 for Windows (HEKA, Lamprecht, Germany) was used [1]. With this setup, high-throughput measurements were possible compared to conventional patch-clamping. Both WERI-Rb1 cell types were prepared in the same way. At first, for improving the seal quality by removing any cell debris and remaining culture medium, a cell suspension was washed out with

phosphate buffer saline (PBS) [78]. Afterwards, cells were diluted in the external patch-clamp solution containing (in mM): 140 NaCl, 4 KCl, 1 $MgCl_2$, 2 $CaCl_2$, 5 D-glucose monohydrate and 10 HEPES (pH ≈ 7.4; osmolarity ≈ 298 mOsM) (Fig. 1D). At the beginning of every experiment, the intracellular solution was applied to the inside of the microchip with a mean resistance of 3 - 5 MOhm (Nanion, Munich, Germany) [79]. To avoid interference by potassium channel currents, this solution contains (in mM): 50 CsCl, 10 NaCl, 60 CsF, 20 EGTA, and 10 HEPES (pH ≈ 7.2 and ≈ 288 mOsM). Next, the aforementioned external solution was applied to the outer side of the microchip. All measurements were performed at room temperature ~ 20 – 23°C. Finally, the software-controlled pump (Suction Control Pro, Nanion, Munich, Germany) was started and the cell suspension was pipetted onto the upper side of the chip to establish cell contact and sealing. Pump suction was applied to break into and to maintain whole-cell configuration. Before starting each experiment, the cells were kept in the whole-cell mode for ~ 10 min to offset substantial resulting leak currents, which ensures the stability of recordings. Currents were measured every 5 s over a voltage range of −60 to +130 mV without steps, each protocol for 500 ms.

Mean access resistance was 26 ± 3 MΩ and mean membrane capacitance was 8 ± 2 pF for both etoposide-resistant (n = 16) and -sensitive (n = 19) WERI-Rb1 cells [1]. The liquid junction potential was calculated and corrected by the software (≈ 3.8 mV) [80]. To eliminate any possible contribution of voltage-dependent Ca^{2+} and Na^{+} channels, the holding potential (HP) was set to 0 mV. Leak currents were subtracted from all recordings and only those below 100 pA were analyzed.

2.8 Data analyses and statistics

To determine whether a parametric or non-parametric statistical test should be used, a normality test was performed to ascertain if there is a Gaussian distribution of tested values. Thereafter, Student's-t-tests were used as parametric tests. Alternatively, for paired tested values the non-parametric Wilcoxon test and for unpaired tested values the Mann-Whitney-U test were used. For all tests a p value < 0.05 was considered as statistically significant. Data are shown by means/ percentage of control ± standard error mean (SEM). For the creation of diagrams and statistical evaluation, SigmaPlot version 12.5 for Windows (Systat Software, Inc., Point Richmond, California USA) and GraphPad Prism software version 5.00 for Windows (La Jolla, California, USA) were used [1].

This study was conducted in accordance to the guidelines of „Grundsätze der Charité zur Sicherung guter wissenschaftlicher Praxis" of the Charité, Universitätsmedizin Berlin.

3 RESULTS

3.1 Asc-induced Ca^{2+} influx is larger in etoposide-resistant WERI-Rb1 than in etoposide-sensitive WERI-Rb1 cells

1 mM Asc induced significant increases in intracellular Ca^{2+} levels in both WERI-Rb1 cell lines. The fluorescence ratio corresponds to intracellular Ca^{2+} concentration. At t = 300 s, this ratio was set to 100% as a positive control. Interestingly, the Asc-mediated increase in the f_{340}/f_{380} ratio was greater in the etoposide-resistant group of cells. Specifically, the ratio rose from 0.1008 ± 0.0002 (t = 60 s; n = 91) to 0.3446 ±

0.0048 (100%$_{e\text{-}r}$) (t = 300 s; n = 91; p < 0.0001) (Fig. 3). Instead, the fluorescence ratio increased from 0.0998 ± 0.0001 (t = 60 s; n = 57) to only 0.1135 ± 0.0008 (100%$_{e\text{-}s}$) (t = 300 s; n = 57; p < 0.0001) in an etoposide-sensitive WERI-Rb1 group (Fig. 3) [1].

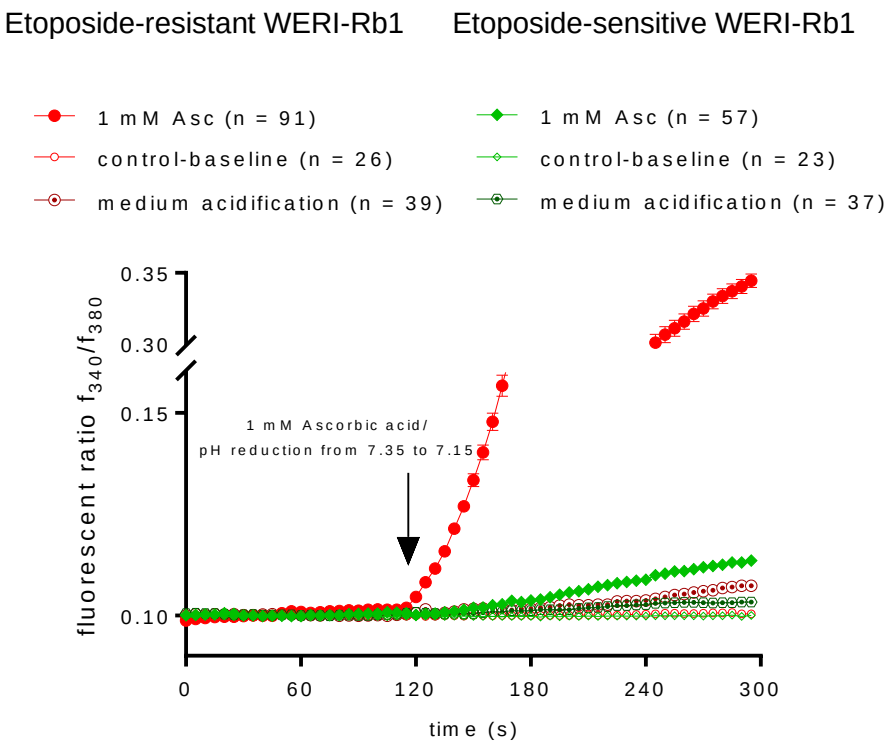

Fig. 3. 1mM Asc induces a larger Ca^{2+} influx in etoposide-resistant WERI-Rb1 cells than in etoposide-sensitive counterpart. Notably, medium acidification does not impact the Ca^{2+} regulation. 1 mM Asc increased intracellular Ca^{2+} influx in both etoposide-resistant (*n* = 91) and etoposide-sensitive (*n* = 57) WERI-Rb1 cells. The untreated control groups maintained a constant Ca^{2+} baseline (etoposide-resistant: *n* = 26; etoposide-sensitive *n* = 23). pH reduction (i.e., from 7.35 to 7.15) did not significantly increase the intracellular Ca^{2+} level (etoposide-resistant: *n* = 39; etoposide-sensitive *n* = 37). Figure modified after Oronowicz et al. [1].

3.2 Asc-induced Ca^{2+} influx is suppressed by TRP channel antagonists

To determine whether TRPs mediate Asc-induced increases in intracellular Ca^{2+} influx in RB cells, both WERI-Rb1 cell lines were preincubated with different TRP channel antagonists. The measurement duration was 5 minutes. 1 mM Asc was

added after 120 s and the fluorescence ratio f_{340}/f_{380} was evaluated at t = 300 s. The Asc-induced increases in Ca^{2+} influx could be clearly suppressed in the presence of TRP channel blockers in both cell lines. As shown in Fig. 4A, the tested TRP blockers suppressed the fluorescence ratio f_{340}/f_{380} as follows: NAC to ~ 54.9 ± 4.2 $\%_{e\text{-}r}$ (n = 56; p < 0.0001); La^{3+} to ~ 22.6 ± 5.8 $\%_{e\text{-}r}$ (n = 15; p < 0.0001); 2-APB to ~ 18.7 ± 2.9 $\%_{e\text{-}r}$ (n = 63; p < 0.0001); and CPZ to ~ 11.4 ± 1.1 $\%_{e\text{-}r}$ (n = 43; p < 0.0001), in the etoposide-resistant WERI-Rb1. Similar results were obtained in etoposide-sensitive cells where CPZ was also the most efficient TRP inhibitor. In this cell group, the aforementioned blockers suppressed the fluorescence f_{340}/f_{380} ratio respectively: La^{3+} to ~ 76.9 ± 5.0 $\%_{e\text{-}s}$ (n = 65, p < 0.005); 2-APB to ~ 72.5 ± 6.7 $\%_{e\text{-}s}$ (n = 15; p < 0.05); NAC to ~ 50.3 ± 8.9 $\%_{e\text{-}s}$ (n = 38; p < 0.0001); and CPZ to ~ 26.7 ± 3.0 $\%_{e\text{-}s}$ (n = 45; p < 0.0001) (Fig. 4B). Since each of these TRP channel blockers reduced the Asc-induced Ca^{2+} influx, these effects indicate that Asc increased TRP channel activity [1].

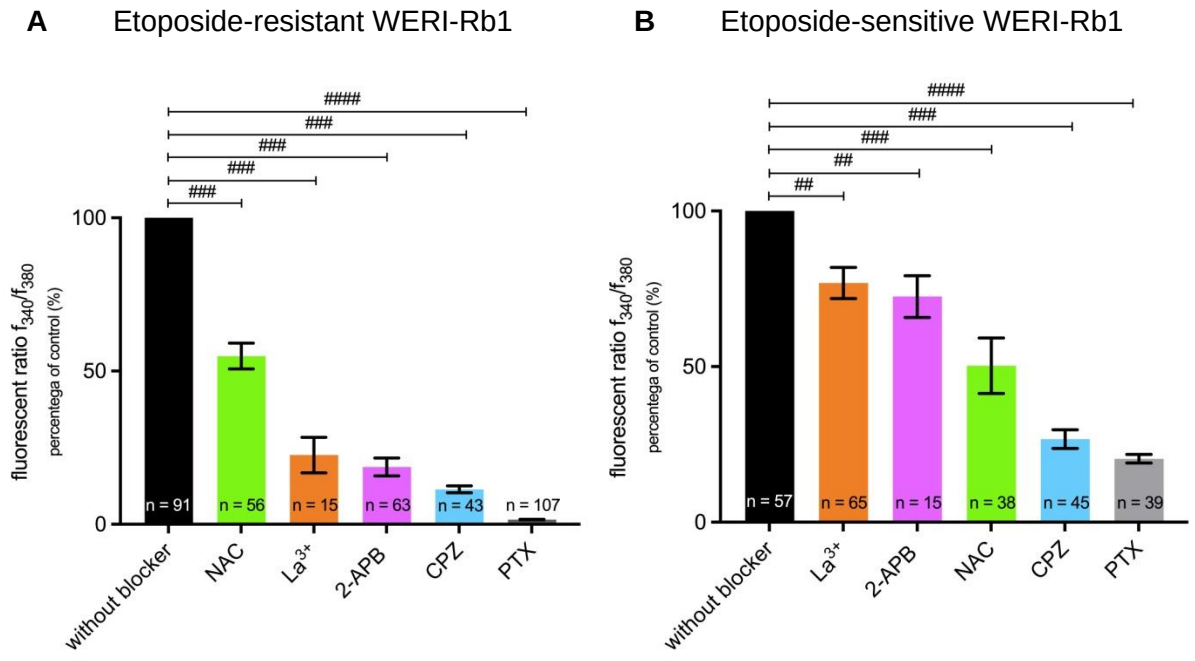

Fig. 4. TRP-channel inhibitors (NAC, La^{3+}, 2-APB, and CPZ) and Gi/o blocker (PTX) suppress Asc-mediated Ca^{2+} influx in WERI-Rb1 cell lines (results at t = 300 s). a) Summary of the inhibitory effects of: 10 mM NAC, 500 µM La^{3+}, 100 µM 2-APB, 100 µM CPZ and 50 ng/ml PTX in etoposide-resistant WERI-Rb1 cells presented as percentage of control (without blocker). The

hashtags (#) indicate significant differences in percentages of fluorescence ratios ($f_{340/380}$) (unpaired tested). **b)** The same summary as in (**a**) but with etoposide-sensitive WERI-Rb1 cells. Figure modified after Oronowicz et al. [1].

3.3 TRP-mediated rises in Ca^{2+} influx are suppressed by PTX

Asc is a modulator of aminergic GPCRs [81]. Owing to the fact that GPCRs and TRPs are on a linked signaling pathway axis [38], the effect was investigated of PTX, which is a GPCR blocker, on Asc-induced influx of Ca^{2+}. To suppress GPCRs, cells were preincubated with PTX (50 ng/ml) for 18 hours [81-83].

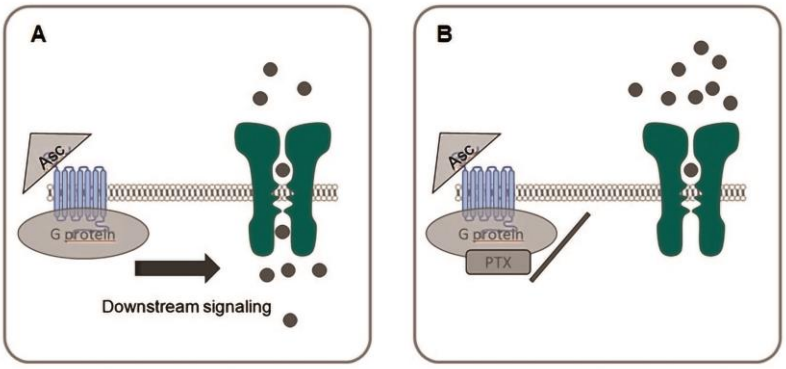

Fig. 5. PTX effect on TRP channels - schematic depiction. Co-expressed GPCRs (blue) and TRPs (green) can be described as a functional GPCR-TRP axis. Accordingly, GPCRs can impact the responses of TRPs and vice versa [38]. **a)** Asc is a well-known aminergic GPCR modulator [81] and can enhance the activity of these receptors, triggering the TRP channel activity. **b)** PTX is an GPCR inhibitor. Specifically, it can ribosylate the Gi/o proteins [83], leading to the suppression of TRP channel activity. Figure by Oronowicz et al. [1].

Like the TRP channel blockers, PTX was even more effective than any of them at suppressing the Asc-induced increases in Ca^{2+} influx (Fig. 4A-B). More specifically, the f_{340}/f_{380} fluorescence ratio in etopoiside-resistant WERI-Rb1 cells was suppressed to 1.55 ± 0.1 $\%_{e\text{-}r}$ (0.1038 ± 0.0003) (t = 300 s; n = 107; p < 0.0001) (Fig. 4A), while in etoposide-sensitive counterpart to 20.4 ± 1.4 $\%_{e\text{-}s}$ (0.1027 ± 0.0002) (t = 300 s; n = 39; p < 0.0001) (Fig. 4B). These large inhibitory effects of PTX are supportive of the involvement of GPCR-TRP signaling axis in mediating Asc-induced increases in Ca^{2+} influx in both cell types [1, 38].

3.4 Dependence of Asc-induced intracellular Ca^{2+} level increases on rises in plasma membrane Ca^{2+} influx

The source was determined of Asc-induced rises in intracellular Ca^{2+} levels by evaluating the effect of Asc on this response in a Ca^{2+}-free conditions (in a bathing solution containing 1 mM EGTA). The procedure included two phases. Specifically the Ca^{2+}-containing bathing solution was substituted with the Ca^{2+}-free bathing solution. In the second step, 1 mM Asc was added. Interestingly, in both WERI-Rb1 groups of cells similar changes occurred. In the etoposide-resistant RB cells, the f_{340}/f_{380} ratio decreased after the first step to 0.0865 ± 0.0018 (t = 60 s before Asc addition; n = 11), as expected. Extracellular application of Asc (1 mM) did not show any effect on the Ca^{2+} increase (0.0766 ± 0.0021 at t = 180 s after Asc addition; n = 11; $p < 0.0001$) (Fig. 6A). Similar results were obtained in the etoposide-sensitive counterpart. After the first stage, the f_{340}/f_{380} ratio decreased to 0.0924 ± 0.0013 (t = 60 s before Asc addition; n = 12). Furthermore, it was lowered to 0.0909 ± 0.0014 (t = 180 s after Asc addition; n = 12; $p < 0.0001$), after 1 mM Asc supplementation (Fig. 6B). To sum up, Asc had no effect in a Ca^{2+}-free external measuring solution suggesting that the Asc-induced Ca^{2+} increase is solely attributable to the activation of plasma membrane delimited pathways and Ca^{2+} influx, regardless of possible intracellular Ca^{2+} stores modulation [1].

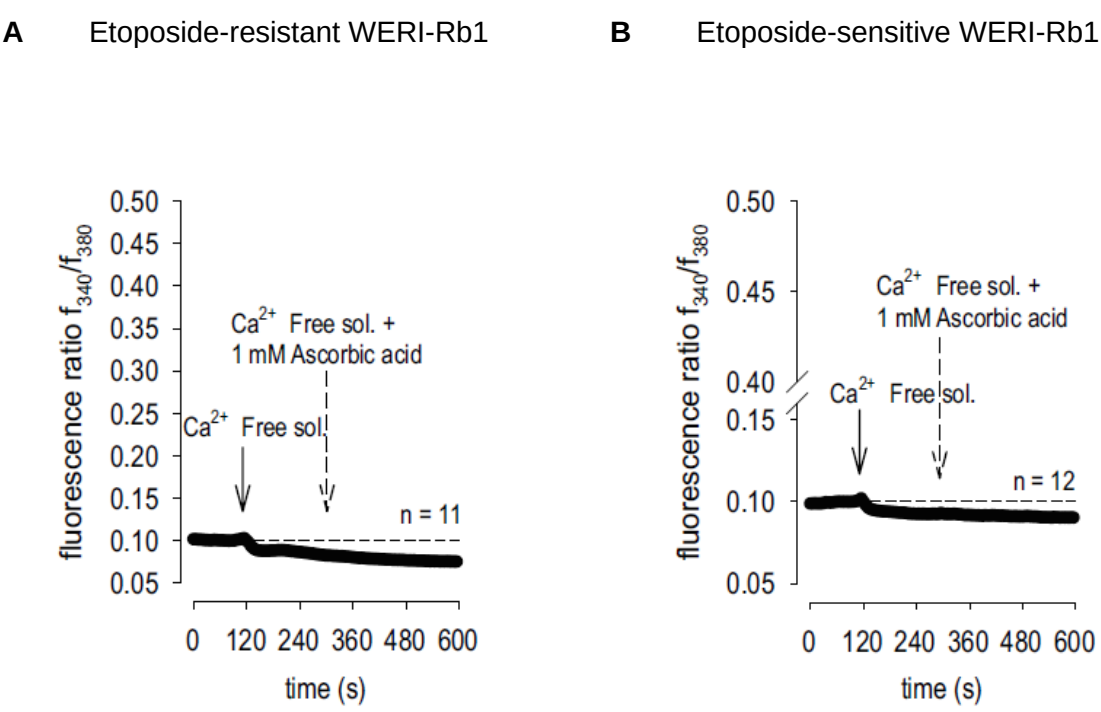

Fig. 6. Extracellular Ca^{2+} is needed for Asc-induced intracellular Ca^{2+} increase. a/b) 1 mM Asc supplementation under Ca^{2+}-free external conditions had no effect on Ca^{2+} regulation in etoposide-resistant and-sensitive WERI-Rb1 cells. Figure by Oronowicz et al. [1].

3.5 Asc leads to whole-cell currents increases in WERI-Rb1 cells

Whole-cell currents were measured to ascertain whether TRPs activity on the cell membrane corresponds with Ca^{2+} influx. Accordingly, a voltage stimulation ramp from −60 to +130 mV was used to monitor current responses with and without Asc (1 mM) in both RB cell lines.

Interestingly, the results presented in Figure 7 were very similar to one another in both WERI-Rb1 cells. The inward current density (pA/pF) increased respectively: in etoposide-resistant WERI-Rb1 from -25 ± 2 pA/pF to -81 ± 8 pA/pF ($n = 16$; $p < 0.0005$) and in the etoposide-sensitive counterpart from -24 ± 2 pA/pF to -66 ± 4 pA/pF ($n = 19$; $p < 0.0001$). An analogous trend could be observed regarding the outward current densities, which also rose: in the etoposide-resistant WERI-Rb1 cells

from 397 ± 38 pA/pF to 529 ± 51 pA/pF (n = 16; p < 0.0001) and in the etoposide-sensitive cell line from 309 ± 23 pA/pF to 464 ± 34 pA/pF (n = 19; p < 0.0005).

In summary, the correspondence between the Asc-mediated whole-cell currents increases and Ca^{2+} influx confirm that increases in plasma membrane ionic currents underlie these responses [1].

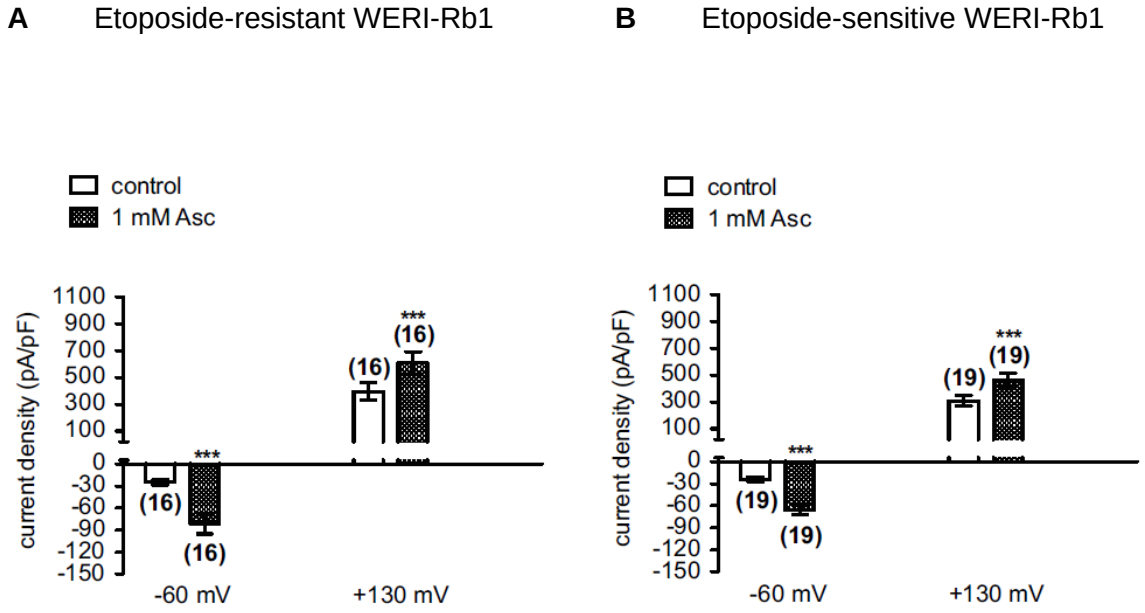

Fig. 7. Increases in whole-cell currents induced by 1 mM Asc supplementation in both etoposide-resistant and -sensitive WERI-Rb1 cells. a) Summarized patch-clamp control experiments with 1 mM Asc addition in etoposide-resistant WERI-Rb1 cells (*n* = 16). Asc led to an increase of whole-cell currents (filled columns) compared to control currents (open columns). The asterisks (*) indicate statistical significance of whole-cell currents increase after supplementation with 1 mM Asc (paired tested). **b)** Summary corresponding to (**a**) but in the etoposide-sensitive WERI-Rb1 cell line (*n* = 19). Figure by Oronowicz et al. [1].

3.6 Asc-induced whole-cell currents increases are suppressed by TRP channel inhibitors

The effects of three different broad spectrum Ca^{2+} channel inhibitors on Asc (1 mM)-induced rises in whole-cell currents in both types of WERI-Rb1 cells were evaluated.

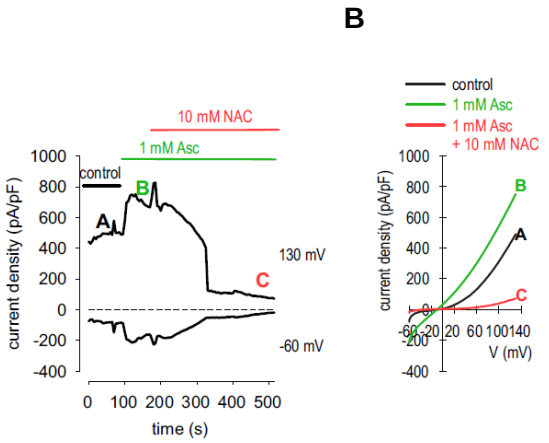

Fig. 8. Asc-mediated increases in whole-cell currents are inhibited by NAC. Representative electrophysiological measurement in etoposide-resistant WERI-Rb1 cells (1/2). a) Time course recording of the whole-cell currents changes (Asc-triggered increase and NAC-mediated decrease). **b)** Current/voltage plot (I-V plot) under control conditions (black trace labeled as A), during 1 mM Asc application (green trace labeled as B) and following 10 mM NAC addition (red trace labeled as C). The current densities were normalized by dividing the currents by the membrane capacitance (pA/pF). The recordings were selected from the traces shown in (**a**). Figure by Oronowicz et al. [1].

The inward currents in etoposide-resistant WERI-Rb1 were decreased by: CPZ to 31.9 ± 10.4 $\%_{e\text{-}r}$ (n = 5; p < 0.05), La^{3+} to 27.8 ± 7.2 $\%_{e\text{-}r}$ (n = 4; p < 0.05) and NAC to 22.2 ± 11.2 $\%_{e\text{-}r}$ (n = 5; p < 0.05) (Fig. 8/9/10A). Comparable effects were observed in etoposide-sensitive RB cells. The inward currents were lowered by: CPZ to 43.3 ± 6.6 $\%_{e\text{-}s}$ (n = 6; p < 0.005), La^{3+} to 34.3 ± 8.4 $\%_{e\text{-}s}$ (n = 7; p < 0.0005) and NAC to 11.5 ± 3.6 $\%_{e\text{-}s}$ (n = 5; p < 0.0005) (Fig. 10B).

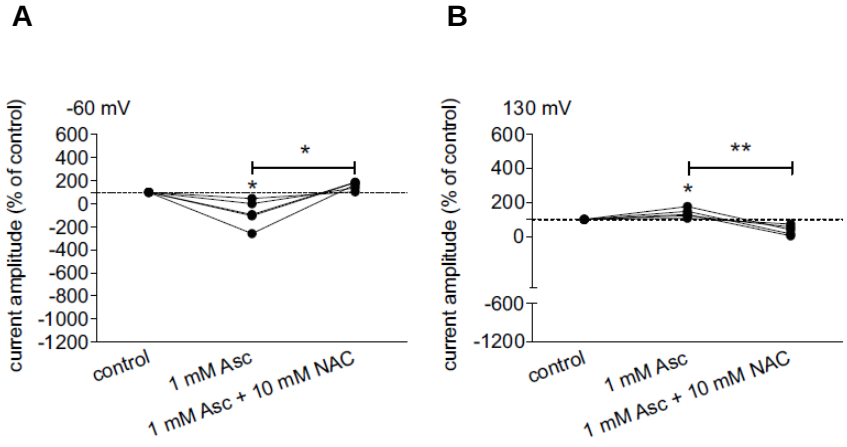

Fig. 9. Asc-mediated increases in whole-cell currents are inhibited by NAC. Representative electrophysiological measurement in etoposide-resistant WERI-Rb1 cells (2/2). a) Inward currents measured after a voltage stimulation from 0 mV to −60 mV without steps before supplementation of drugs (control set to 100%) and in the presence of Asc/NAC. NAC was able to suppress the Asc-induced increase of whole-cell inward currents. **b)** Identical diagram as in (**a**) but the outward currents

after a voltage stimulation from 0 mV to +130 mV are presented. The asterisks (*) indicate significantly increased inward/outward currents after 1 mM Asc addition and suppressed inward/outward currents after the supplementation of 10 mM NAC (paired tested). Figure by Oronowicz et al. [1].

The outward currents were also suppressed with similar efficacy of all TRP blockers. In etoposide-resistant WERI-Rb1, these currents were inhibited by: CPZ to 51.0 ± 13.6 $\%_{e\text{-}r}$ (n = 5; p > 0.05), La^{3+} to 48.5 ± 9.7 $\%_{e\text{-}r}$ (n = 4; p < 0.05) and NAC to 29.5 ± 11.7 $\%_{e\text{-}r}$ (n = 5; p < 0.05) (Fig. 8/9/10A). Similar effects were obtained in the etoposide-sensitive RB cells, in which the outward currents were diminished by: CPZ to 70.5 ± 7.3 $\%_{e\text{-}s}$ (n = 6; p > 0.05), by La^{3+} to 52.9 ± 7.3 $\%_{e\text{-}s}$ (n = 7; p < 0.005) and by NAC to 24.6 ± 4.1 $\%_{e\text{-}s}$ (n = 5; p < 0.005) (Fig. 10B). Overall, the TRP blockers-mediated suppression of Ca^{2+} influxes indicates that the obtained Asc-induced effects are due to the TRPs activation on the cell membrane [1].

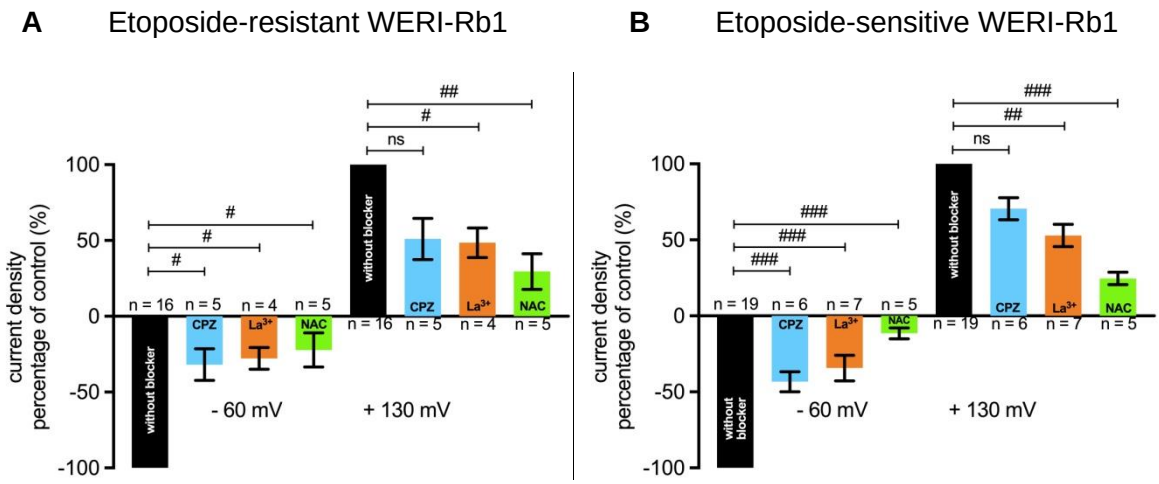

Fig. 10. Asc-mediated increase in whole-cell currents are suppressed by different TRP channel blockers (CPZ, LA^{3+}, NAC) in both etoposide-resistant and -sensitive WERI-Rb1 cells. a) Summarized patch-clamp measurements after extracellular application of 1 mM Asc and TRP channel antagonists (100 µM CPZ, 500 µM La^{3+}, 10 mM NAC) in etoposide-resistant WERI-Rb1. The hashtags (#) indicate significance of the whole-cell current decreases after antagonist supplementation (unpaired tested). ns - not significant (unpaired tested). **b)** Summary corresponding to (**a**) but in the etoposide-sensitive WERI-Rb1 cell line. Figure modified after Oronowicz et al. [1].

3.7 Medium acidification leads to a minor Asc-mediated Ca^{2+} increase

As Asc is a weak acid in solution, it lowered the pH of a bathing solution at room temperature ~ 20 – 23°C from ~7.35 to ~7.15. Since the activity of different TRPs could be pH sensitive, we determined whether this slight acidification accounts for the effects of Asc-stimulated Ca^{2+} influx. Accordingly, the effect of medium acidification with HCl was used to mimic the Asc-induced pH decline. As a result, a slight increase of the f_{340}/f_{380} ratio in both groups of WERI-Rb1 cells could be observed. More specifically, the fluorescence ratio in etoposide-resistant WERI-Rb1 cells increased from 0.1004 ± 0.0001 to 0.1073 ± 0.0008 (t = 300 s; n = 39; p < 0.0001), while in etoposide-sensitive counterpart it rose from 0.0999 ± 0.0001 to 0.1033 ± 0.0004 (t = 300 s; n = 37; p < 0.0001) (Fig. 3). These effects of HCl on the f_{340}/f_{380} ratio did not mimic the much larger increases induced by Asc suggesting that Asc does not induce this response as a consequence of medium acidification [1].

3.8 Asc inhibits the viability of WERI-Rb1 cells

As pharmacological doses of Asc induce cytotoxicity through acting as an oxidant, we evaluated its effects on both etoposide-resistant and etoposide-sensitive WERI-Rb1cell viability. One approach was to compare the effects of exposure to 1 mM Asc on cell density. The density of initially confluent layers had declined (Fig. 11A/B; 11F/G) compared to untreated cells (Fig. 11B vs D; 11G vs I) by the fifth day after Asc incubation, in both WERI-Rb1 cell lines. A partial recovery was observed after lowering the medium Asc concentration through dilution. Nevertheless, these revived cell populations lost their ability to expand by forming clusters as they normally do in an untreated cell culture (Fig. 11C vs D; 11H vs I). A following set of experiments

shows the impact of 1 mM Asc on already grown culture (four days after centrifugation). The confluent RB cultures, treated with Asc, fell apart while the cell density continuously declined in both WERI-Rb1 cell lines (Fig. 11D/E; 11I/J).

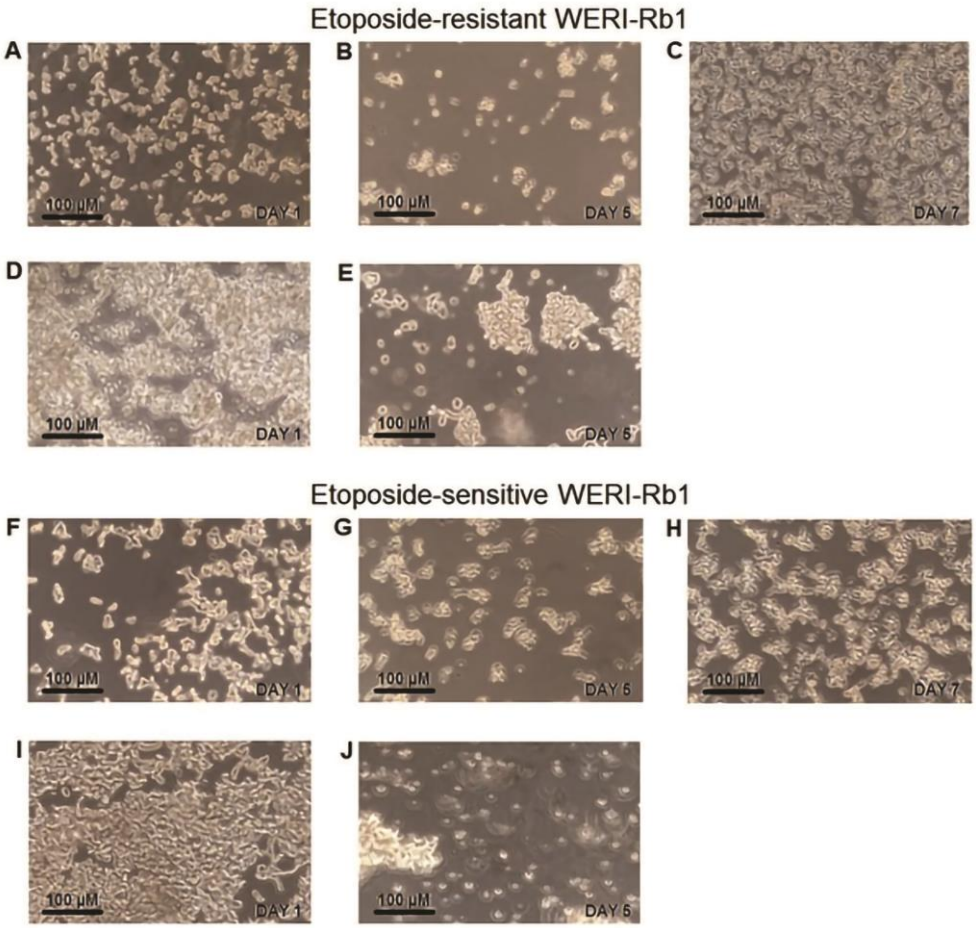

Fig. 11. 1 mM Asc decreases the growth and density of RB cell culture (a–e - etoposide-resistant WERI-Rb1 cells; f–j - etoposide-sensitive WERI-Rb1 cells). Light microscopic images. Asc was added to the new-passaged **(a)** group of etoposide-resistant RB cells. After four days, a reduced cell density was observed **(b)** and the medium was diluted with RPMI-1640. On the seventh day, an increase of cell density could be observed **(c)**. The second set of experiments in this group presents the cells, which were cultured for four days without 1mM Asc **(d)**. Asc was supplemented after the evaluation of cell culture and the reduced cell density was observed after another four days **(e)**. **f–j)** present the etoposide-sensitive WERI-Rb1 cells which underwent the same observations as their etoposide-resistant counterpart (**a**–**e**). Similarly, treatment with 1 mM Asc led to decreases in cell density that was partially recoverable following medium dilution. Figure by Oronowicz et al. [1].

These observations regarding Asc-induced cytotoxicity prompted us to determine the dependence of changes in cell density and viability. The cytotoxic effects were

evaluated on viability based on the results of the Trypan Blue dye exclusion of freshly diluted WERI-Rb1 cells after four days of 1 mM Asc incubation (Fig. 12). This high dose of ascorbate decreased the survivability of both groups of WERI-Rb1 cells. The percentage of dead cells rose from 6.1 ± 0.6% (n = 8) (Fig. 12A) (in the untreated group) to 93.7 ± 1.5% (n = 16) (p = 0.0001) in the group supplied with 1 mM Asc (Fig. 12B). The percentage of dead cells in the etoposide-sensitive counterpart also rose from 5.8 ± 1.0% (n = 8) to 93.9 ± 1.3% (n = 16) (p = 0.0001), respectively (Fig. 12C vs D).

Overall, 1 mM Asc had cytotoxic effects in both etoposide-resistant and -sensitive WERI-Rb1 cell lines [1].

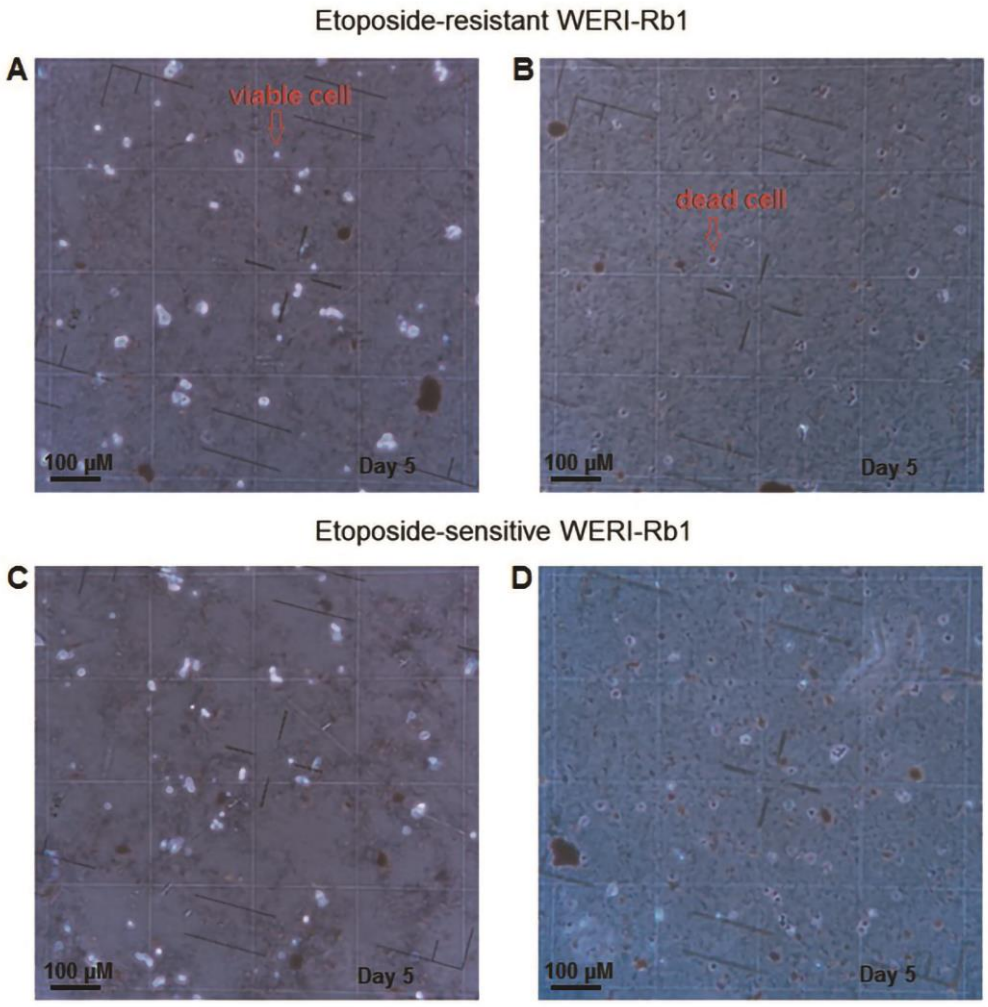

Fig. 12. RB cell viability can be suppressed by 1 mM Asc. The comparison of cytotoxic effects of Asc in both WERI-Rb1 cell lines, using Trypan Blue dye exclusion method. Neubauer counting chamber (divided into equal fields) can be seen in the background. Light microscopic images. **a)** The etoposide-resistant WERI-Rb1 control group of cells can be seen. Large majority of the cells seem bright (e.g., marked with an arrow)—viable cells that were not stained with the Trypan Blue dye. **b)** The etoposide-resistant WERI-Rb1 cells after four days of 1 mM Asc treatment. Most visible cells seem dark (e.g., marked with an arrow)—dead cells stained with the Trypan Blue dye. **c/d)** present the etoposide-sensitive WERI-Rb1 cells which underwent the same experiment as their etoposide-resistant counterpart (**a**, **b**). Figure by Oronowicz et al. [1].

4 DISCUSSION

This study demonstrates the cytotoxic effects of 1 mM Asc on etoposide-resistant and -sensitive WERI-Rb1 cells. Irrespective of a difference in etoposide sensitivity, a pharmacological dose of Asc decreased cell viability in both cell lines. It was presumably due to GPCR-dependent activation of TRPs followed by increases in intracellular Ca^{2+} influx from the external bathing solution suggesting the involvement of a so-called GPCR-TRP signaling pathways axis in mediating this response [38]. Notably, the prooxidative effects of Asc could be responsible for its cytotoxicity since millimolar doses of this agent were reported to reduce cell viability [2, 18]. Furthermore, this study agrees with some other analyses which described the oxidation-dependent cytotoxic effects of pharmacological doses of Asc in different cell lines [5, 9, 13].

4.1 Role of TRP channels

Based on the assumption that Asc (1 mM) treatment induces cell death through creating oxidative stress, the involvement was evaluated of the different TRP subtypes known to be oxidation-sensitive. Therefore, this study was undertaken to investigate the following oxidative stress sensitive TRP subtype channels: TRPA1

[22, 23]; TRPC5 [24, 25]; TRPM2 [26]; TRPM7 [28]; TRPV4 [1, 27]. These TRPs are important not only because of their sensitivity to oxidative stress but also due to some other properties which allow them to play a significant role in cell growth processes (in RB: TRPM7) [55]. Furthermore, TRPV1 and TRPM8 were considered as important factors in tumorigenesis [84]. Both genetic and functional expression levels of aforementioned channels were investigated in etoposide-resistant and -sensitive WERI-Rb1 cells. qRT-PCR data were kindly provided by Jacqueline Reinhard-Recht from Ruhr University Bochum-Germany. The results revealed a TRP channel gene expression pattern similar to those identified in previous reports [54, 55]. A downregulation in gene expression levels of TRPV1, TRPV4, TRPM8, TRPM2, TRPC5 and TRPA1could be observed in the etoposide-resistant WERI-Rb1 cells. Besides, the gene expression levels of TRPM7 were similar in both RB cell lines [1]. To determine the pathways of Asc-mediated effects, selective TRP channel inhibitors and broad spectrum Ca^{2+} channel blockers were used (already characterized in methods).

4.2 Possible mechanisms of TRP channel activation by Asc

Various tumor cells are escaping sensitivity to pharmacological treatment through spontaneous mutations, gaining resistances. This study was undertaken to investigate whether the pharmacological doses of Asc can trigger any TRP-dependent cytotoxic effects and if these responses are different in etoposide-resistant and -sensitive WERI-Rb1 cells. Surprisingly, the results of control measurements clarified that the etoposide-resistant cells are more sensitive to 1 mM Asc than their etoposide-sensitive counterpart (Fig. 3). The contribution of TRPs to these effects was demonstrated, showing that extracellular application of different

TRP/Ca^{2+} channel blockers inhibited the Asc-mediated increases in Ca^{2+} influx (Fig. 4). Knowing that Asc can trigger aminergic GPCRs [81], the RB cells were pretreated with PTX, a widely-used Gi/o blocker, to verify whether Asc interaction with GPCR accounts for the TRP-mediated Ca^{2+} responses. This hypothesis was confirmed since Asc did not induce a significant intracellular Ca^{2+} increase in the presence of the aforementioned blocker (Fig. 4). Therefore, inhibition of the GPCR-TRP signaling pathway axis accounts for how Asc induces responses in etoposide-resistance and -sensitive WERI-Rb1 cell lines [38].

Intracellular Ca^{2+} increase can arise from increases in plasma membrane Ca^{2+} influx as well as the release of Ca^{2+} from intracellular stores. In the current study, Asc-induced increases in intracellular Ca^{2+} influx are solely ascribable to increases from the external medium since Ca^{2+} omission from the bathing solution blocked Asc-induced rises in intracellular Ca^{2+} levels (Fig. 6).

To support this conclusion, patch-clamp experiments were performed. Whole-cell currents were measured in the presence of Asc and Ca^{2+} channel antagonists. Outward and inward currents increased after 1 mM Asc application and were suppressed after supplementation with different TRP channel blockers in both WERI-Rb1 cell groups, similarly. The relation between the effects of channel blockers on whole-cell currents and intracellular Ca^{2+} transients confirms that increases in Ca^{2+} influx across TRPs on the plasma membrane accounts for the currents induced by Asc (Fig. 7-10).

Most of our findings suggest the involvement of TRPs in Asc-induced intracellular Ca^{2+} increases. However, certain mechanisms are not clear. Therefore, it is suggested that one of the trigger factors which activate TRPs could be the increased

generation of H_2O_2, which is caused by the oxidation-mediated mechanisms of high Asc doses, as suggested by other authors [85-88].

Medium acidification by Asc was ruled out as a mediator of Asc -induced intracellular Ca^{2+} transients since mimicking the Asc medium acidification from ~7.35 to ~7.15 failed to mimic the larger increases in intracellular Ca^{2+} influx induced by Asc. Nevertheless, this pH decline had a relatively negligible impact on the Ca^{2+} influx in both WERI-Rb1 cell groups. The observed results were minimal in comparison to Asc-induced effects (Fig. 3). Furthermore, knowing that the reported values of medium pH which triggered TRP-induced currents were below 6.0, it is unlikely that the obtained increases in Ca^{2+} influx were caused by a slight pH acidification [89-91]. These observations are consistent with the results of Garrity *et al*., who reported that primary reason for pH-dependent TRP responses were not extracellular pH changes [92].

The lack of correspondence between the functional and genetic TRP expression levels in both WERI-Rb1 cell lines was obtained. Such discrepancy may be attributable to variability in mRNA turnover caused by modulation of other factors. It is conceivable that instead a closer correlation between protein functional activity and expression levels exists. This supposition can be supported because the level of mRNA expression frequently occurs quicker than protein expression turnover.

4.3 Cytotoxic effects of Asc lead to reduced RB cell viability

Cytotoxicity induced by 1 mM Asc was confirmed based on decreases in Trypan Blue exclusion experiments in etoposide-resistant and -sensitive WERI-Rb1 cells. Such declines in cell viability of almost 94% after 4 days were consistent with similar falls in cell density (Fig. 11/12). The current study focused only on the roles of Ca^{2+}-

dependent pathways in mediating Asc-induced cytotoxicity. Even though they contribute to controlling tumorigenesis there are other possible cytotoxicity-inducing mechanisms that should be considered. In any case, the observed effects are similar to those obtained by Chen *et al*., who described the reduction of cell viability in ascorbate-treated cells [5].

Asc-generated H_2O_2 was reported to be the main factor that compromises cell viability [2, 18]. It should be considered as the central redox agent modulating oxidative pathways [13, 93, 94]. Other studies support this thesis by showing that primarily the extracellular concentration of H_2O_2 led to cell death [12]. This could explain why a high intracellular concentration of Asc does not protect the cells from tumorigenic processes. Although oxidative stress could be the main factor that limited cell viability, other supportive mechanisms such as glutathione depletion should be considered [18]. Most of the Asc-mediated oxidative-dependent effects can result from disruption of mitochondrial function [26]. H_2O_2-induced response was observed in podocytes [95] and Asc-dependent ROS-modulated cell death was reported in thyroid cancer cells [96]. Analogous but oxidative stress-independent effects were obtained in retinal ganglion or breast cancer cells [97, 98]. One of the pathways that can lead to cell apoptosis regardless of H_2O_2 levels is autophagy-associated caspase-independent axis [99].

However, the mechanisms affecting the viability of RB cells are not elucidated so far. Follow-up studies may determine if other viability decreasing mechanisms described in different tumor cells can also underlie the Asc-induced cytotoxicity in WERI-Rb1 cell lines.

4.4 Clinical relevance

Nowadays, the number of patients afflicted with hardly curable tumors is still increasing [100]. Therefore, the development of multiple kinds of anti-cancer cures becomes even more important. Accordingly, one of the effective methods can be a supportive usage of pharmacological doses of Asc, as reported in many studies that dealt with different tumorigenic cell types [5, 9, 11-13, 18, 99, 101].

At this point, Riordan et al. conducted one of the most meaningful clinical studies up until now. They developed a method of high dosage Asc intravenous administration - "Riordan therapy" [2]. It delimited the relationship between peak- and average Asc plasma concentration and assigned a target level which should result in anti-cancer effects. Primarily, the prooxidative effects of Asc followed by an increase in H_2O_2 levels are responsible for reducing the expansion of cancer cells [2, 18]. H_2O_2-dependent cell death is the central point in most of the aforementioned studies. So far, none of them described any involvement of TRP-related pathways. The possible contribution of TRPs is important since they are associated with many oncogenic mechanisms [102, 103]. Moreover, the role of the Ca^{2+}-permeable channels seems to be crucial as they are responsible for maintaining the Ca^{2+} homeostasis, an important factor which controls different cellular processes i.e. apoptosis [48, 51, 104]. This study shows that Asc-induced cytotoxicity in WERI-Rb1 cells could be mediated by GPCR-TRP-related pathways, resulting in increased transmembrane Ca^{2+} influx [1].

Investigating the interaction between Asc and TRPs is reasonable since they both were reported to play a role in anti-tumor therapies. High doses of ascorbate can sensitize the cells to radio/chemotherapeutic agents or have synergistic effects with them [105-107]. On the other hand, modulating certain TRPs can be used in imaging or therapies [108, 109]. Therefore, our description of a dependence of Asc-induced

cytotoxicity on TRPs activation suggests novel targets for improved therapeutic management of tumorigenesis.

Since the obtained effects of 1 mM Asc in RB cells were significant in the etoposide-resistant WERI-Rb1 cell line, Asc could be considered as a possible adjuvant to develop numerous cures of tumors resistant to common therapies [1].

4.5 Outlook and Limitations

Improving the efficacy of anti-cancer therapies and understanding their mechanisms of action is an ongoing challenge. The impact of this study may be far reaching if follow-up studies are undertaken to clarify the dependence between genetic and functional expression of TRPs in tumor cells. Future experiments should also focus on the efficacious Asc concentration ranges, to provide more desirable therapeutic management of tumorgenesis without any side effects. The effects of pharmacological concentration of Asc should also be investigated in other types of RB cell lines to determine if ascorbate is able to overcome different resistances. We cannot ignore the possible incongruence between our *in vitro* and eventual future *in vivo* studies. Such inconsistency in effects of Asc was already observed in other cells [110].

In order to ensure the highest possible level of significance every effort has been undertaken but some limitations that occurred during this study should be mentioned. One of them was cell cultivation itself, since we cannot exclude that minor differences in a cell passage characteristics could have an impact on how the RB cells reacted during different experiments. Furthermore, the measurements included different number of cells, because of their density, vitality and growth phase. Moreover, some data were scattered, which may have been due to the difficulties in the calibration of

signal-noise ratio of the calcium imaging set-up. Many effects of Asc were unambiguous, but there were also some outliers. This variance could have many reasons. One of them could be a polymodal TRP channel characteristics, which means that they are sensitive to lot of different environmental stimuli. Pipetting, pump suction and room temperature could influence either mechano- or thermosensitive activation [111].

The temperature could impact not only TRP channel activation but also affect Fura-2/AM properties. Besides, this dye is also vulnerable to the high light exposure, which could lead to dye bleaching. Therefore, all measurements were performed in a darkened room, at a constant room temperature ~ 20 – 23°C. Another limitation was a concentration of the dye since it is known that the interaction of Fura-2/AM with Ca^{2+} can have an impact on cell metabolism [112].

Moreover, we have to mention the ability of RB cells to group/sediment rapidly, which interfered with patch-clamp measurements stability.

A minor limitation occurred by counting the cells in dye exclusion viability experiments. The cells were counted only by one person but multiple times.

The last limitation was the cell type. All experiments were performed with only one validated RB (WERI-Rb1) cell line. Although the relationship between Asc and the viability of another group of RB cells (Y-79) was reported, the measurements should be repeated with some different cell lines to obtain more definitive results [6].

REFERENCES

1. Oronowicz, J., J. Reinhard, P.S. Reinach, S. Ludwiczak, H. Luo, M.H. Omar Ba Salem, M.M. Kraemer, H. Biebermann, V. Kakkassery, and S. Mergler, *Ascorbate-induced oxidative stress mediates TRP channel activation and cytotoxicity in human etoposide-sensitive and -resistant retinoblastoma cells.* Lab Invest, 2020.
2. Riordan, N.H., H.D. Riordan, X. Meng, Y. Li, and J.A. Jackson, *Intravenous ascorbate as a tumor cytotoxic chemotherapeutic agent.* Med Hypotheses, 1995. **44**(3): p. 207-13.
3. Riordan, H.D., N.H. Riordan, J.A. Jackson, J.J. Casciari, R. Hunninghake, M.J. González, E.M. Mora, J.R. Miranda-Massari, N. Rosario, and A. Rivera, *Intravenous vitamin C as a chemotherapy agent: a report on clinical cases.* P R Health Sci J, 2004. **23**(2): p. 115-8.
4. Riordan, H.D., J.J. Casciari, M.J. González, N.H. Riordan, J.R. Miranda-Massari, P. Taylor, and J.A. Jackson, *A pilot clinical study of continuous intravenous ascorbate in terminal cancer patients.* P R Health Sci J, 2005. **24**(4): p. 269-76.
5. Chen, Q., M.G. Espey, A.Y. Sun, C. Pooput, K.L. Kirk, M.C. Krishna, D.B. Khosh, J. Drisko, and M. Levine, *Pharmacologic doses of ascorbate act as a prooxidant and decrease growth of aggressive tumor xenografts in mice.* Proc Natl Acad Sci U S A, 2008. **105**(32): p. 11105-9.
6. Roomi, M.W., N. Roomi, B. Bhanap, A. Niedzwiecki, and M. Rath, *Antineoplastic activity of a nutrient mixture in Y-79 malignant retinoblastoma cells.* Oncol Rep, 2013. **29**(1): p. 29-33.
7. Ma, E., P. Chen, H.M. Wilkins, T. Wang, R.H. Swerdlow, and Q. Chen, *Pharmacologic ascorbate induces neuroblastoma cell death by hydrogen peroxide mediated DNA damage and reduction in cancer cell glycolysis.* Free Radic Biol Med, 2017. **113**: p. 36-47.
8. Mikirova, N., N. Riordan, and J. Casciari, *Modulation of Cytokines in Cancer Patients by Intravenous Ascorbate Therapy.* Med Sci Monit, 2016. **22**: p. 14-25.
9. Padayatty, S.J., H.D. Riordan, S.M. Hewitt, A. Katz, L.J. Hoffer, and M. Levine, *Intravenously administered vitamin C as cancer therapy: three cases.* CMAJ, 2006. **174**(7): p. 937-42.
10. Polireddy, K., R. Dong, G. Reed, J. Yu, P. Chen, S. Williamson, P.C. Violet, Z. Pessetto, A.K. Godwin, F. Fan, M. Levine, J.A. Drisko, and Q. Chen, *High Dose Parenteral Ascorbate Inhibited Pancreatic Cancer Growth and Metastasis: Mechanisms and a Phase I/IIa study.* Sci Rep, 2017. **7**(1): p. 17188.
11. Uetaki, M., S. Tabata, F. Nakasuka, T. Soga, and M. Tomita, *Metabolomic alterations in human cancer cells by vitamin C-induced oxidative stress.* Sci Rep, 2015. **5**: p. 13896.
12. Chen, Q., M.G. Espey, M.C. Krishna, J.B. Mitchell, C.P. Corpe, G.R. Buettner, E. Shacter, and M. Levine, *Pharmacologic ascorbic acid concentrations selectively kill cancer cells: action as a pro-drug to deliver hydrogen peroxide to tissues.* Proc Natl Acad Sci U S A, 2005. **102**(38): p. 13604-9.

13. Frei, B. and S. Lawson, *Vitamin C and cancer revisited.* Proc Natl Acad Sci U S A, 2008. **105**(32): p. 11037-8.
14. Hoffer, L.J., M. Levine, S. Assouline, D. Melnychuk, S.J. Padayatty, K. Rosadiuk, C. Rousseau, L. Robitaille, and W.H. Miller, *Phase I clinical trial of i.v. ascorbic acid in advanced malignancy.* Ann Oncol, 2008. **19**(11): p. 1969-74.
15. Jacob, R.A. and G. Sotoudeh, *Vitamin C function and status in chronic disease.* Nutr Clin Care, 2002. **5**(2): p. 66-74.
16. Geeraert, L., *Intravenous high-dose vitamin C*. 2014, CAM-Cancer Consortium: http://cam-cancer.org/en/high-dose-vitamin-c.
17. Brubaker, R.F., W.M. Bourne, L.A. Bachman, and J.W. McLaren, *Ascorbic acid content of human corneal epithelium.* Invest Ophthalmol Vis Sci, 2000. **41**(7): p. 1681-3.
18. Du, J., J.J. Cullen, and G.R. Buettner, *Ascorbic acid: chemistry, biology and the treatment of cancer.* Biochim Biophys Acta, 2012. **1826**(2): p. 443-57.
19. Hediger, M.A., *New view at C.* Nat Med, 2002. **8**(5): p. 445-6.
20. Calero, C.I., E. Vickers, G. Moraga Cid, L.G. Aguayo, H. von Gersdorff, and D.J. Calvo, *Allosteric modulation of retinal GABA receptors by ascorbic acid.* J Neurosci, 2011. **31**(26): p. 9672-82.
21. Vissers, M.C.M. and A.B. Das, *Potential Mechanisms of Action for Vitamin C in Cancer: Reviewing the Evidence.* Front Physiol, 2018. **9**: p. 809.
22. Andersson, D.A., C. Gentry, S. Moss, and S. Bevan, *Transient receptor potential A1 is a sensory receptor for multiple products of oxidative stress.* J Neurosci, 2008. **28**(10): p. 2485-94.
23. Hill, K. and M. Schaefer, *Ultraviolet light and photosensitising agents activate TRPA1 via generation of oxidative stress.* Cell Calcium, 2009. **45**(2): p. 155-64.
24. Yamamoto, S., N. Takahashi, and Y. Mori, *Chemical physiology of oxidative stress-activated TRPM2 and TRPC5 channels.* Prog Biophys Mol Biol, 2010. **103**(1): p. 18-27.
25. Pires, P.W. and S. Earley, *Redox regulation of transient receptor potential channels in the endothelium.* Microcirculation, 2017. **24**(3).
26. Wang, Q., L. Huang, and J. Yue, *Oxidative stress activates the TRPM2-Ca(2+)-CaMKII-ROS signaling loop to induce cell death in cancer cells.* Biochim Biophys Acta Mol Cell Res, 2017. **1864**(6): p. 957-967.
27. Bai, J.Z. and J. Lipski, *Involvement of TRPV4 channels in Aβ(40)-induced hippocampal cell death and astrocytic Ca(2+) signalling.* Neurotoxicology, 2014. **41**: p. 64-72.
28. Abiria, S.A., G. Krapivinsky, R. Sah, A.G. Santa-Cruz, D. Chaudhuri, J. Zhang, P. Adstamongkonkul, P.G. DeCaen, and D.E. Clapham, *TRPM7 senses oxidative stress to release Zn.* Proc Natl Acad Sci U S A, 2017. **114**(30): p. E6079-E6088.
29. Clapham, D.E., L.W. Runnels, and C. Strübing, *The TRP ion channel family.* Nat Rev Neurosci, 2001. **2**(6): p. 387-96.
30. Li, H., *TRP Channel Classification.* Adv Exp Med Biol, 2017. **976**: p. 1-8.
31. Khajavi, N., P.S. Reinach, M. Skrzypski, A. Lude, and S. Mergler, *L-carnitine reduces in human conjunctival epithelial cells hypertonic-induced shrinkage through interacting with TRPV1 channels.* Cell Physiol Biochem, 2014. **34**(3): p. 790-803.

32. Vriens, J., G. Appendino, and B. Nilius, *Pharmacology of vanilloid transient receptor potential cation channels.* Mol Pharmacol, 2009. **75**(6): p. 1262-79.
33. Murayama, T. and I.N. Maruyama, *Alkaline pH sensor molecules.* J Neurosci Res, 2015. **93**(11): p. 1623-30.
34. Tominaga, M. and M.J. Caterina, *Thermosensation and pain.* J Neurobiol, 2004. **61**(1): p. 3-12.
35. Devi, S., R. Kedlaya, N. Maddodi, K.M. Bhat, C.S. Weber, H. Valdivia, and V. Setaluri, *Calcium homeostasis in human melanocytes: role of transient receptor potential melastatin 1 (TRPM1) and its regulation by ultraviolet light.* Am.J.Physiol Cell Physiol, 2009. **297**(3): p. C679-C687.
36. Venkatachalam, K. and C. Montell, *TRP channels.* Annu Rev Biochem, 2007. **76**: p. 387-417.
37. Yekkirala, A.S., *Two to tango: GPCR oligomers and GPCR-TRP channel interactions in nociception.* Life Sci, 2013. **92**(8-9): p. 438-45.
38. Veldhuis, N.A., D.P. Poole, M. Grace, P. McIntyre, and N.W. Bunnett, *The G protein-coupled receptor-transient receptor potential channel axis: molecular insights for targeting disorders of sensation and inflammation.* Pharmacol Rev, 2015. **67**(1): p. 36-73.
39. Altier, C. and G.W. Zamponi, *Analysis of GPCR/ion channel interactions.* Methods Mol Biol, 2011. **756**: p. 215-25.
40. Shapovalov, G., V. Lehen'kyi, R. Skryma, and N. Prevarskaya, *TRP channels in cell survival and cell death in normal and transformed cells.* Cell Calcium, 2011. **50**(3): p. 295-302.
41. Tsavaler, L., M.H. Shapero, S. Morkowski, and R. Laus, *Trp-p8, a novel prostate-specific gene, is up-regulated in prostate cancer and other malignancies and shares high homology with transient receptor potential calcium channel proteins.* Cancer Res, 2001. **61**(9): p. 3760-9.
42. Zhang, L. and G.J. Barritt, *TRPM8 in prostate cancer cells: a potential diagnostic and prognostic marker with a secretory function?* Endocr Relat Cancer, 2006. **13**(1): p. 27-38.
43. Hammock, L., C. Cohen, G. Carlson, D. Murray, J.S. Ross, C. Sheehan, T.M. Nazir, and J.A. Carlson, *Chromogenic in situ hybridization analysis of melastatin mRNA expression in melanomas from American Joint Committee on Cancer stage I and II patients with recurrent melanoma.* J Cutan Pathol, 2006. **33**(9): p. 599-607.
44. Yamada, T., T. Ueda, Y. Shibata, Y. Ikegami, M. Saito, Y. Ishida, S. Ugawa, K. Kohri, and S. Shimada, *TRPV2 activation induces apoptotic cell death in human T24 bladder cancer cells: a potential therapeutic target for bladder cancer.* Urology, 2010. **76**(2): p. 509 e1-7.
45. Prevarskaya, N., R. Skryma, and Y. Shuba, *Ion Channels in Cancer: Are Cancer Hallmarks Oncochannelopathies?* Physiol Rev, 2018. **98**(2): p. 559-621.
46. Shapovalov, G., A. Ritaine, R. Skryma, and N. Prevarskaya, *Role of TRP ion channels in cancer and tumorigenesis.* Semin Immunopathol, 2016. **38**(3): p. 357-69.
47. Fels, B., E. Bulk, Z. Pethő, and A. Schwab, *The Role of TRP Channels in the Metastatic Cascade.* Pharmaceuticals (Basel), 2018. **11**(2).
48. Decuypere, J.P., G. Bultynck, and J.B. Parys, *A dual role for Ca(2+) in autophagy regulation.* Cell Calcium, 2011. **50**(3): p. 242-50.

49. Dubois, C., F. Vanden Abeele, and N. Prevarskaya, *Targeting apoptosis by the remodelling of calcium-transporting proteins in cancerogenesis.* FEBS J, 2013. **280**(21): p. 5500-10.
50. Shinomiya, T., X.K. Li, H. Amemiya, and S. Suzuki, *An immunosuppressive agent, FTY720, increases intracellular concentration of calcium ion and induces apoptosis in HL-60.* Immunology, 1997. **91**(4): p. 594-600.
51. Varghese, E., S.M. Samuel, Z. Sadiq, P. Kubatka, A. Liskova, J. Benacka, P. Pazinka, P. Kruzliak, and D. Büsselberg, *Anti-Cancer Agents in Proliferation and Cell Death: The Calcium Connection.* Int J Mol Sci, 2019. **20**(12).
52. Barnes, S. and L.W. Haynes, *Low-voltage-activated calcium channels in human retinoblastoma cells.* Brain Res, 1992. **598**(1-2): p. 19-22.
53. Hirooka, K., G.E. Bertolesi, M.E. Kelly, E.M. Denovan-Wright, X. Sun, J. Hamid, G.W. Zamponi, A.E. Juhasz, L.W. Haynes, and S. Barnes, *T-Type calcium channel alpha1G and alpha1H subunits in human retinoblastoma cells and their loss after differentiation.* J Neurophysiol, 2002. **88**(1): p. 196-205.
54. Mergler, S., Y. Cheng, S. Skosyrski, F. Garreis, P. Pietrzak, N. Kociok, A. Dwarakanath, P.S. Reinach, and V. Kakkassery, *Altered calcium regulation by thermosensitive transient receptor potential channels in etoposide-resistant WERI-Rb1 retinoblastoma cells.* Exp Eye Res, 2012. **94**(1): p. 157-73.
55. Hanano, T., Y. Hara, J. Shi, H. Morita, C. Umebayashi, E. Mori, H. Sumimoto, Y. Ito, Y. Mori, and R. Inoue, *Involvement of TRPM7 in cell growth as a spontaneously activated Ca2+ entry pathway in human retinoblastoma cells.* J Pharmacol Sci, 2004. **95**(4): p. 403-19.
56. Dimaras, H. and T.W. Corson, *Retinoblastoma, the visible CNS tumor: A review.* J Neurosci Res, 2019. **97**(1): p. 29-44.
57. Lohmann, D., B. Gallie, C. Dommering, and M. Gauthier-Villars, *Clinical utility gene card for: retinoblastoma.* Eur J Hum Genet, 2011. **19**(3).
58. Dimaras, H., T.W. Corson, D. Cobrinik, A. White, J. Zhao, F.L. Munier, D.H. Abramson, C.L. Shields, G.L. Chantada, F. Njuguna, and B.L. Gallie, *Retinoblastoma.* Nat Rev Dis Primers, 2015. **1**: p. 15021.
59. Naseripour, M., *"Retinoblastoma survival disparity": The expanding horizon in developing countries.* Saudi J Ophthalmol, 2012. **26**(2): p. 157-61.
60. Control, U.f.I.C., *RETINOBLASTOMA*. 2014, WHO: Review of Cancer Medicines on the WHO List of Essential Medicines.
61. Busch, M., D. Papior, H. Stephan, and N. Dünker, *Characterization of etoposide- and cisplatin-chemoresistant retinoblastoma cell lines.* Oncol Rep, 2018. **39**(1): p. 160-172.
62. McFall, R.C., T.W. Sery, and M. Makadon, *Characterization of a new continuous cell line derived from a human retinoblastoma.* Cancer Res, 1977. **37**(4): p. 1003-10.
63. Stephan, H., R. Boeloeni, A. Eggert, N. Bornfeld, and A. Schueler, *Photodynamic therapy in retinoblastoma: effects of verteporfin on retinoblastoma cell lines.* Invest Ophthalmol Vis Sci, 2008. **49**(7): p. 3158-63.
64. Liu, Y., H. Hu, M. Liang, Y. Xiong, K. Li, M. Chen, Z. Fan, X. Kuang, F. Deng, X. Liu, C. Xu, and J. Ge, *Regulated differentiation of WERI-Rb-1 cells into retinal neuron-like cells.* Int J Mol Med, 2017. **40**(4): p. 1172-1184.
65. Kakkassery, V., S. Skosyrski, A. Lüth, B. Kleuser, M. van der Giet, R. Tate, J. Reinhard, A. Faissner, S.C. Joachim, and N. Kociok, *Etoposide Upregulates Survival Favoring Sphingosine-1-Phosphate in Etoposide-Resistant Retinoblastoma Cells.* Pathol Oncol Res, 2019. **25**(1): p. 391-399.

66. Reinhard, J., N. Wagner, M.M. Krämer, M. Jarocki, S.C. Joachim, H.B. Dick, A. Faissner, and V. Kakkassery, *Expression Changes and Impact of the Extracellular Matrix on Etoposide Resistant Human Retinoblastoma Cell Lines.* Int J Mol Sci, 2020. **21**(12).
67. Strober, W., *Trypan Blue Exclusion Test of Cell Viability.* Curr Protoc Immunol, 2015. **111**: p. A3 B 1-A3 B 3.
68. Grynkiewicz, G., M. Poenie, and R.Y. Tsien, *A new generation of Ca2+ indicators with greatly improved fluorescence properties.* J Biol Chem, 1985. **260**(6): p. 3440-50.
69. Köse, S.A. and M. Nazıroğlu, *N-acetyl cysteine reduces oxidative toxicity, apoptosis, and calcium entry through TRPV1 channels in the neutrophils of patients with polycystic ovary syndrome.* Free Radic Res, 2015. **49**(3): p. 338-46.
70. Nazıroğlu, M., B. Ciğ, and C. Ozgül, *Neuroprotection induced by N-acetylcysteine against cytosolic glutathione depletion-induced Ca2+ influx in dorsal root ganglion neurons of mice: role of TRPV1 channels.* Neuroscience, 2013. **242**: p. 151-60.
71. Özgül, C. and M. Nazıroğlu, *TRPM2 channel protective properties of N-acetylcysteine on cytosolic glutathione depletion dependent oxidative stress and Ca2+ influx in rat dorsal root ganglion.* Physiol Behav, 2012. **106**(2): p. 122-8.
72. Stenger, B., T. Popp, H. John, M. Siegert, A. Tsoutsoulopoulos, A. Schmidt, H. Mückter, T. Gudermann, H. Thiermann, and D. Steinritz, *N-Acetyl-L-cysteine inhibits sulfur mustard-induced and TRPA1-dependent calcium influx.* Arch Toxicol, 2017. **91**(5): p. 2179-2189.
73. Bouron, A., K. Kiselyov, and J. Oberwinkler, *Permeation, regulation and control of expression of TRP channels by trace metal ions.* Pflugers Arch, 2015. **467**(6): p. 1143-64.
74. Xu, S.Z., F. Zeng, G. Boulay, C. Grimm, C. Harteneck, and D.J. Beech, *Block of TRPC5 channels by 2-aminoethoxydiphenyl borate: a differential, extracellular and voltage-dependent effect.* Br J Pharmacol, 2005. **145**(4): p. 405-14.
75. Parekh, A.B. and J.W. Putney, *Store-operated calcium channels.* Physiol Rev, 2005. **85**(2): p. 757-810.
76. Bootman, M.D., T.J. Collins, L. Mackenzie, H.L. Roderick, M.J. Berridge, and C.M. Peppiatt, *2-aminoethoxydiphenyl borate (2-APB) is a reliable blocker of store-operated Ca2+ entry but an inconsistent inhibitor of InsP3-induced Ca2+ release.* FASEB J, 2002. **16**(10): p. 1145-50.
77. Mergler, S., H. Dannowski, J. Bednarz, K. Engelmann, C. Hartmann, and U. Pleyer, *Calcium influx induced by activation of receptor tyrosine kinases in SV40-transfected human corneal endothelial cells.* Exp Eye Res, 2003. **77**(4): p. 485-95.
78. Milligan, C.J., J. Li, P. Sukumar, Y. Majeed, M.L. Dallas, A. English, P. Emery, K.E. Porter, A.M. Smith, I. McFadzean, D. Beccano-Kelly, Y. Bahnasi, A. Cheong, J. Naylor, F. Zeng, X. Liu, N. Gamper, L.H. Jiang, H.A. Pearson, C. Peers, B. Robertson, and D.J. Beech, *Robotic multiwell planar patch-clamp for native and primary mammalian cells.* Nat Protoc, 2009. **4**(2): p. 244-55.
79. Fertig, N., R.H. Blick, and J.C. Behrends, *Whole cell patch clamp recording performed on a planar glass chip.* Biophys J, 2002. **82**(6): p. 3056-62.

80. Barry, P.H., *JPCalc, a software package for calculating liquid junction potential corrections in patch-clamp, intracellular, epithelial and bilayer measurements and for correcting junction potential measurements.* J Neurosci Methods, 1994. **51**(1): p. 107-16.
81. Root-Bernstein, R. and P.F. Dillon, *A common molecular motif characterizes extracellular allosteric enhancers of GPCR aminergic receptors and suggests enhancer mechanism of action.* Curr Med Chem, 2014. **21**(32): p. 3673-86.
82. Clement, K., H. Biebermann, I.S. Farooqi, L. Van der Ploeg, B. Wolters, C. Poitou, L. Puder, F. Fiedorek, K. Gottesdiener, G. Kleinau, N. Heyder, P. Scheerer, U. Blume-Peytavi, I. Jahnke, S. Sharma, J. Mokrosinski, S. Wiegand, A. Muller, K. Weiss, K. Mai, J. Spranger, A. Gruters, O. Blankenstein, H. Krude, and P. Kuhnen, *MC4R agonism promotes durable weight loss in patients with leptin receptor deficiency.* Nat Med, 2018. **24**(5): p. 551-555.
83. Mangmool, S. and H. Kurose, *G(i/o) protein-dependent and -independent actions of Pertussis Toxin (PTX).* Toxins (Basel), 2011. **3**(7): p. 884-99.
84. Prevarskaya, N., L. Zhang, and G. Barritt, *TRP channels in cancer.* Biochim Biophys Acta, 2007. **1772**(8): p. 937-46.
85. Bari, M.R., S. Akbar, M. Eweida, F.J. Kühn, A.J. Gustafsson, A. Lückhoff, and M.S. Islam, *H2O2-induced Ca2+ influx and its inhibition by N-(p-amylcinnamoyl) anthranilic acid in the beta-cells: involvement of TRPM2 channels.* J Cell Mol Med, 2009. **13**(9B): p. 3260-7.
86. DelloStritto, D.J., P.J. Connell, G.M. Dick, I.S. Fancher, B. Klarich, J.N. Fahmy, P.T. Kang, Y.R. Chen, D.S. Damron, C.K. Thodeti, and I.N. Bratz, *Differential regulation of TRPV1 channels by H2O2: implications for diabetic microvascular dysfunction.* Basic Res Cardiol, 2016. **111**(2): p. 21.
87. Hara, Y., M. Wakamori, M. Ishii, E. Maeno, M. Nishida, T. Yoshida, H. Yamada, S. Shimizu, E. Mori, J. Kudoh, N. Shimizu, H. Kurose, Y. Okada, K. Imoto, and Y. Mori, *LTRPC2 Ca2+-permeable channel activated by changes in redox status confers susceptibility to cell death.* Mol Cell, 2002. **9**(1): p. 163-73.
88. Nicholas, S., S.Y. Yuan, S.J. Brookes, N.J. Spencer, and V.P. Zagorodnyuk, *Hydrogen peroxide preferentially activates capsaicin-sensitive high threshold afferents via TRPA1 channels in the guinea pig bladder.* Br J Pharmacol, 2017. **174**(2): p. 126-138.
89. Dhaka, A., V. Uzzell, A.E. Dubin, J. Mathur, M. Petrus, M. Bandell, and A. Patapoutian, *TRPV1 is activated by both acidic and basic pH.* J Neurosci, 2009. **29**(1): p. 153-8.
90. Du, J., J. Xie, and L. Yue, *Modulation of TRPM2 by acidic pH and the underlying mechanisms for pH sensitivity.* J Gen Physiol, 2009. **134**(6): p. 471-88.
91. Mačianskienė, R., M. Almanaitytė, A. Jekabsone, and K. Mubagwa, *Modulation of Human Cardiac TRPM7 Current by Extracellular Acidic pH Depends upon Extracellular Concentrations of Divalent Cations.* PLoS One, 2017. **12**(1): p. e0170923.
92. Garrity, P.A., *Weakly acidic, but strongly irritating: TRPA1 and the activation of nociceptors by cytoplasmic acidification.* J Gen Physiol, 2011. **137**(6): p. 489-91.

93. Upadhyay, S., S. Vaish, and M. Dhiman, *Hydrogen peroxide-induced oxidative stress and its impact on innate immune responses in lung carcinoma A549 cells.* Mol Cell Biochem, 2019. **450**(1-2): p. 135-147.
94. Sies, H., *Hydrogen peroxide as a central redox signaling molecule in physiological oxidative stress: Oxidative eustress.* Redox Biol, 2017. **11**: p. 613-619.
95. Lu, X.Y., B.C. Liu, L.H. Wang, L.L. Yang, Q. Bao, Y.J. Zhai, A.A. Alli, T.L. Thai, D.C. Eaton, W.Z. Wang, and H.P. Ma, *Acute ethanol induces apoptosis by stimulating TRPC6 via elevation of superoxide in oxygenated podocytes.* Biochim Biophys Acta, 2015. **1853**(5): p. 965-74.
96. Su, X., Z. Shen, Q. Yang, F. Sui, J. Pu, J. Ma, S. Ma, D. Yao, M. Ji, and P. Hou, *Vitamin C kills thyroid cancer cells through ROS-dependent inhibition of MAPK/ERK and PI3K/AKT pathways via distinct mechanisms.* Theranostics, 2019. **9**(15): p. 4461-4473.
97. Ryskamp, D.A., P. Witkovsky, P. Barabas, W. Huang, C. Koehler, N.P. Akimov, S.H. Lee, S. Chauhan, W. Xing, R.C. Rentería, W. Liedtke, and D. Krizaj, *The polymodal ion channel transient receptor potential vanilloid 4 modulates calcium flux, spiking rate, and apoptosis of mouse retinal ganglion cells.* J Neurosci, 2011. **31**(19): p. 7089-101.
98. Wang, Q., Q. Xu, A. Wei, S. Chen, C. Zhang, and L. Zeng, *[High dose vitamin C inhibits proliferation of breast cancer cells through reducing glycolysis and protein synthesis].* Zhejiang Da Xue Xue Bao Yi Xue Ban, 2019. **48**(3): p. 296-302.
99. Du, J., S.M. Martin, M. Levine, B.A. Wagner, G.R. Buettner, S.H. Wang, A.F. Taghiyev, C. Du, C.M. Knudson, and J.J. Cullen, *Mechanisms of ascorbate-induced cytotoxicity in pancreatic cancer.* Clin Cancer Res, 2010. **16**(2): p. 509-20.
100. Sung, H., J. Ferlay, R.L. Siegel, M. Laversanne, I. Soerjomataram, A. Jemal, and F. Bray, *Global Cancer Statistics 2020: GLOBOCAN Estimates of Incidence and Mortality Worldwide for 36 Cancers in 185 Countries.* CA Cancer J Clin, 2021. **71**(3): p. 209-249.
101. Cameron, E. and L. Pauling, *Supplemental ascorbate in the supportive treatment of cancer: Prolongation of survival times in terminal human cancer.* Proc Natl Acad Sci U S A, 1976. **73**(10): p. 3685-9.
102. Gkika, D. and N. Prevarskaya, *Molecular mechanisms of TRP regulation in tumor growth and metastasis.* Biochim Biophys Acta, 2009. **1793**(6): p. 953-8.
103. Prevarskaya, N., H. Ouadid-Ahidouch, R. Skryma, and Y. Shuba, *Remodelling of Ca2+ transport in cancer: how it contributes to cancer hallmarks?* Philos Trans R Soc Lond B Biol Sci, 2014. **369**(1638): p. 20130097.
104. Rizzuto, R., P. Pinton, D. Ferrari, M. Chami, G. Szabadkai, P.J. Magalhães, F. Di Virgilio, and T. Pozzan, *Calcium and apoptosis: facts and hypotheses.* Oncogene, 2003. **22**(53): p. 8619-27.
105. Kurbacher, C.M., U. Wagner, B. Kolster, P.E. Andreotti, D. Krebs, and H.W. Bruckner, *Ascorbic acid (vitamin C) improves the antineoplastic activity of doxorubicin, cisplatin, and paclitaxel in human breast carcinoma cells in vitro.* Cancer Lett, 1996. **103**(2): p. 183-9.
106. Ghavami, G. and S. Sardari, *Synergistic Effect of Vitamin C with Cisplatin for Inhibiting Proliferation of Gastric Cancer Cells.* Iran Biomed J, 2020. **24**(2): p. 119-27.

107. Herst, P.M., K.W. Broadley, J.L. Harper, and M.J. McConnell, *Pharmacological concentrations of ascorbate radiosensitize glioblastoma multiforme primary cells by increasing oxidative DNA damage and inhibiting G2/M arrest.* Free Radic Biol Med, 2012. **52**(8): p. 1486-93.
108. Beck, B., G. Bidaux, A. Bavencoffe, L. Lemonnier, S. Thebault, Y. Shuba, G. Barrit, R. Skryma, and N. Prevarskaya, *Prospects for prostate cancer imaging and therapy using high-affinity TRPM8 activators.* Cell Calcium, 2007. **41**(3): p. 285-94.
109. Stock, K., J. Kumar, M. Synowitz, S. Petrosino, R. Imperatore, E.S. Smith, P. Wend, B. Purfürst, U.A. Nuber, U. Gurok, V. Matyash, J.H. Wälzlein, S.R. Chirasani, G. Dittmar, B.F. Cravatt, S. Momma, G.R. Lewin, A. Ligresti, L. De Petrocellis, L. Cristino, V. Di Marzo, H. Kettenmann, and R. Glass, *Neural precursor cells induce cell death of high-grade astrocytomas through stimulation of TRPV1.* Nat Med, 2012. **18**(8): p. 1232-8.
110. Shatzer, A.N., M.G. Espey, M. Chavez, H. Tu, M. Levine, and J.I. Cohen, *Ascorbic acid kills Epstein-Barr virus positive Burkitt lymphoma cells and Epstein-Barr virus transformed B-cells in vitro, but not in vivo.* Leuk Lymphoma, 2013. **54**(5): p. 1069-78.
111. Reinach, P.S., W. Chen, and S. Mergler, *Polymodal roles of transient receptor potential channels in the control of ocular function.* Eye Vis (Lond), 2015. **2**: p. 5.
112. Noble, D. and T. Powell, *The slowing of Ca2+ signals by Ca2+ indicators in cardiac muscle.* Proc Biol Sci, 1991. **246**(1316): p. 167-72.

Eidesstattliche Versicherung

„Ich, Jakub Oronowicz, versichere an Eides statt durch meine eigenhändige Unterschrift, dass ich die vorgelegte Dissertation mit dem Thema: *Effects of ascorbic acid on TRP channel-mediated Ca^{2+} homeostasis and cell viability in etoposide-resistant and -sensitive retinoblastoma cells / Auswirkungen von Ascorbinsäure auf die TRP-Kanal-vermittelte Ca^{2+}-Homöostase und Zelllebensfähigkeit in Etoposid-resistenten und -empfindlichen Retinoblastomzellen* selbstständig und ohne nicht offengelegte Hilfe Dritter verfasst und keine anderen als die angegebenen Quellen und Hilfsmittel genutzt habe.

Alle Stellen, die wörtlich oder dem Sinne nach auf Publikationen oder Vorträgen anderer Autoren/innen beruhen, sind als solche in korrekter Zitierung kenntlich gemacht. Die Abschnitte zu Methodik (insbesondere praktische Arbeiten, Laborbestimmungen, statistische Aufarbeitung) und Resultaten (insbesondere Abbildungen, Graphiken und Tabellen) werden von mir verantwortet.

Ich versichere ferner, dass ich die in Zusammenarbeit mit anderen Personen generierten Daten, Datenauswertungen und Schlussfolgerungen korrekt gekennzeichnet und meinen eigenen Beitrag sowie die Beiträge anderer Personen korrekt kenntlich gemacht habe (siehe Anteilserklärung). Texte oder Textteile, die gemeinsam mit anderen erstellt oder verwendet wurden, habe ich korrekt kenntlich gemacht.

Meine Anteile an etwaigen Publikationen zu dieser Dissertation entsprechen denen, die in der untenstehenden gemeinsamen Erklärung mit dem Erstbetreuer, angegeben sind. Für sämtliche im Rahmen der Dissertation entstandenen Publikationen wurden die Richtlinien des ICMJE (International Committee of Medical Journal Editors; www.icmje.org) zur Autorenschaft eingehalten. Ich erkläre ferner,

dass ich mich zur Einhaltung der Satzung der Charité – Universitätsmedizin Berlin zur Sicherung Guter Wissenschaftlicher Praxis verpflichte.

Weiterhin versichere ich, dass ich diese Dissertation weder in gleicher noch in ähnlicher Form bereits an einer anderen Fakultät eingereicht habe.
Die Bedeutung dieser eidesstattlichen Versicherung und die strafrechtlichen Folgen einer unwahren eidesstattlichen Versicherung (§§156, 161 des Strafgesetzbuches) sind mir bekannt und bewusst.“

Datum Unterschrift

Anteilserklärung an den erfolgten Publikationen

Jakub Oronowicz hatte folgenden Anteil an den folgenden Publikationen:

Publikation 1: Jakub Oronowicz, Jacqueline Reinhard, Peter Sol Reinach, Szymon Ludwiczak, Huan Luo, Marah Hussain Omar Ba Salem, Miriam Monika Kraemer, Heike Biebermann, Vinodh Kakkassery, Stefan Mergler, *Ascorbate-induced oxidative stress mediates TRP channel activation and cytotoxicity in human etoposide-sensitive and -resistant retinoblastoma cells.* Lab Invest, 2020.

Beitrag im Einzeln:

-Vorschlagen des Themas, der Hypothese und einplanen des Designs (mit Literaturrecherche) dieser Studie.

-Durchführung aller dargestellten Experimente (mit Ausnahme qRT-PCR), einschließlich Auswertung der Rohdaten und Diagrammerstellung: Calciummessungen (Fig. 3 - 5 und 10) und Patch-Clamp Experimente (Fig. 6 - 9), zytotoxische Untersuchungen (Fig. 11 - 12), inklusive der Handhabung der Zellkulturen (Fig. 1).

-Durchführung aller statistischen Analysen, Interpretation der Ergebnisse.

-Alle Teile dieser Studie wurden nach der entsprechenden Einweisung seitens Erstbetreuers durchgeführt.

_____

Unterschrift, Datum und Stempel des/der erstbetreuenden Hochschullehrers/in

_____

Unterschrift des Doktoranden/der Doktorandin

Auszug aus der Journal Summary List

Journal Data Filtered By: **Selected JCR Year: 2018** Selected Editions: SCIE,SSCI
Selected Categories: **"MEDICINE, RESEARCH and EXPERIMENTAL"**
Selected Category Scheme: WoS
Gesamtanzahl: 136 Journale

Rank	Full Journal Title	Total Cites	Journal Impact Factor	Eigenfactor Score
1	NATURE MEDICINE	79,243	30.641	0.162840
2	Science Translational Medicine	30,485	17.161	0.121980
3	JOURNAL OF CLINICAL INVESTIGATION	108,879	12.282	0.139970
4	TRENDS IN MOLECULAR MEDICINE	9,946	11.028	0.018900
5	JOURNAL OF EXPERIMENTAL MEDICINE	63,983	10.892	0.071790
6	EMBO Molecular Medicine	7,507	10.624	0.025980
7	Annual Review of Medicine	6,068	10.091	0.009030
8	MOLECULAR THERAPY	16,991	8.402	0.030050
9	MOLECULAR ASPECTS OF MEDICINE	5,568	8.313	0.009020
10	Theranostics	8,769	8.063	0.020270
11	EBioMedicine	5,401	6.680	0.022310
12	ALTEX-Alternatives to Animal Experimentation	1,361	6.183	0.001920
13	Wiley Interdisciplinary Reviews-Nanomedicine and Nanobiotechnology	2,345	6.140	0.004130
14	JCI Insight	4,351	6.014	0.020440
15	Molecular Therapy-Nucleic Acids	3,189	5.919	0.010410
16	Molecular Therapy-Oncolytics	486	5.710	0.001990
17	Nanomedicine-Nanotechnology Biology and Medicine	10,131	5.570	0.014480
18	Cold Spring Harbor Perspectives in Medicine	6,223	5.564	0.016730
19	CLINICAL SCIENCE	10,951	5.237	0.014190
20	JOURNAL OF BIOMEDICAL SCIENCE	4,083	5.203	0.006300

Rank	Full Journal Title	Total Cites	Journal Impact Factor	Eigenfactor Score
21	npj Vaccines	282	5.020	0.001120
22	AMYLOID-JOURNAL OF PROTEIN FOLDING DISORDERS	1,335	4.919	0.003270
23	Translational Research	3,669	4.915	0.008530
24	Molecular Therapy-Methods & Clinical Development	1,078	4.875	0.004020
25	Vaccines	1,077	4.760	0.003910
26	JOURNAL OF MOLECULAR MEDICINE-JMM	7,195	4.746	0.010880
27	EXPERIMENTAL AND MOLECULAR MEDICINE	4,046	4.743	0.007380
28	Stem Cell Reviews and Reports	2,436	4.697	0.004690
29	CANCER GENE THERAPY	2,842	4.681	0.003200
30	EPMA Journal	815	4.661	0.001320
31	JOURNAL OF CELLULAR AND MOLECULAR MEDICINE	12,391	4.658	0.015760
32	Stem Cell Research & Therapy	6,132	4.627	0.015810
33	Cancer Biology & Medicine	1,043	4.467	0.003040
34	EXPERT REVIEWS IN MOLECULAR MEDICINE	1,758	4.407	0.001450
35	mAbs	4,415	4.405	0.011150
36	MOLECULAR PHARMACEUTICS	16,792	4.396	0.028020
37	CYTOTHERAPY	5,969	4.297	0.009690
38	JOURNAL OF INHERITED METABOLIC DISEASE	5,868	4.287	0.008410
39	PPAR Research	1,434	4.186	0.001600
40	ARCHIVES OF PATHOLOGY & LABORATORY MEDICINE	10,039	4.151	0.012620
41	Journal of Translational Medicine	10,831	4.098	0.022910
42	CTS-Clinical and Translational Science	1,351	3.989	0.003190

Selected JCR Year: 2018; Selected Categories: "MEDICINE, RESEARCH and EXPERIMENTAL"

Rank	Full Journal Title	Total Cites	Journal Impact Factor	Eigenfactor Score
43	HUMAN GENE THERAPY	5,639	3.855	0.007540
44	Nucleic Acid Therapeutics	854	3.780	0.003000
45	GENE THERAPY	7,223	3.749	0.007040
46	BIOMEDICINE & PHARMACOTHERAPY	14,983	3.743	0.023480
47	Annals of Translational Medicine	3,430	3.689	0.010900
48	Orphanet Journal of Rare Diseases	6,654	3.687	0.015860
* 49	LABORATORY INVESTIGATION	10,025	3.684	0.009110
50	MOLECULAR GENETICS AND METABOLISM	7,018	3.610	0.009900
51	EXPERT OPINION ON BIOLOGICAL THERAPY	4,481	3.585	0.007720
52	Wiley Interdisciplinary Reviews-Systems Biology and Medicine	1,165	3.542	0.002190
53	XENOTRANSPLANTATION	1,689	3.484	0.002390
54	CELL TRANSPLANTATION	5,941	3.477	0.009210
55	JOURNAL OF IMMUNOTHERAPY	3,142	3.455	0.004000
56	LIFE SCIENCES	21,687	3.448	0.016400
57	VACCINE	40,222	3.269	0.070760
58	American Journal of Translational Research	5,434	3.266	0.012240
59	ADVANCES IN THERAPY	3,008	3.260	0.006540
60	STEM CELLS AND DEVELOPMENT	7,899	3.147	0.013510
61	Drug Delivery and Translational Research	1,298	3.111	0.002430
62	Journal of Diabetes Research	3,653	3.040	0.011530
63	EXPERIMENTAL BIOLOGY AND MEDICINE	6,301	3.005	0.007610
64	MOLECULAR MEDICINE	4,918	2.991	0.004770

Selected JCR Year: 2018; Selected Categories: "MEDICINE, RESEARCH and EXPERIMENTAL"

Publikation

Laboratory Investigation (2021) 101:70–88
https://doi.org/10.1038/s41374-020-00485-2

ARTICLE

Ascorbate-induced oxidative stress mediates TRP channel activation and cytotoxicity in human etoposide-sensitive and -resistant retinoblastoma cells

Jakub Oronowicz[1] · Jacqueline Reinhard[2] · Peter Sol Reinach[3] · Szymon Ludwiczak[1] · Huan Luo[1] · Marah Hussain Omar Ba Salem[1] · Miriam Monika Kraemer[2] · Heike Biebermann[4] · Vinodh Kakkassery[5] · Stefan Mergler[1]

Received: 7 February 2020 / Revised: 29 July 2020 / Accepted: 11 August 2020 / Published online: 18 September 2020

Abstract

There are indications that pharmacological doses of ascorbate (Asc) used as an adjuvant improve the chemotherapeutic management of cancer. This favorable outcome stems from its cytotoxic effects due to prooxidative mechanisms. Since regulation of intracellular Ca^{2+} levels contributes to the maintenance of cell viability, we hypothesized that one of the effects of Asc includes disrupting regulation of intracellular Ca^{2+} homeostasis. Accordingly, we determined if Asc induced intracellular Ca^{2+} influx through activation of pertussis sensitive Gi/o-coupled GPCR which in turn activated transient receptor potential (TRP) channels in both etoposide-resistant and -sensitive retinoblastoma (WERI-Rb1) tumor cells. Ca^{2+} imaging, whole-cell patch-clamping, and quantitative real-time PCR (qRT-PCR) were performed in parallel with measurements of RB cell survival using Trypan Blue cell dye exclusion. *TRPM7* gene expression levels were similar in both cell lines whereas *TRPV1*, *TRPM2*, *TRPA1*, *TRPC5*, *TRPV4*, and *TRPM8* gene expression levels were downregulated in the etoposide-resistant WERI-Rb1 cells. In the presence of extracellular Ca^{2+}, 1 mM Asc induced larger intracellular Ca^{2+} transients in the etoposide-resistant WERI-Rb1 than in their etoposide-sensitive counterpart. With either 100 µM CPZ, 500 µM La^{3+}, 10 mM NAC, or 100 µM 2-APB, these Ca^{2+} transients were markedly diminished. These inhibitors also had corresponding inhibitory effects on Asc-induced rises in whole-cell currents. Pertussis toxin (PTX) preincubation blocked rises in Ca^{2+} influx. Microscopic analyses showed that after 4 days of exposure to 1 mM Asc cell viability fell by nearly 100% in both RB cell lines. Taken together, one of the effects underlying oxidative mediated Asc-induced WERI-Rb1 cytotoxicity stems from its promotion of Gi/o coupled GPCR mediated increases in intracellular Ca^{2+} influx through TRP channels. Therefore, designing drugs targeting TRP channel modulation may be a viable approach to increase the efficacy of chemotherapeutic treatment of RB. Furthermore, Asc may be indicated as a possible supportive agent in anti-cancer therapies.

✉ Vinodh Kakkassery
vinodh.kakkassery@gmail.com

✉ Stefan Mergler
stefan.mergler@charite.de

[1] Klinik für Augenheilkunde, Charité – Universitätsmedizin Berlin, Corporate Member of Freie Universität Berlin, Humboldt-Universität zu Berlin and Berlin Institute of Health, Berlin, Germany

[2] Department of Cell Morphology and Molecular Neurobiology, Faculty of Biology and Biotechnology, Ruhr University Bochum, Bochum, Germany

[3] School of Ophthalmology and Optometry, Wenzhou Medical University, Wenzhou, PR China

[4] Institut für Experimentelle Pädiatrische Endokrinologie, Charité – Universitätsmedizin Berlin, Corporate Member of Freie Universität Berlin, Humboldt-Universität zu Berlin and Berlin Institute of Health, Berlin, Germany

[5] Universität zu Lübeck, Klinik für Augenheilkunde – Universitätsklinikum Schleswig-Holstein (Campus Lübeck), Lübeck, Germany

Introduction

Retinoblastoma (RB) is the most common intraocular cancer solely expressed in children. It is the only central nervous system tumor that can be easily observed without dedicated medical equipment [1]. RB is due to a mutation of both RB1 alleles, which increases both formation of a phosphorylated protein product (pRB) and tumorous cell proliferation [2, 3]. In the absence of metastasis, the RB survival rate is variable in different countries. In developed countries, it has risen to over 90%, while it is <50% in lower-income countries having a higher incidence of RB patients [4, 5]. The first-line therapy in the worst cases is still enucleation despite numerous alternative options such as etoposide chemotherapy [3]. However, the efficacy of etoposide may be limited since some RB cells develop resistance [6]. Accordingly, there remains a need to develop novel approaches to treat this disease.

Dysfunctional regulation of intracellular calcium levels can disrupt control of responses that may underlie some types of RB neoplasms. In recent years, some progress was made in clarifying a relationship between alterations underlying tumorgenesis and dysfunctional transient receptor potential (TRP) channel expression [7–9]. One example includes an association between altered TRP channel expression and intracellular calcium regulation, which was recently described in healthy ocular cells and benign as well as malignant ocular tumor cells [10–12]. Sustained rises in intracellular calcium levels above 100 nM can lead to some damaging effects such as increases in apoptosis, autophagy, or even decreases in cell proliferation [13–16]. TRP channel involvement in regulating these responses suggests that they are potential drug targets to inhibit RB cell viability and survival.

The TRP channel superfamily is a heterogenous group of more than 28 channel genes that are divided into seven subfamilies based on protein and DNA sequence homology: TRPC (classical), TRPV (vanilloid), TRPM (melastatin), TRPA (ankyrin), TRPP (polycyclin), TRPML (mycolipin) and TRPN (NOMPC) [17–20]. RB cells express voltage-operated Ca^{2+} channels [21, 22] and TRPs [11, 23]. Through regulating Ca^{2+} influx, TRPs function as biosensors and transducers. They undergo polymodal activation in response to a wide variety of environmental stresses, including temperature fluctuation [24], tissue injury [25], anisoosmolarity [26], UV-light [27], pH reduction [28], certain ligands (e.g., capsaicin [29]), exocytosis, pathways coupled to phospholipase C stimulation and many others [30]. Changes in specific TRP expression levels and function are diagnostic of some malignant transformations [8, 31]. For example, either TRPV6 or TRPM8 upregulation is used as a marker for establishing a prostatic cancer prognosis [32, 33]. Therefore, identifying TRP channel expression patterns may broaden their use as prognostic tumor markers in various cancerous diseases [34].

Aside from acting as biosensors and transducers of a host of different environmental cues, TRP stimulation can also be triggered by the activation of G protein-coupled receptors (GPCRs), which are the largest family of signaling proteins in mammals [35, 36]. GPCRs and TRPs are both cell surface proteins of neuronal and non-neuronal cells. GPCRs and Ca^{2+} permeable TRPs are also a component of a GPCR-TRP signaling pathway axis and may function as a unit [37, 38].

Ascorbic acid (Asc) is being evaluated as a therapeutic option in treating oncologic diseases [39–41]. This treatment is becoming more widely used because of its beneficial effects in different groups of patients [42–46]. Pharmacological doses (i.e., 1–20 mM) of Asc administered through intravenous injection provide therapeutic benefit. In over 40 different tumor cell lines (including breast, lung, renal, ovarian cancer, and Y-79 RB cell line) Asc reduced cell survival [47, 48]. Even if a pharmacological dose of Asc administered as an adjuvant did not have a favorable outcome, millimolar levels of extracellular Vitamin C selectively killed cancer cells [49, 50] whereas these high dosages were well tolerated by healthy cells [41, 51].

Asc concentrations less than a millimolar are referred to as being physiological since they are similar to those reported in plasma (<0.2 mM). At these levels, Asc acts as an antioxidant. On the other hand, Asc at pharmacological doses is present in the plasma reaching the millimolar range in which case it acts instead as an oxidant generating hydrogen peroxide (H_2O_2), reactive oxygen species (ROS), and hydroxyl radicals [46, 47, 52]. In this study, 1 mM Asc was used, which is the same concentration used in a previous report [46].

Notably, Asc is present in human ocular tissues at millimolar levels. In this range, it is speculated that Asc protects these tissues from short-wavelength solar radiation damage [53]. Specifically, in ocular tissues the intracellular Asc concentration is reported as follows: lens: 2.5 to 3.4 mM; aqueous humour: 0.4–1.1 mM; corneal epithelium ~12,5 mM; retina > 1 mM [54, 55]. It is suggested that during intravenous ascorbate therapy Asc may reach comparable or even higher levels at the extracellular side of the retina through the ophthalmic artery. It is relevant because cell death depends on extracellular rather than the intracellular Asc concentration [49].

We show here that 1 mM Asc, presumably acting as an oxidant, had similar cytotoxic effects on etoposide-sensitive and etoposide-resistant WERI-Rb1 cell

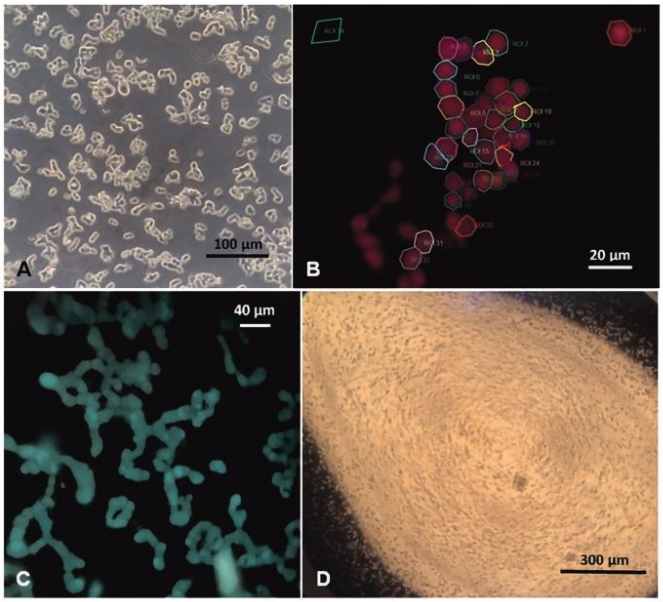

Fig. 1 Microscopic images of RB cells. a Light microscopic image of etoposide-resistant WERI-Rb1 cells. **b** Fluorescence microscopic image (510 nm; red colored by imaging software) showing single etoposide-resistant WERI-Rb1 cells on a poly-L-lysine coated coverslip. The circumscribed zones point out some single cells that are regions of interest (ROIs) for fluorescence measurements. **c** Fluorescence microscopic image (510 nm) shows cells growing in chains. **d** Light microscopic view of a single-cell suspension prepared for patch-clamp recordings.

viability. This response included increases in Gi/o coupled GPCR activity resulting in increases in intracellular Ca^{2+} influx through TRP channels. The involvement of this channel family was confirmed based on (1) TRP gene expression patterns in the etoposide-sensitive and -resistant WERI-Rb1 cells; (2) Asc-induced increases in Ca^{2+} influx and underlying currents that are attributable to TRP channel activation; (3) association between the effects of TRP channel inhibitors and the two different aforementioned responses to Asc.

Materials and methods

Materials

Medium and supplements for cell culture were purchased from Biochrom AG (Berlin, Germany) or GIBCO Invitrogen (Karlsruhe, Germany). All reagents (e.g., Ascorbic acid A4403; Trypan Blue T8154), except those specified below, were purchased from Sigma-Aldrich (Deisenhofen, Germany). Capsazepine was purchased from Cayman Chemical Company (Ann Arbor, Mi, USA). The internal and external solutions for planar patch-clamping were provided by Nanion Company (Munich, Germany). Fura2/AM was purchased from PromoCell (Heidelberg, Germany).

Cell culture and cultivation

The etoposide-sensitive and -resistant WERI-Rb1 cell lines were established [6, 56, 57] and cultured as previously described [11, 58, 59]. In brief, both cell lines were cultivated in RPMI-1640 Medium [60], supplemented with 10% fetal bovine serum (FBS) and 100 IU/ml penicillin/streptomycin, in an incubator at 37 °C in 5% CO_2 and 80% humidity. Cells were seeded on 12 well plastic culture plates (Fig. 1a) and medium was exchanged three times per week.

Microscopic analyses of cell viability

The RB cells were prepared as described above. Subsequently, microscopic images were captured on the first, the fifth, and the seventh day. Two sets of experiments were performed in order to ascertain whether Asc altered viability of etoposide-resistant and -sensitive WERI-Rb1 cells. In the first set of experiments, freshly diluted cells were observed and 1 mM Asc was subsequently added to the medium. On the fifth day, cell density was again recorded and fresh RPMI-1640 medium was added to the cell culture to evaluate reversibility of perceived changes. On the seventh day, cell density images were captured and evaluated. In the second set of experiments, following culturing the cell suspensions for 4 days, 1 mM Asc was added to the

medium. After another 4 days, the effect of this addition on cell density was reevaluated.

To ascertain if cell death accounted for the changes in their density, 0.4% Trypan Blue dye exclusion was used to evaluate cells viability. As only dead cells are stainable, on the fifth day 250 µl of the cell suspension were removed from each flask and diluted with an equal volume of Trypan Blue. With the Neubauer counting chamber (A. Hartenstein GmbH, Wuerzburg, Germany) stained cells were counted and expressed as a percent of the total cell population.

RNA-isolation, cDNA synthesis, and qRT-PCR analysis

The Gene Elute Mammalian Total RNA Miniprep Kit from Sigma-Aldrich (St. Louis, USA) was used according to the manufacturer's instructions to extract RNA from 5×10^6 etoposide-sensitive and -resistant WERI-Rb1 cells. Concentration and purity of RNA were evaluated with a BioSpectrometer (Eppendorf, Hamburg, Germany). The First Strand cDNA Synthesis Kit was used for reverse-transcription of 1 µg RNA (Thermo Fisher Scientific, Waltham, MA, USA). qRT-PCR was performed using the FastStart essential DNA Green Master Mix. Reactions were run in a Light Cycler® 96 (Roche Applied Science, Mannheim, Germany). Conditions were as follows: 10 min at 95 °C; 10 s at 95 °C, 30 s at 60 °C; 10 s at 72 °C for 45 cycles; 10 s at 95 °C, 60 s at 65 °C, 1 s at 97 °C and 30 s at 37 °C. Oligonucleotides were designed using the Probe-Finder Assay Design Center (Roche Applied Science; Table 1). Efficiency of oligonucleotide pairs was calculated by a cDNA dilution series of 5 ng to 125 ng. For normalization and relative quantification, expression of the housekeeping gene *RPS18* was analyzed. Table 1 provides a list of oligonucleotides used for TRP-cation channel mRNA expression analyses of the aforementioned cell lines.

Fluorescence calcium imaging

Cells were preincubated with culture medium containing 1 µM Fura-2/AM and, if needed, with TRP-channel antagonists (for 20–30 min, except for N-acetylcysteine (NAC): 4–5 days) or Gi/o inhibitor—pertussis toxin (PTX) (for 18 h) at 37 °C and 5% CO_2. Coverslips were additionally coated with poly-L-lysine to attach the RB cells. If dimethyl sulfoxide (DMSO) was used to dissolve a drug, its final concentration did not exceed 0.1%. At this concentration, it was not cytotoxic. Afterward, the cells were washed with a Ringer-like solution (containing in mM: 150 NaCl, 6 CsCl, 1 $MgCl_2$, 10 HEPES acid, 10 glucose and 1.5 $CaCl_2$ at pH ~7.35) in order to stop Fura-2/AM uptake and to remove any cell debris and dead cells [61]. Thereafter, fluorescence measurements were performed at room temperature ~20–23 °C using a digital imaging system (Olympus Europa Holding GmbH, Hamburg, Germany) in conjunction with an inverted

Table 1 List of oligonucleotides used for TRP-cation channel mRNA expression analyses in human etoposide-sensitive and -resistant WERI-Rb1 by qRT-PCR.

Gene	Oligonucleotide sequence	Product size (bp)	Oligonucleotide efficiency	GenBank accession number
*TRPA1*_for	TGGACACCTTCTTCTTGCATT	103	1.0	NM_007332
*TRPA1*_rev	TCATCCATTTCATGCAGCAC			
*TRPC5*_for	TGGTAACTGGTTCAACAACACC	99	1.0	NM_012471
*TRPC5*_rev	CTGTCAGCATTGCGTTCTG			
*RPS18*_for	CTTCCACAGGAGGCCTACAC	82	1.0	NM_022551
*RPS18*_rev	CGCAAAATATGCTGGAACTTT			
*TRPM2*_for	CGAGGACATCAGCAATAAGGT	75	0.836	NM_003307
*TRPM2*_rev	ATGGAGCCCGACCTCTTC			
*TRPM7*_for	TTGACATTGCCAAAAATCATGT	66	1.0	NM_017672
*TRPM7*_rev	CTTGTTCCAAGGATCCAACC			
*TRPM8*_for	GGTCCTGTACTCGCTGGTCT	67	1.0	NM_024080
*TRPM8*_rev	CACCCCATTTACGTACCACTG			
*TRPV1*_for	CTACAGCAGCAGCGAGACC	71	0.899	NM_080704
*TRPV1*_rev	CCTGCAGGAGTCGGTTCA			
*TRPV4*_for	CAACAACGACGGCCTCTC	74	1.0	NM_021625
*TRPV4*_rev	GGATGATGTGCTGAAAGATCC			

bp base pairs, *for* forward, *rev* reverse.

The oligonucleotide sequence, predicted product size, oligonucleotide efficiency, and GenBank accession number are indicated. For relative quantification of mRNA levels, *RPS18* served as reference gene.

microscope (Olympus BX50WJ), a LED light source (LED-Hub by Omikron, Rodgau–Dudenhoven, Germany) and a digital camera (Olympus XM-10). Alternate fluorescence wavelength excitation was isolated at 340 nm and 380 nm. Ratios (f_{340}/f_{380}) of emission at 510 nm were used to obtain relative values of intracellular Ca^{2+} levels with imaging software (cellSens, Olympus Europa Holding GmbH, Hamburg, Germany) (Fig. 1b, c) [62]. Drug application was done by pipetting it into the static measuring chamber. Results are shown as mean traces of the fluorescence ratio ± SEM (with bidirectional error bars). n-values indicate the number of measured cells. The fluorescence ratios f_{340}/f_{380} were normalized (control set to 0.1).

Planar patch-clamp recordings

Following removal with phosphate buffer saline (PBS) of any cell debris to improve seal quality [63], a single-cell suspension was bathed in the external solution containing (in mM): 140 NaCl, 4 KCl, 1 $MgCl_2$, 2 $CaCl_2$, 5 D-glucose monohydrate and 10 HEPES (pH ≈ 7.4; osmolarity ≈ 298 mOsM) (Fig. 1d). Microchips (Nanion, Munich, Germany) with a mean resistance of 3–5 MOhm were used. First of all, the internal measuring solution was applied to the internal side of the chip (in mM): 50 CsCl, 10 NaCl, 60 CsF, 20 EGTA, and 10 HEPES (pH ≈ 7.2 and ≈ 288 mOsM). An external solution was then added to the external measuring side of the chip coupled to a planar patch-clamp system (Port-a-Patch®, Nanion, Munich, Germany), an EPC 10 amplifier (HEKA, Lamprecht, Germany), and PatchMaster version 2.6 for Windows (HEKA, Lamprecht, Germany) [64]. Furthermore, 5–10 µL of the single-cell suspension was added to the upper side of the microchip at ~20–23 °C. The software controlled the pump (Suction Control Pro, Nanion, Munich, Germany) in order to achieve and maintain the whole-cell configuration and also to read and evaluate the data. The recordings were started ~10 min after breaking into a whole-cell configuration and confirming the settings [65]. Currents were recorded every 5 s following a voltage ramp protocol of −60 to + 130 mV range without steps and 500 ms duration. Resulting currents were normalized to cell membrane capacitance to obtain current density (pA/pF). The software calculated mean access resistance (for etoposide-sensitive WERI-Rb1: 26 ± 3 MΩ; $n = 19$; for etoposide-resistant WERI-Rb1: 26 ± 3 MΩ; $n = 16$) and mean membrane capacitance (for etoposide-sensitive WERI-Rb1: 8 ± 2 pF; $n = 19$; for etoposide-resistant WERI-Rb1: 8 ± 2 pF; $n = 16$). The liquid junction potential was calculated (≈3.8 mV) and software corrected [66]. All current recordings were leak-subtracted. Only leak currents below 100 pA were used, while all other recordings were excluded from analyses. In order to avoid possible interference of voltage-dependent Ca^{2+} channels, the holding potential (HP) was set to 0 mV.

Data analyses and statistics

Statistical significance was determined depending on whether the data passed the normality test. For data passing the normality test, paired or unpaired Student's-t-test was used. Otherwise, the Wilcoxon test for matched pairs or Mann–Whitney *U* test for unpaired data were used. All other values are reported as means ± SEM. *P* values < 0.05 were considered as significant both for paired (*) and unpaired (#) tests. All analyses were performed using SigmaPlot version 12.5 for Windows (Systat Software, Inc., Point Richmond, California USA) and GraphPad Prism software version 5.00 for Windows (La Jolla, California, USA).

For statistical evaluation of qRT-PCR analysis, data were analyzed by REST 2009 (relative expression software tool; Qiagen GmbH, Hilden, Germany) using a pairwise fixed reallocation and randomization test. *P* values < 0.05 were considered statistically significant.

Results

TRP mRNA expression in etoposide-sensitive and -resistant WERI-Rb1 cells

Figure 2 provides a comparison of the gene expression levels of *TRPA1*, *TRPC5*, *TRPM2*, *TRPM7*, *TRPM8*, *TRPV1*, and *TRPV4* in etoposide-sensitive and -resistant WERI-Rb1 cells. Even though both cell lines had a

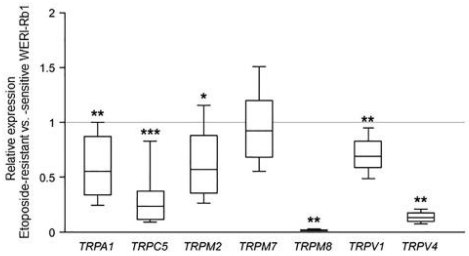

Fig. 2 Analyses of relative TRP mRNA expression by qRT-PCR. Expression of TRPs was observed in etoposide-sensitive and -resistant WERI-Rb1 cells. Both cell lines show a comparable *TRPM7* mRNA expression. In contrast, *TRPA1*, *TRPC5*, *TRPM2*, *TRPM8*, *TRPV1*, and *TRPV4* mRNA levels were significantly downregulated in etoposide-resistant in comparison to the -sensitive WERI-Rb1 cells. Data are shown as median±quartile±minimum/maximum ($n = 6$).

comparable *TRPM7* mRNA expression level (0.920-fold; $p = 0.556$), *TRPC5* (0.239-fold; $p < 0.001$), *TRPM8* (0.015-fold; $p = 0.001$) as well as *TRPV4* (0.131-fold; $p = 0.001$) were markedly downregulated in the etoposide-resistant WERI-Rb1 cell line. In addition, *TRPA1* (0.556-fold; $p = 0.002$), *TRPM2* (0.570-fold; $p = 0.012$) and *TRPV1* (0.687-fold; $p = 0.001$) expression levels were lower in the etoposide-resistant WERI-Rb1 cells. Overall, the gene expression levels of all of these TRPs were lower in etoposide-resistant WERI-Rb1 cell line, except for *TRPM7*.

Asc induces larger Ca^{2+} increases in etoposide-resistant WERI-Rb1 cells

Asc (1 mM) induced larger increases in the f_{340}/f_{380} fluorescence ratio in etoposide-resistant WERI-Rb1 cells than in their etoposide-sensitive counterpart. It increased the ratio in etoposide-resistant WERI-Rb1 cells from 0.1008 ± 0.0002 ($t = 60$ s; $n = 91$) to 0.3446 ± 0.0048 ($t = 300$ s; $n = 91$; $p < 0.0001$) (Fig. 3a, c), while in an etoposide-sensitive WERI-Rb1 group the fluorescence ratio increased only from 0.0998 ± 0.0001 ($t = 60$ s; $n = 57$) to 0.1135 ± 0.0008 ($t = 300$ s; $n = 57$; $p < 0.0001$) (Fig. 3b, d).

TRP-channel antagonists suppress Asc-induced Ca^{2+} influx

The contribution by TRP channel activation to Asc-induced rises was evaluated based on comparing the inhibitory effects of various modulators of this response. Both RB cell lines were individually pretreated with either 100 µM capsazepine (CPZ), 500 µM Lanthanum-III-chloride (La^{3+}), 10 mM n-acetyl cysteine (NAC), or 100 µM 2-aminoethyl diphenylborinate (2-APB). The results shown in Fig. 3c–f indicate that each of these inhibitors reduced Asc-induced increases in Ca^{2+} influx in both RB cell lines. Specifically, CPZ preincubation reduced the Asc-induced influx to 0.1278 ± 0.0026 ($t = 300$ s; $n = 43$; $p < 0.0001$) in etoposide-resistant WERI-Rb1 cells (Fig. 3c) and to 0.1036 ± 0.0004 ($t = 300$ s; $n = 45$; $p < 0.0001$) in etoposide-sensitive WERI-Rb1 cells (Fig. 3d). La^{3+} decreased the fluorescence ratios (f_{340}/f_{380}) in etoposide-resistant WERI-Rb1 cells to 0.1548 ± 0.0142 ($t = 300$ s; $n = 15$; $p < 0.0001$) and in etoposide-sensitive WERI-Rb1 cells to 0.1104 ± 0.0007 ($t = 300$ s; $n = 65$, $p < 0.005$), respectively (Fig. 3c, d). With NAC both RB cell lines were preincubated for 4–5 days, whereas preincubation time with the other TRP channel blockers was only 20–30 min [67]. This time for NAC is the longest possible because after a longer period cell viability declined, what affected measuring conditions. NAC also reduced the fluorescence ratios, in etoposide-resistant WERI-Rb1cells to 0.2344 ± 0.0103 ($t = 300$ s; $n = 56$; $p < 0.0001$) (Fig. 3e) and in etoposide-sensitive WERI-Rb1 cells to 0.1068 ± 0.0012 ($t = 300$ s; $n = 38$; $p < 0.0001$) (Fig. 3f). Preincubation with 2-APB reduced the fluorescence ratios to 0.1453 ± 0.0071 ($t = 300$ s; $n = 63$; $p < 0.0001$) in etoposide-resistant WERI-Rb1 cells (Fig. 3e) and to 0.1098 ± 0.0009 ($t = 300$ s; $n = 15$; $p < 0.05$) in etoposide-sensitive WERI-Rb1 cells (Fig. 3f). The inhibition of Asc-induced increases in intracellular Ca^{2+} levels shows that TRP channel activity contributes to these rises.

PTX suppresses Asc-induced Ca^{2+} influx

Since one of the effects of Asc is modulation of aminergic GPCRs in some cell types, both RB cell lines were preincubated with PTX (50 ng/ml) for 18 h to determine if Gi/o modulation by Asc contributes to controlling Ca^{2+} influx [68–71]. PTX preincubation blunted the Asc-induced rise in Ca^{2+} influx in both cell lines compared to untreated cells (Figs. 3a, b and 4a, b). Specifically, the fluorescence ratio in etoposide-resistant WERI-Rb1 only slightly increased from 0.1004 ± 0.0001 ($t = 60$ s) to 0.1038 ± 0.0003 ($t = 300$ s; $n = 107$; $p < 0.0001$) (Fig. 4a, c). Similarly, this ratio increased only to 0.1027 ± 0.0002 ($t = 300$ s; $n = 39$; $p < 0.0001$) in etoposide-sensitive WERI-Rb1 cells (Fig. 4b, c). Taken together, inactivation of Gi/o proteins nearly completely suppressed the Asc-induced activation of TRPs in both RB cell lines. This result suggests that Asc-induced stimulation of TRP activity is mediated through enhancement of a Gi/o coupled GPCR.

Asc-induced increases in intracellular Ca^{2+} levels depend on extracellular Ca^{2+}

To assess the source of Ca^{2+} in mediating the Asc-induced increases in intracellular Ca^{2+} levels, the effects of Asc on this response were determined in a Ca^{2+}-free bathing solution containing 1 mM EGTA. This substitution decreased the fluorescence ratio to 0.0865 ± 0.0018 ($t = 60$ s before Asc addition; $n = 11$) in etoposide-resistant WERI-Rb1 cells. 1 mM Asc supplementation instead decreased it further to 0.0766 ± 0.0021 ($t = 180$ s after Asc addition; $n = 11$; $p < 0.0001$) (Fig. 5a). These declines were essentially the same in the etoposide-sensitive WERI-Rb1 cells. Namely, replacing the extracellular Ca^{2+} containing solution with the Ca^{2+}-free bathing solution, the fluorescence ratio decreased to 0.0924 ± 0.0013 ($t = 60$ s before Asc addition; $n = 12$). Afterward, 1 mM Asc supplementation even further decreased this ratio to 0.0909 ± 0.0014 ($t = 180$ s after Asc addition; $n = 12$; $p < 0.0001$) (Fig. 5b). Taken together, these opposing effects of Asc in the absence of extracellular Ca^{2+} indicate that this oxidant induces rises in Ca^{2+} influx from the exterior through plasma membrane delimited pathways.

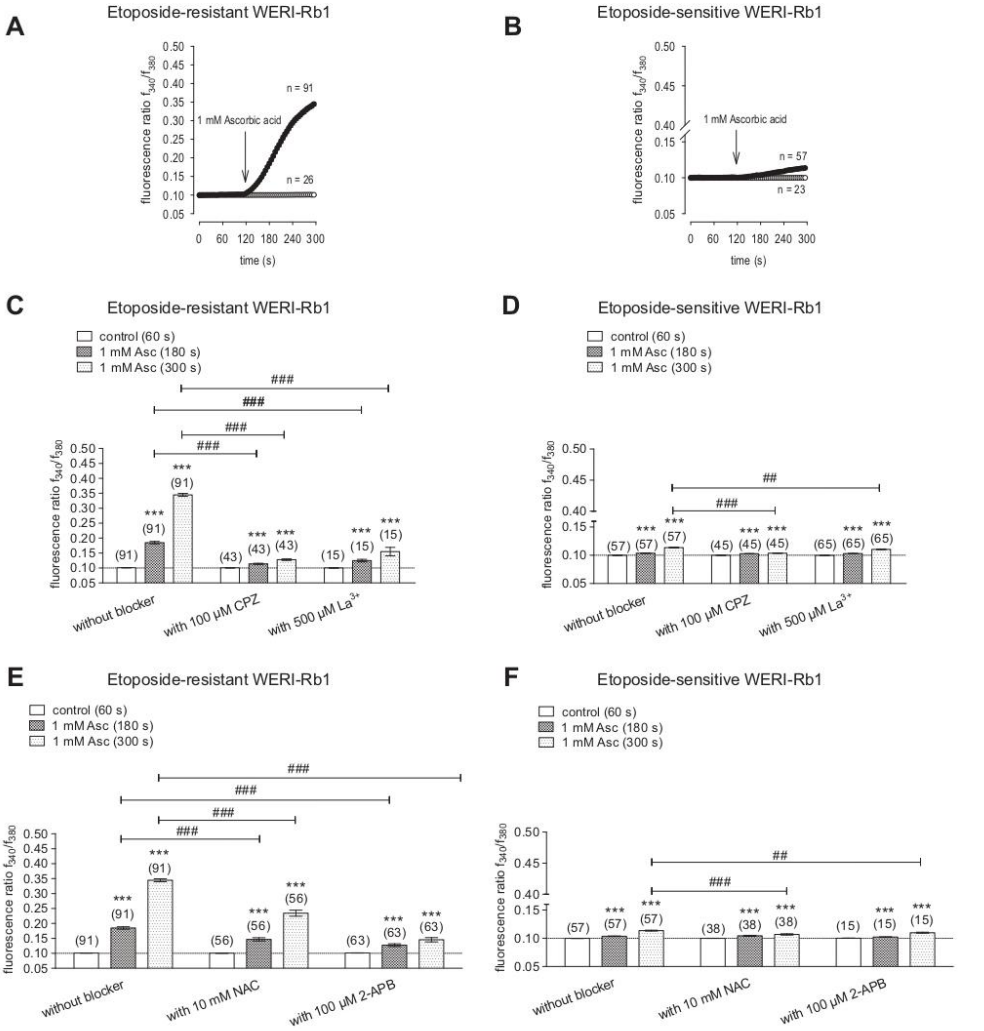

Fig. 3 1mM Asc induces an increase in intracellular Ca^{2+} influx in both RB cell lines. TRP-channel antagonists (CPZ, La^{3+}, NAC, and 2-APB) suppress Asc-induced Ca^{2+} influx. a 1 mM Asc led to an increase in intracellular Ca^{2+} influx ($n = 91$) in etoposide-resistant WERI-Rb1 cells, whereas non-treated control cells maintained a constant Ca^{2+} baseline ($n = 26$). **b** The same experiment as shown in (**a**) but carried out with etoposide-sensitive WERI-Rb1 cells. **c** Summary of the experiments with 1 mM Asc and TRP-channel antagonists (100 µM CPZ, 500 µM La^{3+}) in etoposide-resistant WERI-Rb1 cells. The asterisks (*) designate a significant increase in fluorescence ratios ($f_{340/380}$) in the groups of cells with and without TRP-channel antagonists after addition of Asc to the medium (paired tested). The hashtags (#) indicate significant differences in fluorescence ratios ($f_{340/380}$) (unpaired tested). **d** Summary of the same experiments as in (**c**) but with etoposide-sensitive WERI-Rb1 cells. **e** Summary of the experiments with 1 mM Asc and TRP-channel antagonists (10 mM NAC and 100 µM 2-APB) in etoposide-resistant WERI-Rb1 cells. The asterisks (*) designate a significant increase in fluorescence ratios ($f_{340/380}$) in the groups of cells with and without TRP-channel antagonists after addition of Asc to the medium (paired tested). The hashtags (#) indicate significant differences in fluorescence ratios ($f_{340/380}$) (unpaired tested). **f** Summary of the same experiments as in (**e**) but with etoposide-sensitive WERI-Rb1 cells (unpaired tested only at $t = 300$ s). Asc Ascorbic acid, CPZ Capsazepine, La^{3+} Lanthanum-III-chloride, NAC N-acetylcysteine, 2-APB 2-aminoethyl diphenylborinate.

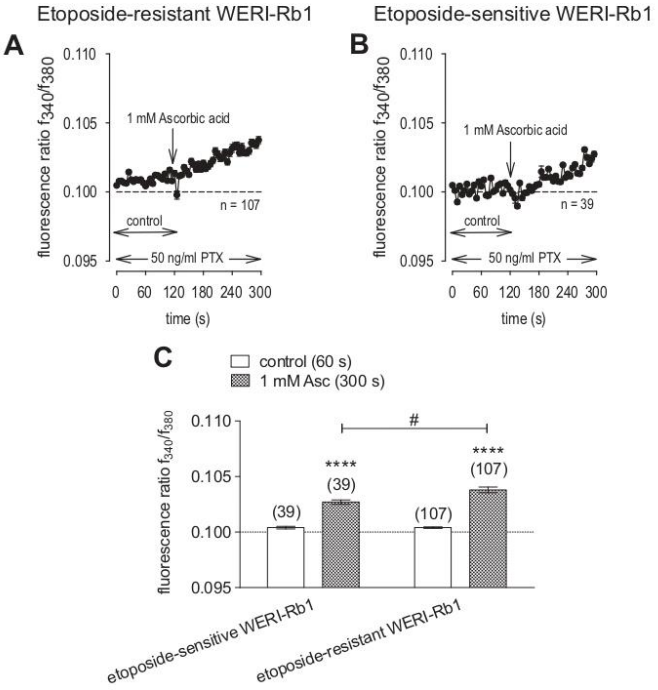

Fig. 4 PTX suppresses Asc-induced Ca^{2+} influx in both RB cell lines. a Mean trace of etoposide-resistant WERI-Rb1 cells after addition of 1 mM Asc to the medium bathing cells pretreated with 50 ng/ml PTX ($n = 107$) for 18 h. **b** Mean trace of etoposide-sensitive WERI-Rb1 cells after addition of 1 mM Asc to the medium bathing cells pretreated with 50 ng/ml PTX ($n = 39$). **c** Summary of Asc experiments in the presence of PTX in etoposide-sensitive and -resistant WERI-Rb1 cells. The asterisks (*) designate a significant increase in fluorescence ratios ($f_{340/380}$) after addition of Asc to the medium bathing each group of cells (paired tested) ($t = 300$ s). The hashtag (#) indicates a significant difference in fluorescence ratios ($f_{340/380}$) between both RB cell lines (unpaired tested).
PTX Pertussis toxin.

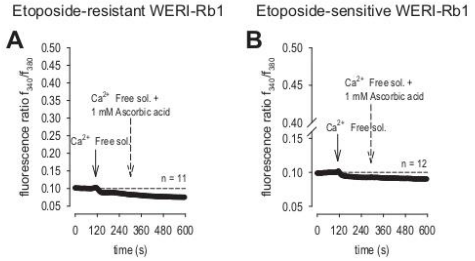

Fig. 5 Asc-induced intracellular Ca^{2+} increase depends on extracellular Ca^{2+} in the bathing medium. a Substitution of Ca^{2+} containing medium with Ca^{2+}-free solution led to a slight decrease of intracellular Ca^{2+} level in etoposide-resistant WERI-Rb1 cells ($n = 11$). Notable, addition of 1 mM Asc failed to increase the intracellular Ca^{2+} concentration as it took place in the presence of extracellular Ca^{2+}. **b** The same experiment as shown in (**a**), but carried out with etoposide-sensitive WERI-Rb1 cells ($n = 12$).

Asc induces increases in whole-cell currents

To confirm that 1 mM Asc-induced increases in Ca^{2+} influx are mainly reflective of the rises in ion channel currents, its effects were determined on whole-cell currents induced by applying a voltage ramp from −60 to + 130 mV, in both etoposide-resistant and -sensitive WERI-Rb1 cells. Specifically, in the etoposide-resistant WERI-Rb1 cells, the inward current density increased from -25 ± 2 pA/pF to -81 ± 8 pA/pF ($n = 16$; $p < 0.0005$). Similarly, the outward currents increased from 397 ± 38 pA/pF to 529 ± 51 pA/pF ($n = 16$; $p < 0.0001$) (Fig. 6a). Comparable results were observed in a group of etoposide-sensitive WERI-Rb1 cells. The inward current density increased from -24 ± 2 pA/pF to -66 ± 4 pA/pF ($n = 19$; $p < 0.0001$), while the outward currents increased markedly from 309 ± 23 pA/pF to 464 ± 34 pA/pF ($n = 19$; $p < 0.0005$) (Fig. 6b). Interestingly, there were no significant differences in the whole-cell current densities between both cell lines. These results confirm that Asc-induced increases in whole-cell currents underlie rises in Ca^{2+} influx.

TRP-channel antagonists suppress Asc-induced increases in whole-cell currents

TRP channel inhibitors were used at the same concentration as those in the Ca^{2+} imaging experiments, except for 2-APB that was not used. Each of them suppressed whole-cell currents in both etoposide-resistant and -sensitive WERI-Rb1

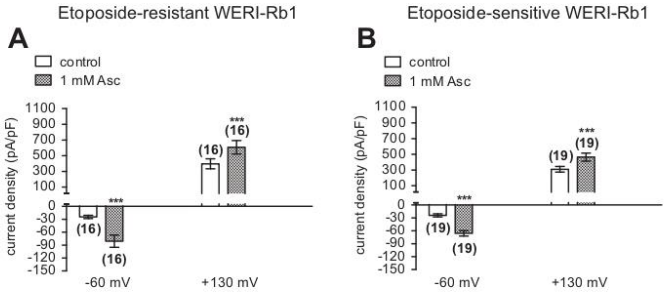

Fig. 6 1mM Asc induces increases in whole-cell currents in both etoposide-resistant and -sensitive WERI-Rb1 cells. a Summary of patch-clamp experiments with Asc in etoposide-resistant WERI-Rb1 cells ($n = 16$). The asterisks (*) indicate statistically significant increase in whole-cell currents after application of 1 mM Asc (paired tested). **b** Same summary as in (**a**) except etoposide-sensitive WERI-Rb1 cells are instead analyzed ($n = 19$). Asc Ascorbic acid.

cells. NAC suppressed the Asc-induced rises in inward currents in the etoposide-resistant WERI-Rb1 cells from -125 ± 11 pA/pF to -14 ± 1 ($n = 5$; $p < 0.05$), while the outward currents markedly decreased from 810 ± 70 pA/pF to 144 ± 13 pA/pF ($n = 5$; $p < 0.05$) (Figs. 7 and 9e). Similar results were obtained in etoposide-sensitive WERI-Rb1 cells. In this cell line, the inward current density decreased from -72 ± 3 pA/pF to -7 ± 0 pA/pF ($n = 5$; $p < 0.0005$), while the outward currents fell from 537 ± 34 pA/pF to 121 ± 5 pA/pF ($n = 5$; $p < 0.005$) (Figs. 8 and 9f). CPZ had similar effects since the inward current density in etoposide-resistant WERI-Rb1 cells declined from -69 ± 7 pA/pF to -18 ± 3 pA/pF ($n = 5$; $p < 0.05$) along with the outward currents, which decreased from 652 ± 42 pA/pF to 296 ± 33 pA/pF ($n = 5$; $p > 0.05$) (Fig. 9a, e). Similarly, in etoposide-sensitive WERI-Rb1 the inward current density decreased from -57 ± 5 pA/pF to -21 ± 2 pA/pF ($n = 6$; $p < 0.005$), which was accompanied by declines in the outward currents from 394 ± 30 pA/pF to 281 ± 24 pA/pF ($n = 6$; $p > 0.05$) (Fig. 9c, f). With La^{3+}, the inward currents in etoposide-resistant WERI-Rb1 cells decreased from -61 ± 5 pA/pF to -15 ± 1 pA/pF ($n = 4$; $p < 0.05$) along with the outward currents, which fell from 451 ± 25 pA/pF to 233 ± 21 pA/pF ($n = 4$; $p < 0.05$) (Fig. 9b, e). Also, in etoposide-sensitive WERI-Rb1 cells, the inward current density decreased from -63 ± 3 pA/pF to -20 ± 2 pA/pF ($n = 7$; $p < 0.0005$). The outward currents were suppressed from 414 ± 32 pA/pF to 203 ± 12 ($n = 7$; $p < 0.005$) in the presence of La^{3+} (Fig. 9d, f). These inhibitory effects confirm that Asc-induced TRP channel activation contributes to increases in Ca^{2+} influx.

Medium acidification has less influence on Ca^{2+} regulation

As medium acidification is one of the factors that can induce TRP channel activation, we determined if such a change contributes to how Asc stimulates TRPs. This possibility warranted consideration since 1 mM Asc decreased the bathing solution pH from ~7.35 to ~7.15, at room temperature ~20–23 °C. To replicate such a decline, we determined if merely acidifying the bathing solution with HCl also increased the fluorescence ratio f_{340}/f_{380} in RB cells. Indeed, the fluorescence level slightly rose from 0.1004 ± 0.0001 to 0.1073 ± 0.0008 ($t = 300$ s; $n = 39$; $p < 0.0001$), in etoposide-resistant WERI-Rb1 cells. Similarly, this ratio increased from 0.0999 ± 0.0001 to 0.1033 ± 0.0004 ($t = 300$ s; $n = 37$; $p < 0.0001$) in etoposide-sensitive WERI-Rb1 cells (Fig. 10). Taken together, minor medium acidification slightly increased intracellular Ca^{2+}, but the effect is too small to fully account for how Asc stimulates TRPs.

Asc suppresses RB cell viability

The cell culture images shown in Figs. 11 and 12 are indicative of the cytotoxic effects of 1 mM Asc in both the etoposide-sensitive and -resistant WERI-Rb1 cell groups. After 4 days of incubating freshly diluted cells with Asc, the cell densities declined in both types of RB cells (Fig. 11a, b, f, g). Comparing Fig. 11b vs. d and Fig. 11g vs. i shows that the cell densities fell compared to those in untreated cells. Diluting the medium with fresh RPMI-1640 medium led to a recovery of the cell density. Interestingly, these rescued cells failed to cluster together to form any compact groups (Fig. 11b, c, g, h). In the second set of experiments, 1 mM Asc was added to the medium 4 days after the cells were passaged. Subsequently, these clumped groups separated during the time when the cell density progressively declined (Fig. 11d, e, i, j).

To determine if declines in cell density are reflective of losses in cell viability, Trypan Blue dye exclusion was used to evaluate the viability of RB cells after 4 days in culture

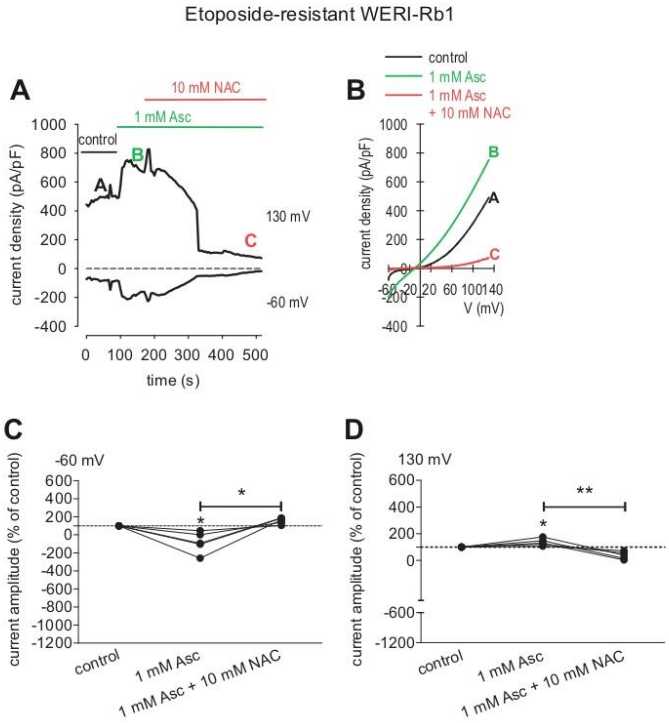

Fig. 7 NAC blocks the Asc-induced increase in whole-cell currents in etoposide-resistant WERI-Rb1 cells. a Time course recording of the currents increase induced by 1 mM Asc and currents decrease after application of 10 mM NAC. **b** Original traces of Asc-induced current responses to voltage ramps [current/voltage plot (I-V plot)]. Current densities are shown as a control without drugs (black trace labeled as A), during application of 1 mM Asc (green trace labeled as B) and after addition of 10 mM NAC (red trace labeled as C). Calculated current densities obtained by normalizing currents to membrane capacitance as function of imposed voltage were derived from the traces shown in (**a**). **c** Maximal negative inward current amplitudes induced by a voltage step from 0 mV to −60 mV, shown in percent of control values before application of drugs (control set to 100%). The asterisks (*) designate a significant increase in inward currents after application of 1 mM Asc and a significant suppression of inward currents after addition of 10 mM NAC (paired tested). **d** Same diagram but related to maximal outward current amplitudes induced by a voltage step from 0 mV to +130 mV. Asc Ascorbic acid, NAC N-acetylcysteine.

(in the first set of experiments) (Fig. 12). In etoposide-resistant WERI-Rb1, the percentage of dead cells increased from 6.1 ± 0.6% ($n = 8$) in the untreated group shown in Fig. 12a (analogical to Fig. 11d) to 93.7 ± 1.5% ($n = 16$) ($p = 0.0001$) in the Asc-treated counterpart shown in Fig. 12b (analogical to Fig. 11b). Similarly, this percentage increased from 5.8 ± 1.0% ($n = 8$) to 93.9 ± 1.3% ($n = 16$) ($p = 0.0001$) in the etoposide-sensitive WERI-Rb1 cells. This difference is evident by comparing the results shown in Fig. 12c, d (analogical to Fig. 11i, g).

In summary, 1 mM Asc led to the cell death as indicated by the declines in the density of etoposide-resistant and etoposide-sensitive WERI-Rb1 cells, which was partially reversible upon dilution with fresh medium.

Discussion

In agreement with numerous studies in other cell lines, we show here that a 1 mM pharmacological dose of Asc had similar cytotoxic effects on both etoposide-resistant and -sensitive WERI-Rb1 cells through acting allegedly as an oxidant [44, 47, 50]. The results indicate that these declines in cell viability are mediated through increases in Gi/o activity which in turn stimulate TRP channels resulting in increases in intracellular Ca^{2+} influx. At this concentration, it is presumed that Asc acts as prooxidant and generates H_2O_2 and ROS as well as other oxidative species, which reduce cell viability [39, 54]. Therefore, our results provide for

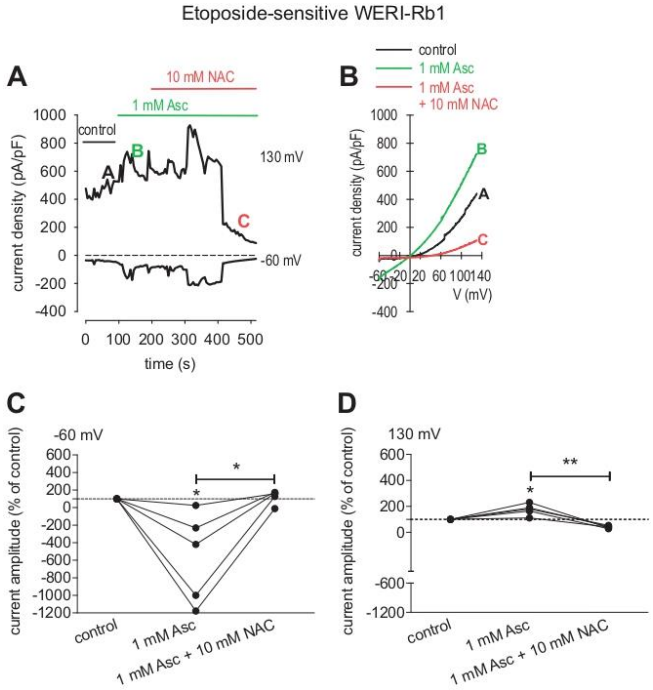

Fig. 8 NAC blocks the Asc-induced increase in whole-cell currents in etoposide-sensitive WERI-Rb1 cells. a Time course recording of the currents increase induced by 1 mM Asc and currents decrease after application of 10 mM NAC. **b** Original traces of Asc-induced current responses to voltage ramps [current/voltage plot (I-V plot)]. Current densities are shown as a control without drugs (black trace labeled as A), during application of 1 mM Asc (green trace labeled as B) and after addition of 10 mM NAC (red trace labeled as C). Calculated current densities obtained by normalizing currents to membrane capacitance as function of imposed voltage were derived from the traces shown in (**a**). **c** Maximal negative inward current amplitudes induced by a voltage step from 0 mV to -60 mV, shown in percent of control values before application of drugs (control set to 100%). The asterisks (*) designate a significant increase in inward currents after application of 1 mM Asc and a significant suppression of inward currents after addition of 10 mM NAC (paired tested). **d** Same diagram but related to maximal outward current amplitudes induced by a voltage step from 0 mV to +130 mV. Asc Ascorbic acid, NAC N-acetylcysteine.

the first time some insight into an interaction between Gi/o coupled GPCR and TRP activity in mediating Asc-induced cytotoxicity in both etoposide-sensitive and -resistant WERI-Rb1 cells.

A pattern of TRP channel gene expression was identified that agrees with a previously identified grouping in both WERI-Rb1 cell lines (i.e., Fig. 2) [11, 23]. Since both a battery of a relatively selective TRP channel antagonists combined with broad spectrum Ca^{2+} channel blockers inhibited Asc-induced rises in Ca^{2+} influx, activation of different TRP channel subtypes contributes to this response in RB cells (Fig. 3). Asc failed to increase such influx during exposure to PTX, suggesting that TRP channel activation is dependent on Asc interaction with the Gi/o coupled GPCR proteins (Fig. 4).

It is already known that excessive uncompromised rises in intracellular Ca^{2+} levels can lead to cell death or deregulate cancerogenic pathways [72, 73]. However, the identity of the mechanisms mediating such control still requires clarification. This study revealed for the first time that TRP channel activation on the cell membrane contributes to the Asc-induced Ca^{2+} influx in RB cells (Figs. 5–9). Mimicking with HCl addition the slight acidifying effect of Asc, it had a minor impact on intracellular Ca^{2+} levels. This suggests that a small decline in pH is not the sole mechanism accounting for how Asc induces TRP activation (Fig. 10). In the presence of Asc, RB cell density markedly declined due to inhibition of cell viability (Figs. 11 and 12). This cytotoxic effect of Asc agrees with similar studies reporting reduced viability of

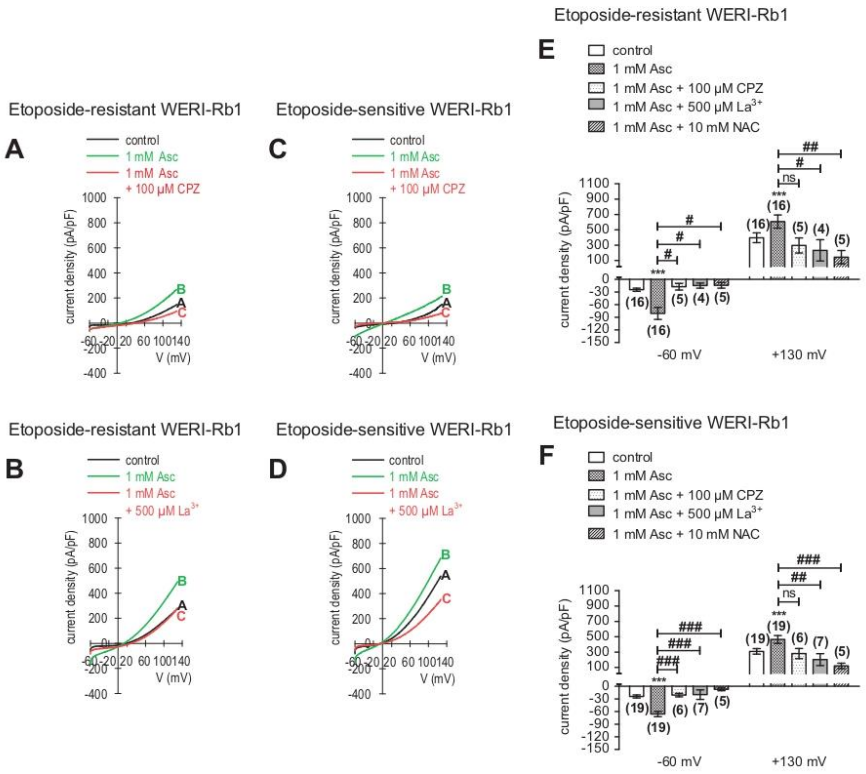

Fig. 9 TRP antagonists (CPZ, LA^{3+}, NAC) can block Asc-induced increase in whole-cell currents in both etoposide-resistant and -sensitive WERI-Rb1 cells. a Original traces of Asc-induced current responses to voltage ramps [current/voltage plot (I-V plot)] in etoposide-resistant WERI-Rb1 cells. Current densities are shown as a control without drugs (labeled as A), during application of 1 mM Asc (labeled as B) and after addition of 100 µM CPZ (labeled as C). **b** The same experiment as in (**a**), but with 500 µM La^{3+} in etoposide-resistant WERI-Rb1 cells. **c** Same experiment as in (**a**) but with etoposide-sensitive WERI-Rb1 cells. **d** Same experiment as in (**b**) but with etoposide-sensitive WERI-Rb1 cells. **e** Summary of patch-clamp experiments with Asc and TRP-channel antagonists (CPZ, La^{3+}, NAC) in etoposide-resistant WERI-Rb1. The asterisks (*) indicate a significant increase in whole-cell currents after application of 1 mM Asc (paired tested). The hashtags (#) designate significant decreases in whole-cell currents after adding TRP-channel antagonists (100 µM CPZ, 500 µM La^{3+}, 10 mM NAC) (unpaired tested). ns not significant (unpaired tested). **f** Same summary as in (**e**) but concerning etoposide-sensitive WERI-Rb1 cells. Asc Ascorbic acid, CPZ Capsazepine, La^{3+} Lanthanum-III-chloride, NAC N-acetylcysteine.

cells treated with ascorbate [47]. Interestingly, the Asc-induced Ca^{2+} increases in etoposide-resistant WERI-Rb1 cells were greater than those in etoposide-sensitive WERI-Rb1 cells. This difference suggests that Asc could be used as an anti-cancer adjuvant to overcome etoposide resistance that may be present in some types of cancerous growth.

Role of Asc

Asc has numerous possible modes of action including mediating cellular redox reactions [50, 54]. In addition, Asc can directly modulate different receptors such as GABA [74]. Furthermore, Asc at concentrations of 1 mM or higher is able to inhibit tumor growth [75]. By acting as an oxidant, Asc generates H_2O_2 through reactions such as autooxidation [54]. Notably, H_2O_2 is the central redox molecule in oxidative stress [50, 76, 77] and was suggested to be the main factor that limited cell viability [39, 54]. Furthermore, cell death is dependent on extracellular but not intracellular Asc since this cytotoxic effect is mediated by extracellular H_2O_2 [49]. Interestingly, Chen et al. suggested that ascorbate radicals and H_2O_2 were present only in the extracellular fluid but were not

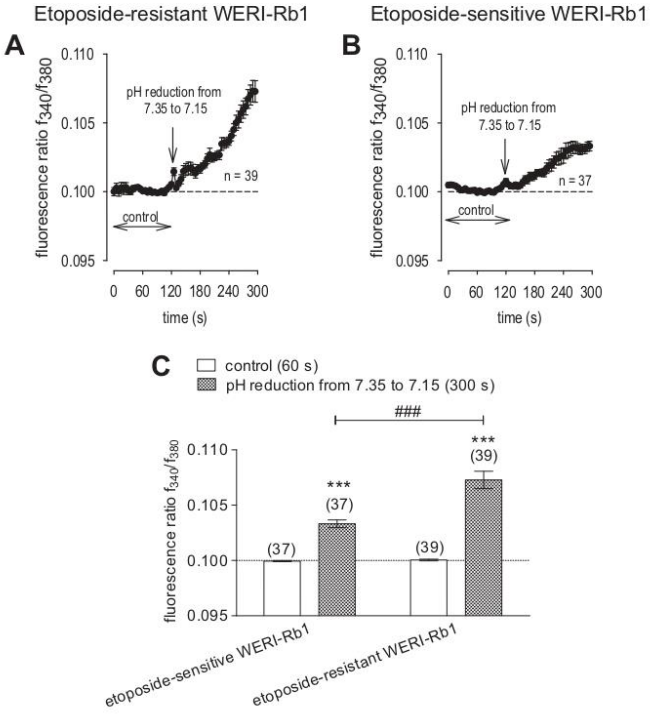

Fig. 10 Medium acidification has less influence on Ca^{2+} regulation. a Mean trace of etoposide-resistant WERI-Rb1 cells under pH reduction (i.e., from 7.35 to 7.15) ($n = 39$). **b** Mean trace of etoposide-sensitive WERI-Rb1 cells under pH reduction (i.e., from 7.35 to 7.15) ($n = 37$). **c** Summary of pH reduction experiments compared to control values of etoposide-sensitive and -resistant WERI-Rb1 cells. pH reduction induced larger Ca^{2+} influx in etoposide-resistant WERI-Rb1 cells. The asterisks (*) designate a significant increase in fluorescence ratios ($f_{340/380}$) after pH reduction in each group of cells (paired tested) ($t = 300$ s). The hashtags (#) indicate significant differences in fluorescence ratios ($f_{340/380}$) between both RB cell lines (unpaired tested).

detectable in whole blood [78]. The cell viability was also affected by intracellular GSH (glutathione) depletion, which increased oxidative stress [54] and by autophagy-associated caspase-independent cell death [79]. Moreover, Asc-induced oxidative stress can disrupt mitochondrial function [80]. Noteworthy is the finding that millimolar levels of extracellular Asc selectively induce tumor cell death [49, 50].

Mechanisms of Asc-induced TRP-channel activation

We hypothesized that TRP channel subtypes are involved in mediating the cytotoxic effects of oxidant promoting Asc since some of them are sensitive to oxidative stress. They include: TRPA1 [81, 82], TRPV4 [83], TRPM7 [84], TRPM2, and TRPC5 [80, 85, 86]. Besides, TRPM7 channel modulation also affects RB cell growth [23]. Furthermore, changes in TRPV1 and TRPM8 expression levels were reported to play a significant role in tumorigenesis [87]. We investigated both functional and genetic expression of these channels in etoposide-resistant and -sensitive WERI-Rb1 cells. Accordingly, the effects were determined of the TRP channel antagonists with different specificity and selectivity, i.e., 100 µM CPZ that blocks TRPV1 and TRPM8 and 500 µM La^{3+} which is a broad spectrum Ca^{2+} channel blocker [88]. Moreover, CPZ can also potentiate the apoptotic effects of TRAIL (TNF-related apoptosis-inducing ligand) via ROS-JNK-CHOP pathway or downregulate the nuclear transcription factor-kappa B (NF-κB) [89, 90]. The non-selective inhibitors included also 2-APB (100 µM) which blocks TRPC5 and presumably TRPM2 as well as store operated calcium channel entry [67, 91–93]. Another broad-spectrum antagonist was 10 mM NAC, which blocks TRPA1, TRPV1, and TRPM2 [67, 94–96]. Besides, NAC has this classification, because it can also quench free radicals and impact GSH regeneration [96]. As several reports suggested using a longer pretreatment period [67, 95], we incubated the RB cells for up to 5 days with NAC rather than ~20–30 min, which was the incubation time for all the other antagonists. This was the longest period that did not reduce cell viability and did not impact measuring conditions. As the inhibitory effects of NAC were at some times larger than those of other inhibitors, it is conceivable that Asc induces rises in Ca^{2+} influx through additional pathways.

The effects of Asc were dependent on Gi/o interaction with TRP channels since preincubation with PTX inhibited

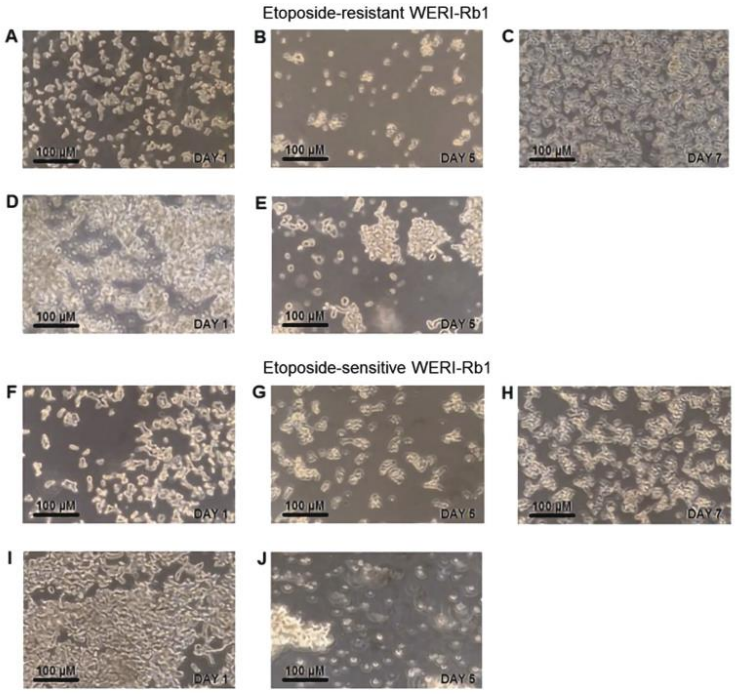

Fig. 11 Effects of exposure to Asc on RB cell viability (a–e—etoposide-resistant WERI-Rb1 cells; f–j—etoposide-sensitive WERI-Rb1 cells). **a** Microscopic image of freshly diluted cells on the first day. Subsequently, 1 mM Asc was added. **b** The same cells as shown in (**a**), but on the fifth day after Asc treatment. A clear reduction of cell density is visible. Subsequently, medium dilution with fresh RPMI-1640 medium. **c** The same cells as in (**a**) and (**b**), but 2 days after adding fresh RPMI-1640 medium. The cell density again increased. **d** Microscopic image showing etoposide-resistant WERI-Rb1 cells which were maintained for 4 days in culture. At this time, 1 mM Asc was added. **e** The same cells as in (**d**), but on the fifth day after Asc treatment. The cell density declined. **f–j** The same experimental design as that shown in (**a–e**), but etoposide-sensitive WERI-Rb1 cells were used. Similar to the etoposide-resistant WERI-Rb1 cells, cell density declined after Asc treatment and recovered after diluting the medium.

Asc-induced increases in Ca^{2+} influx through these channels (Fig. 4). This dependence is in accord with other studies showing that GPCR activation triggers TRPs and vice versa (reviewed by Veldhuis et al. [37]). Furthermore, Asc is a well-characterized aminergic GPCR enhancer and many aminergic GPCRs are coupled to Gi/o [68] (Fig. 13).

The effects of Asc are dependent on its interaction with plasma membrane delimited channels since Asc had no effects on intracellular Ca^{2+} levels in an external Ca^{2+}-free medium (Fig. 5). A similar dependence was reported for some other drugs [97].

Extracellular Asc application increased the inward and outward currents in both RB cell types. The correspondence between the Asc-induced increases in currents, Ca^{2+} transients, and the effects of the different blockers indicates that most of the current increases are attributable to a rise in Ca^{2+} influx (Figs. 6–9). Even though it is uncertain if 1 mM Asc induces these changes through acting as an oxidant, some studies show that increases in H_2O_2 generation induce TRP channel activation [98–102].

Since some TRPs are pH-sensitive and 1 mM Asc decreased the medium pH by 0.2 pH units (i.e., from ~7.35 to ~7.15), we determined if such an effect on pH by Asc accounts for TRP channel activation. Significant increases in Ca^{2+} influx were detected, but they were much smaller than those induced by 1 mM Asc (Fig. 10). Therefore, it is unlikely that these Ca^{2+} increases were induced by a decline in pH since a potentiating effect on TRP-induced mean current amplitude was reported to occur only if the medium pH was lowered below 6.0 [103–105]. In this case, these cell lines possibly possess other pH sensitive pathways since we still observed significant increases in Ca^{2+} influx. Interestingly, Garrity et al. also reported that TRP channel responses increased with decreasing pH, but these effects were probably caused by intracellular rather than by extracellular pH changes [106]. Therefore, pH acidification is unlikely to account for TRP channel activation since in this study the bathing solution pH was always >7.0.

It is noteworthy that there is a lack of correlation between the levels of functional TRP expression and corresponding gene expression levels in the two different cell types. In some other studies such a disconnect has been attributed to the possibility that mRNA turnover is variable due to modulation by other factors. Perhaps there is a closer correspondence instead between protein expression level changes and functional activity since protein expression turnover frequently occurs less rapidly than mRNA expression levels.

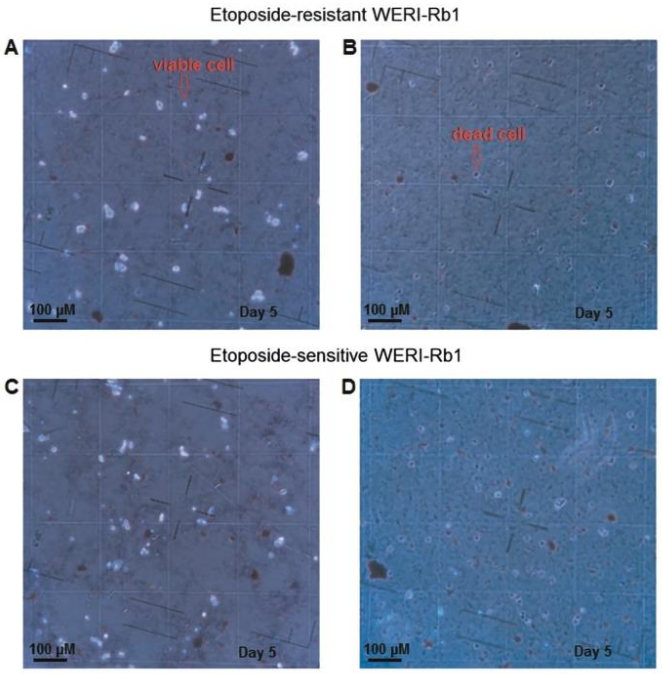

Fig. 12 1mM Asc suppresses RB cell viability. Trypan Blue dye exclusion capability is compared between control and Asc-exposed WERI-Rb1 cells, on the fifth day after Asc treatment. In the background, is shown the cell counting chamber divided into square fields. **a** Light microscopic image of etoposide-resistant WERI-Rb1 cells. Most cells are viable (e.g., marked with a red arrow)—excluded the Trypan Blue dye. **b** The same group of cells as in (**a**), but exposed to 1 mM Asc. Most cells are dead (e.g., marked with a red arrow)—Trypan Blue dye stains cell interior. **c**, **d** These panels show the same conditions as in (**a**, **b**) except that a group of etoposide-sensitive WERI-Rb1 cells are shown instead.

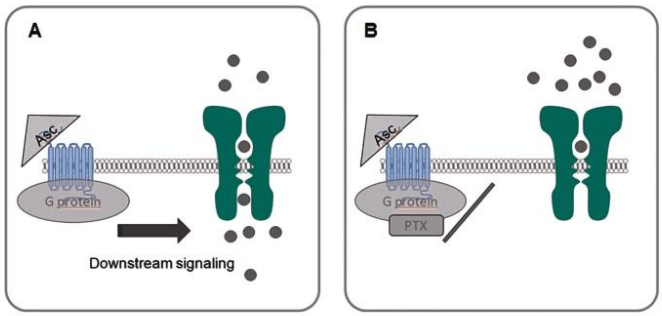

Fig. 13 Schematic illustration of PTX effect on TRP channel. GPCRs (blue) and TRP channels (green) are often co-expressed in cells. It is accepted that activation of GPCRs modify the function of TRPs [37]. **a** Asc was reported as a modulator of aminergic GPCRs [68] and thereby might enhance the constitutive activity of these receptors. Therefore, downstream signaling effects might stimulate the activity of TRPs. **b** PTX is known to ADP-ribosylation of Gi/o proteins [71] that result in their inaction, thus reduce the activity of TRPs. Asc Ascorbic acid, PTX Pertussis toxin.

RB cells viability under Asc incubation

Chen et al. suggested that Asc can affect the viability of breast, lung, renal, ovarian, and other cancer cells. They calculated the Asc concentration that was able to reduce cell survival by 50% [47]. Asc was also reported to affect the viability of Y-79 RB cell line [48]. In the current study, Trypan Blue dye exclusion was used to determine the effects of 1 mM Asc on cell viability. Such treatment decreased cell density in both etoposide-resistant and -sensitive WERI-Rb1 cells (Fig. 11a, b, f, g), compared to the untreated control groups (Fig. 11b vs. d; Fig. 11g vs i). Furthermore, Asc also

dispersed preformed cell clusters (Fig. 11d, e, i, j). As shown in Fig. 11b, c, g, h, the reversal of declines in cell density may be attributable to a decrease in Asc concentration due to dilution of the medium and to the fact that after 5 days of Asc incubation about 6% of the cells retained viability in the cell culture (Fig. 12). The cytotoxic effects of a pharmacological dose of Asc could stem from increases in H_2O_2 generation, which was reported to promote cell death [49]. Such effects in another study induced apoptosis in podocytes [107]. Similarly, Asc-induced ROS-dependent apoptosis in thyroid cancer cells [108]. Comparable effects were obtained in breast cancer cells or retinal ganglion cells, independent from increases in H_2O_2 generation [109, 110]. Future studies are warranted to determine if Asc decreases RB cell viability through the same mechanisms described in a number of other different cancer cell types.

Clinical relevance

Many studies described the possible therapeutic effects of Asc in different types of cancers [44, 46, 47, 49, 50, 54, 79, 111]. Nowadays, in an era of increasing numbers of cancer patients, more options are needed to improve therapeutic management of this disease.

In some clinical studies similar to those performed by Riordan et al., Asc is administered in a trial called "Riordan therapy" [39]. This group developed a protocol for administering a high intravenous Asc dose. It is likely that the Asc concentration is high enough for it to act as an oxidant rather than as a reductant. By acting as an oxidant, it promotes H_2O_2 generation and cytotoxicity, which is responsible for reducing cancer cell expansion [39, 54]. The current study is unique because it shows that Asc induces increase in cytotoxicity in RB cells through interacting with the Gi/o signaling pathway axis which in turn elicits increases in TRP channel activity followed by rises in intracellular Ca^{2+} influx. These results are relevant since TRPs were reported as an important factor in tumorigenesis [34, 112]. Furthermore, the current findings have an impact on gaining insight into how Ca^{2+} homeostasis is maintained and such control plays an important role in apoptosis and other cellular processes [13, 16, 113].

As already reported, targeting certain TRPs with either Asc or other drugs could serve as a main or supportive kind of cure in tumor diseases [114–118].

Since Asc-induced Ca^{2+} influx was larger in etoposide-resistant WERI-Rb1 cells than in the etoposide-sensitive WERI-Rb1 cells, Asc has the potential to serve as an adjuvant to improve the therapy of not only etoposide-sensitive but also cytostatic-resistant tumor cells.

Acknowledgements We thank Petra Temming, Alexander Schramm, and Harald Stephan (University of Duisburg-Essen, Essen, Germany) for providing the etoposide-sensitive and -resistant WERI-Rb1 cell lines. Kindly, Andreas Faissner (Department of Cell Morphology and Molecular Neurobiology, Faculty of Biology and Biotechnology, Ruhr University Bochum) supported this study. Finally, we thank May Amer, Stephanie Chun, and Sandra Lata for excellent technical assistance. Open Access funding provided by Projekt DEAL.

Funding SM was supported by the German Research Foundation (DFG, ME 1706/18-1) for a TRP channel related research project. The planar patch-clamp equipment and parts of the photometry setup were partially funded by Sonnenfeld-Stiftung (Berlin, Germany). VK was supported by Dr. Werner Jackstädt-Stiftung (S 134-10.063) and the KinderAugenKrebsStiftung (KAKS 20191118 f - UKM). MMK was supported by the Karl und Charlotte Spohn Stiftung.

Author contributions JO designed the study, analyzed the data, wrote and edited the manuscript. JR and MMK performed and evaluated qRT-PCR analyses. SM, VK, JR, PSR, and HB contributed with their expertise, discussed data and their interpretation, and helped to edit the manuscript. JO and SM performed calcium measurements and plot analyses. JO performed planar patch-clamp recordings as well as corresponding plot analyses. JO, JR, MMK, and SM created diagrams. SL, HL, and MBS performed calcium measurements and plot analyses concerning supplemented data.

Compliance with ethical standards

Conflict of interest The authors declare that the research was conducted in the absence of any commercial or financial relationships that could be construed as a potential conflict of interest.

Publisher's note Springer Nature remains neutral with regard to jurisdictional claims in published maps and institutional affiliations.

References

1. Dimaras H, Corson TW. Retinoblastoma, the visible CNS tumor: a review. J Neurosci Res. 2019;97:29–44.
2. Lohmann D, Gallie B, Dommering C, Gauthier-Villars M. Clinical utility gene card for: retinoblastoma. Eur J Hum Genet. 2011;19. https://doi.org/10.1038/ejhg.2010.200.
3. Dimaras H, Corson TW, Cobrinik D, White A, Zhao J, Munier FL, et al. Retinoblastoma. Nat Rev Dis Primers. 2015;1:15021.
4. Naseripour M. "Retinoblastoma survival disparity": the expanding horizon in developing countries. Saudi J Ophthalmol. 2012;26:157–61.
5. Control UfIC. RETINOBLASTOMA. review of cancer medicines on the WHO list of essential medicines. WHO; 2014.

https://www.who.int/selection_medicines/committees/expert/20/applications/Retinoblastoma.pdf?ua=1.
6. Busch M, Papior D, Stephan H, Dünker N. Characterization of etoposide- and cisplatin-chemoresistant retinoblastoma cell lines. Oncol Rep. 2018;39:160–72.
7. Bernardini M, Fiorio Pla A, Prevarskaya N, Gkika D. Human transient receptor potential (TRP) channel expression profiling in carcinogenesis. Int J Dev Biol. 2015;59:399–406.
8. Shapovalov G, Ritaine A, Skryma R, Prevarskaya N. Role of TRP ion channels in cancer and tumorigenesis. Semin Immunopathol. 2016;38:357–69.
9. Fels B, Bulk E, Pethő Z, Schwab A. The role of TRP channels in the metastatic cascade. Pharmaceuticals (Basel). 2018;11. https://www.mdpi.com/1424-8247/11/2/48.
10. Mergler S, Derckx R, Reinach PS, Garreis F, Böhm A, Schmelzer L, et al. Calcium regulation by temperature-sensitive transient receptor potential channels in human uveal melanoma cells. Cell Signal. 2014;26:56–69.
11. Mergler S, Cheng Y, Skosyrski S, Garreis F, Pietrzak P, Kociok N, et al. Altered calcium regulation by thermosensitive transient receptor potential channels in etoposide-resistant WERI-Rb1 retinoblastoma cells. Exp Eye Res. 2012;94:157–73.
12. Garreis F, Schröder A, Reinach PS, Zoll S, Khajavi N, Dhandapani P, et al. Upregulation of transient receptor potential vanilloid type-1 channel activity and Ca2+ influx dysfunction in human pterygial cells. Invest Ophthalmol Vis Sci. 2016;57:2564–77.
13. Decuypere JP, Bultynck G, Parys JB. A dual role for Ca(2+) in autophagy regulation. Cell Calcium. 2011;50:242–50.
14. Dubois C, Vanden Abeele F, Prevarskaya N. Targeting apoptosis by the remodelling of calcium-transporting proteins in cancerogenesis. FEBS J. 2013;280:5500–10.
15. Shinomiya T, Li XK, Amemiya H, Suzuki S. An immunosuppressive agent, FTY720, increases intracellular concentration of calcium ion and induces apoptosis in HL-60. Immunology. 1997;91:594–600.
16. Varghese E, Samuel SM, Sadiq Z, Kubatka P, Liskova A, Benacka J, et al. Anti-cancer agents in proliferation and cell death: the calcium connection. Int J Mol Sci. 2019;20. https://www.mdpi.com/1422-0067/20/12/3017.
17. Clapham DE, Runnels LW, Strübing C. The TRP ion channel family. Nat Rev Neurosci. 2001;2:387–96.
18. Flockerzi V. An introduction on TRP channels. Handb Exp Pharmacol. 2007;179:1–19.
19. Nilius B, Owsianik G, Voets T, Peters JA. Transient receptor potential cation channels in disease. Physiol Rev. 2007;87:165–217.
20. Song MY, Yuan JX. Introduction to TRP channels: structure, function, and regulation. Adv Exp Med Biol. 2010;661:99–108.
21. Barnes S, Haynes LW. Low-voltage-activated calcium channels in human retinoblastoma cells. Brain Res. 1992;598:19–22.
22. Hirooka K, Bertolesi GE, Kelly ME, Denovan-Wright EM, Sun X, Hamid J, et al. T-Type calcium channel alpha1G and alpha1H subunits in human retinoblastoma cells and their loss after differentiation. J Neurophysiol. 2002;88:196–205.
23. Hanano T, Hara Y, Shi J, Morita H, Umebayashi C, Mori E, et al. Involvement of TRPM7 in cell growth as a spontaneously activated Ca2+ entry pathway in human retinoblastoma cells. JPharmacolSci. 2004;95:403–19.
24. Tominaga M, Caterina MJ. Thermosensation and pain. J Neurobiol. 2004;61:3–12.
25. Gees M, Owsianik G, Nilius B, Voets T. TRP channels. Compr Physiol. 2012;2:563–608.
26. Khajavi N, Reinach PS, Skrzypski M, Lude A, Mergler S. L-carnitine reduces in human conjunctival epithelial cells hypertonic-induced shrinkage through interacting with TRPV1 channels. Cell Physiol Biochem. 2014;34:790–803.
27. Devi S, Kedlaya R, Maddodi N, Bhat KM, Weber CS, Valdivia H, et al. Calcium homeostasis in human melanocytes: role of transient receptor potential melastatin 1 (TRPM1) and its regulation by ultraviolet light. AmJPhysiol Cell Physiol. 2009;297:C679–C687.
28. Murayama T, Maruyama IN. Alkaline pH sensor molecules. J Neurosci Res. 2015;93:1623–30.
29. Vriens J, Appendino G, Nilius B. Pharmacology of vanilloid transient receptor potential cation channels. Mol Pharmacol. 2009;75:1262–79.
30. Venkatachalam K, Montell C. TRP channels. Annu Rev Biochem. 2007;76:387–417.
31. Prevarskaya N, Skryma R, Shuba Y. Ion channels in cancer: are cancer hallmarks oncochannelopathies? Physiol Rev. 2018;98:559–621.
32. Fixemer T, Wissenbach U, Flockerzi V, Bonkhoff H. Expression of the Ca2+-selective cation channel TRPV6 in human prostate cancer: a novel prognostic marker for tumor progression. Oncogene. 2003;22:7858–61.
33. Zhang L, Barritt GJ. TRPM8 in prostate cancer cells: a potential diagnostic and prognostic marker with a secretory function? Endocr Relat Cancer. 2006;13:27–38.
34. Prevarskaya N, Ouadid-Ahidouch H, Skryma R, Shuba Y. Remodelling of Ca2+ transport in cancer: how it contributes to cancer hallmarks? Philos Trans R Soc Lond B Biol Sci. 2014;369:20130097.
35. Regard JB, Sato IT, Coughlin SR. Anatomical profiling of G protein-coupled receptor expression. Cell. 2008;135:561–71.
36. Yekkirala AS. Two to tango: GPCR oligomers and GPCR-TRP channel interactions in nociception. Life Sci. 2013;92:438–45.
37. Veldhuis NA, Poole DP, Grace M, McIntyre P, Bunnett NW. The G protein-coupled receptor-transient receptor potential channel axis: molecular insights for targeting disorders of sensation and inflammation. Pharmacol Rev. 2015;67:36–73.
38. Altier C, Zamponi GW. Analysis of GPCR/ion channel interactions. Methods Mol Biol. 2011;756:215–25.
39. Riordan NH, Riordan HD, Meng X, Li Y, Jackson JA. Intravenous ascorbate as a tumor cytotoxic chemotherapeutic agent. Med Hypotheses. 1995;44:207–13.
40. Riordan HD, Riordan NH, Jackson JA, Casciari JJ, Hunninghake R, González MJ, et al. Intravenous vitamin C as a chemotherapy agent: a report on clinical cases. P R Health Sci J. 2004;23:115–8.
41. Riordan HD, Casciari JJ, González MJ, Riordan NH, Miranda-Massari JR, Taylor P, et al. A pilot clinical study of continuous intravenous ascorbate in terminal cancer patients. P R Health Sci J. 2005;24:269–76.
42. Ma E, Chen P, Wilkins HM, Wang T, Swerdlow RH, Chen Q. Pharmacologic ascorbate induces neuroblastoma cell death by hydrogen peroxide mediated DNA damage and reduction in cancer cell glycolysis. Free Radic Biol Med. 2017;113:36–47.
43. Mikirova N, Riordan N, Casciari J. Modulation of cytokines in cancer patients by intravenous ascorbate therapy. Med Sci Monit. 2016;22:14–25.
44. Padayatty SJ, Riordan HD, Hewitt SM, Katz A, Hoffer LJ, Levine M. Intravenously administered vitamin C as cancer therapy: three cases. CMAJ. 2006;174:937–42.
45. Polireddy K, Dong R, Reed G, Yu J, Chen P, Williamson S, et al. High dose parenteral ascorbate inhibited pancreatic cancer growth and metastasis: mechanisms and a phase I/IIa study. Sci Rep. 2017;7:17188.
46. Uetaki M, Tabata S, Nakasuka F, Soga T, Tomita M. Metabolomic alterations in human cancer cells by vitamin C-induced oxidative stress. Sci Rep. 2015;5:13896.

47. Chen Q, Espey MG, Sun AY, Pooput C, Kirk KL, Krishna MC, et al. Pharmacologic doses of ascorbate act as a prooxidant and decrease growth of aggressive tumor xenografts in mice. Proc Natl Acad Sci USA. 2008;105:11105–9.
48. Roomi MW, Roomi N, Bhanap B, Niedzwiecki A, Rath M. Antineoplastic activity of a nutrient mixture in Y-79 malignant retinoblastoma cells. Oncol Rep. 2013;29:29–33.
49. Chen Q, Espey MG, Krishna MC, Mitchell JB, Corpe CP, Buettner GR, et al. Pharmacologic ascorbic acid concentrations selectively kill cancer cells: action as a pro-drug to deliver hydrogen peroxide to tissues. Proc Natl Acad Sci USA. 2005;102:13604–9.
50. Frei B, Lawson S. Vitamin C and cancer revisited. Proc Natl Acad Sci USA. 2008;105:11037–8.
51. Hoffer LJ, Levine M, Assouline S, Melnychuk D, Padayatty SJ, Rosadiuk K, et al. Phase I clinical trial of i.v. ascorbic acid in advanced malignancy. Ann Oncol. 2008;19:1969–74.
52. Geeraert L. Intravenous high-dose vitamin C. http://cam-cancer.org/en/high-dose-vitamin-c: CAM-Cancer Consortium, 2014.
53. Brubaker RF, Bourne WM, Bachman LA, McLaren JW. Ascorbic acid content of human corneal epithelium. Invest Ophthalmol Vis Sci. 2000;41:1681–3.
54. Du J, Cullen JJ, Buettner GR. Ascorbic acid: chemistry, biology and the treatment of cancer. Biochim Biophys Acta. 2012;1826:443–57.
55. Hediger MA. New view at C. Nat Med. 2002;8:445–6.
56. McFall RC, Sery TW, Makadon M. Characterization of a new continuous cell line derived from a human retinoblastoma. Cancer Res. 1977;37:1003–10.
57. Stephan H, Boeloeni R, Eggert A, Bornfeld N, Schueler A. Photodynamic therapy in retinoblastoma: effects of verteporfin on retinoblastoma cell lines. Invest Ophthalmol Vis Sci. 2008;49:3158–63.
58. Kakkassery V, Skosyrski S, Lüth A, Kleuser B, van der Giet M, Tate R, et al. Etoposide Upregulates Survival Favoring Sphingosine-1-Phosphate in Etoposide-Resistant Retinoblastoma Cells. Pathol Oncol Res. 2019;25:391–9.
59. Reinhard J, Wagner N, Krämer MM, Jarocki M, Joachim SC, Dick HB, et al. Expression changes and impact of the extracellular matrix on etoposide resistant human retinoblastoma cell lines. Int J Mol Sci. 2020;21. https://www.mdpi.com/1422-0067/21/12/4322.
60. Liu Y, Hu H, Liang M, Xiong Y, Li K, Chen M, et al. Regulated differentiation of WERI-Rb-1 cells into retinal neuron-like cells. Int J Mol Med. 2017;40:1172–84.
61. Voets T, Droogmans G, Wissenbach U, Janssens A, Flockerzi V, Nilius B. The principle of temperature-dependent gating in cold- and heat-sensitive TRP channels. Nature. 2004;430:748–54.
62. Grynkiewicz G, Poenie M, Tsien RY. A new generation of Ca2+ indicators with greatly improved fluorescence properties. J Biol Chem. 1985;260:3440–50.
63. Milligan CJ, Li J, Sukumar P, Majeed Y, Dallas ML, English A, et al. Robotic multiwell planar patch-clamp for native and primary mammalian cells. Nat Protoc. 2009;4:244–55.
64. Bruggemann A, Stoelzle S, George M, Behrends JC, Fertig N. Microchip technology for automated and parallel patch-clamp recording. Small. 2006;2:840–6.
65. Pusch M, Neher E. Rates of diffusional exchange between small cells and a measuring patch pipette. Pflugers Arch. 1988;411:204–11.
66. Barry PH. JPCalc, a software package for calculating liquid junction potential corrections in patch-clamp, intracellular, epithelial and bilayer measurements and for correcting junction potential measurements. J Neurosci Methods. 1994;51:107–16.
67. Köse SA, Nazıroğlu M. N-acetyl cysteine reduces oxidative toxicity, apoptosis, and calcium entry through TRPV1 channels in the neutrophils of patients with polycystic ovary syndrome. Free Radic Res. 2015;49:338–46.
68. Root-Bernstein R, Dillon PF. A common molecular motif characterizes extracellular allosteric enhancers of GPCR aminergic receptors and suggests enhancer mechanism of action. Curr Med Chem. 2014;21:3673–86.
69. Clement K, Biebermann H, Farooqi IS, Van der Ploeg L, Wolters B, Poitou C, et al. MC4R agonism promotes durable weight loss in patients with leptin receptor deficiency. Nat Med. 2018;24:551–5.
70. Mühlhaus J, Dinter J, Nürnberg D, Rehders M, Depke M, Golchert J, et al. Analysis of human TAAR8 and murine Taar8b mediated signaling pathways and expression profile. Int J Mol Sci. 2014;15:20638–55.
71. Mangmool S, Kurose H. G(i/o) protein-dependent and -independent actions of Pertussis Toxin (PTX). Toxins (Basel). 2011;3:884–99.
72. Monteith GR, McAndrew D, Faddy HM, Roberts-Thomson SJ. Calcium and cancer: targeting Ca2+ transport. Nat Rev Cancer. 2007;7:519–30.
73. Monteith GR, Davis FM, Roberts-Thomson SJ. Calcium channels and pumps in cancer: changes and consequences. J Biol Chem. 2012;287:31666–73.
74. Calero CI, Vickers E, Moraga Cid G, Aguayo LG, von Gersdorff H, Calvo DJ. Allosteric modulation of retinal GABA receptors by ascorbic acid. J Neurosci. 2011;31:9672–82.
75. Vissers MCM, Das AB. Potential mechanisms of action for Vitamin C in cancer: reviewing the evidence. Front Physiol. 2018;9:809.
76. Upadhyay S, Vaish S, Dhiman M. Hydrogen peroxide-induced oxidative stress and its impact on innate immune responses in lung carcinoma A549 cells. Mol Cell Biochem. 2019;450:135–47.
77. Sies H. Hydrogen peroxide as a central redox signaling molecule in physiological oxidative stress: oxidative eustress. Redox Biol. 2017;11:613–9.
78. Chen Q, Espey MG, Sun AY, Lee JH, Krishna MC, Shacter E, et al. Ascorbate in pharmacologic concentrations selectively generates ascorbate radical and hydrogen peroxide in extracellular fluid in vivo. Proc Natl Acad Sci USA. 2007;104:8749–54.
79. Du J, Martin SM, Levine M, Wagner BA, Buettner GR, Wang SH, et al. Mechanisms of ascorbate-induced cytotoxicity in pancreatic cancer. Clin Cancer Res. 2010;16:509–20.
80. Wang Q, Huang L, Yue J. Oxidative stress activates the TRPM2-Ca(2+)-CaMKII-ROS signaling loop to induce cell death in cancer cells. Biochim Biophys Acta Mol Cell Res. 2017;1864:957–67.
81. Andersson DA, Gentry C, Moss S, Bevan S. Transient receptor potential A1 is a sensory receptor for multiple products of oxidative stress. J Neurosci. 2008;28:2485–94.
82. Hill K, Schaefer M. Ultraviolet light and photosensitising agents activate TRPA1 via generation of oxidative stress. Cell Calcium. 2009;45:155–64.
83. Bai JZ, Lipski J. Involvement of TRPV4 channels in Aβ(40)-induced hippocampal cell death and astrocytic Ca(2+) signalling. Neurotoxicology. 2014;41:64–72.
84. Abiria SA, Krapivinsky G, Sah R, Santa-Cruz AG, Chaudhuri D, Zhang J, et al. TRPM7 senses oxidative stress to release Zn. Proc Natl Acad Sci U S A. 2017;114:E6079–88.
85. Yamamoto S, Takahashi N, Mori Y. Chemical physiology of oxidative stress-activated TRPM2 and TRPC5 channels. Prog Biophys Mol Biol. 2010;103:18–27.
86. Pires PW, Earley S. Redox regulation of transient receptor potential channels in the endothelium. Microcirculation. 2017;24. https://onlinelibrary.wiley.com/doi/abs/10.1111/micc.12329.

87. Prevarskaya N, Zhang L, Barritt G. TRP channels in cancer. Biochim Biophys Acta. 2007;1772:937–46.
88. Bouron A, Kiselyov K, Oberwinkler J. Permeation, regulation and control of expression of TRP channels by trace metal ions. Pflugers Arch. 2015;467:1143–64.
89. Sung B, Prasad S, Ravindran J, Yadav VR, Aggarwal BB. Capsazepine, a TRPV1 antagonist, sensitizes colorectal cancer cells to apoptosis by TRAIL through ROS-JNK-CHOP-mediated upregulation of death receptors. Free Radic Biol Med. 2012;53:1977–87.
90. Yang MH, Jung SH, Sethi G, Ahn KS. Pleiotropic pharmacological actions of capsazepine, a synthetic analogue of capsaicin, against various cancers and inflammatory diseases. Molecules 2019;24. https://www.mdpi.com/1420-3049/24/5/995.
91. Xu SZ, Zeng F, Boulay G, Grimm C, Harteneck C, Beech DJ. Block of TRPC5 channels by 2-aminoethoxydiphenyl borate: a differential, extracellular and voltage-dependent effect. Br J Pharmacol. 2005;145:405–14.
92. Parekh AB, Putney JW. Store-operated calcium channels. Physiol Rev. 2005;85:757–810.
93. Bootman MD, Collins TJ, Mackenzie L, Roderick HL, Berridge MJ, Peppiatt CM. 2-aminoethoxydiphenyl borate (2-APB) is a reliable blocker of store-operated Ca2+ entry but an inconsistent inhibitor of InsP3-induced Ca2+ release. FASEB J. 2002;16:1145–50.
94. Stenger B, Popp T, John H, Siegert M, Tsoutsoulopoulos A, Schmidt A, et al. N-Acetyl-L-cysteine inhibits sulfur mustard-induced and TRPA1-dependent calcium influx. Arch Toxicol. 2017;91:2179–89.
95. Nazıroğlu M, Ciğ B, Ozgül C. Neuroprotection induced by N-acetylcysteine against cytosolic glutathione depletion-induced Ca2+ influx in dorsal root ganglion neurons of mice: role of TRPV1 channels. Neuroscience. 2013;242:151–60.
96. Özgül C, Nazıroğlu M. TRPM2 channel protective properties of N-acetylcysteine on cytosolic glutathione depletion dependent oxidative stress and Ca2+ influx in rat dorsal root ganglion. Physiol Behav. 2012;106:122–8.
97. Walcher L, Budde C, Böhm A, Reinach PS, Dhandapani P, Ljubojevic N, et al. TRPM8 activation via 3-Iodothyronamine blunts VEGF-induced transactivation of TRPV1 in human uveal melanoma cells. Front Pharmacol. 2018;9:1234.
98. Bari MR, Akbar S, Eweida M, Kühn FJ, Gustafsson AJ, Lückhoff A, et al. H2O2-induced Ca2+ influx and its inhibition by N-(p-amylcinnamoyl) anthranilic acid in the beta-cells: involvement of TRPM2 channels. J Cell Mol Med. 2009;13:3260–7.
99. DelloStritto DJ, Connell PJ, Dick GM, Fancher IS, Klarich B, Fahmy JN, et al. Differential regulation of TRPV1 channels by H2O2: implications for diabetic microvascular dysfunction. Basic Res Cardiol. 2016;111:21.
100. Hara Y, Wakamori M, Ishii M, Maeno E, Nishida M, Yoshida T, et al. LTRPC2 Ca2+-permeable channel activated by changes in redox status confers susceptibility to cell death. Mol Cell. 2002;9:163–73.
101. Kashio M, Tominaga M. The TRPM2 channel: a thermosensitive metabolic sensor. Channels (Austin). 2017;11:426–33.
102. Nicholas S, Yuan SY, Brookes SJ, Spencer NJ, Zagorodnyuk VP. Hydrogen peroxide preferentially activates capsaicin-sensitive high threshold afferents via TRPA1 channels in the guinea pig bladder. Br J Pharmacol. 2017;174:126–38.
103. Dhaka A, Uzzell V, Dubin AE, Mathur J, Petrus M, Bandell M, et al. TRPV1 is activated by both acidic and basic pH. J Neurosci. 2009;29:153–8.
104. Du J, Xie J, Yue L. Modulation of TRPM2 by acidic pH and the underlying mechanisms for pH sensitivity. J Gen Physiol. 2009;134:471–88.
105. Mačianskienė R, Almanaitytė M, Jekabsone A, Mubagwa K. Modulation of human cardiac TRPM7 current by extracellular acidic pH depends upon extracellular concentrations of divalent cations. PLoS One. 2017;12:e0170923.
106. Garrity PA. Weakly acidic, but strongly irritating: TRPA1 and the activation of nociceptors by cytoplasmic acidification. J Gen Physiol. 2011;137:489–91.
107. Lu XY, Liu BC, Wang LH, Yang LL, Bao Q, Zhai YJ, et al. Acute ethanol induces apoptosis by stimulating TRPC6 via elevation of superoxide in oxygenated podocytes. Biochim Biophys Acta. 2015;1853:965–74.
108. Su X, Shen Z, Yang Q, Sui F, Pu J, Ma J, et al. Vitamin C kills thyroid cancer cells through ROS-dependent inhibition of MAPK/ERK and PI3K/AKT pathways via distinct mechanisms. Theranostics. 2019;9:4461–73.
109. Ryskamp DA, Witkovsky P, Barabas P, Huang W, Koehler C, Akimov NP, et al. The polymodal ion channel transient receptor potential vanilloid 4 modulates calcium flux, spiking rate, and apoptosis of mouse retinal ganglion cells. J Neurosci. 2011;31:7089–101.
110. Wang Q, Xu Q, Wei A, Chen S, Zhang C, Zeng L. [High dose vitamin C inhibits proliferation of breast cancer cells through reducing glycolysis and protein synthesis]. Zhejiang Da Xue Xue Bao Yi Xue Ban. 2019;48:296–302.
111. Cameron E, Pauling L. Supplemental ascorbate in the supportive treatment of cancer: Prolongation of survival times in terminal human cancer. Proc Natl Acad Sci U S A. 1976;73:3685–9.
112. Gkika D, Prevarskaya N. Molecular mechanisms of TRP regulation in tumor growth and metastasis. Biochim Biophys Acta. 2009;1793:953–8.
113. Rizzuto R, Pinton P, Ferrari D, Chami M, Szabadkai G, Magalhães PJ, et al. Calcium and apoptosis: facts and hypotheses. Oncogene. 2003;22:8619–27.
114. Beck B, Bidaux G, Bavencoffe A, Lemonnier L, Thebault S, Shuba Y, et al. Prospects for prostate cancer imaging and therapy using high-affinity TRPM8 activators. Cell Calcium. 2007;41:285–94.
115. Herst PM, Broadley KW, Harper JL, McConnell MJ. Pharmacological concentrations of ascorbate radiosensitize glioblastoma multiforme primary cells by increasing oxidative DNA damage and inhibiting G2/M arrest. Free Radic Biol Med. 2012;52:1486–93.
116. Kurbacher CM, Wagner U, Kolster B, Andreotti PE, Krebs D, Bruckner HW. Ascorbic acid (vitamin C) improves the antineoplastic activity of doxorubicin, cisplatin, and paclitaxel in human breast carcinoma cells in vitro. Cancer Lett. 1996;103:183–9.
117. Stock K, Kumar J, Synowitz M, Petrosino S, Imperatore R, Smith ES, et al. Neural precursor cells induce cell death of high-grade astrocytomas through stimulation of TRPV1. Nat Med. 2012;18:1232–8.
118. Ghavami G, Sardari S. Synergistic effect of vitamin C with cisplatin for inhibiting proliferation of gastric cancer cells. Iran Biomed J. 2020;24:119–27.

Curriculum Vitae

Mein Lebenslauf wird aus datenschutzrechtlichen Gründen in der elektronischen Version meiner Arbeit nicht veröffentlicht.

Publikationsliste

Oronowicz J, Reinhard J, Reinach PS, Ludwiczak S, Luo H, Omar Ba Salem MH, Kraemer MM, Biebermann H, Kakkassery V, Mergler S: **Ascorbate-induced oxidative stress mediates TRP channel activation and cytotoxicity in human etoposide-sensitive and -resistant retinoblastoma cells**. *Lab Invest* 2020.

DOI: 10.1038/s41374-020-00485-2

Journal Impact Factor: 3.684

Eigenfactor: 0.009110

Danksagung

Mein besonderer Dank gilt meinem Doktorvater Herrn PD Dr. phil. nat. Stefan Mergler für die Einführung in die Forschung, die enorme Unterstützung bei der Durchführung dieses Projekts und wunderbare Betreuung. Außerdem danke ich meinem Co-Autor Prof. Peter S. Reinach für die konstruktive wissenschaftliche Zusammenarbeit und Verbesserungsvorschläge bei der Anfertigung meiner Arbeit. Ganz besonders danke ich auch meiner Co-Betreuerin Prof. Dr. rer. nat. Heike Biebermann für die stetige fachliche Unterstützung. Darüber hinaus möchte ich unserer Kooperationspartnerin Dr. Jacqueline Reinhard-Recht für die Durchführung der PCR-Analysen und die Bereitstellung der Zellen, PD Dr. med. Vinodh Kakkassery als Initiator der Kooperation, May Amer für die technischen Unterstützung und der Validierung einiger Ergebnisse sowie allen Co-Autoren der Publikation bedanken. Besonderer Dank gilt meiner Familie und meinen Freunden für die unbeschränkte Unterstützung.